Optimisation studies of a single-machine power system.

Lu, Henry

Award date:
1979

Awarding institution:
University of Bath

OPTIMISATION STUDIES OF A SINGLE-MACHINE POWER SYSTEM

submitted by Henry LU M.Sc. D.I.C.

for the degree of Ph.D.

of the University of Bath

1979

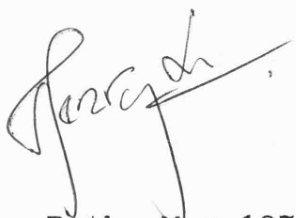

Bath, May 1979

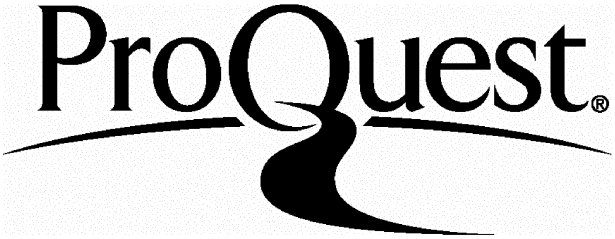

S U M M A R Y

This dissertation is, in the main, concerned with the synthesis of excitation feedback controllers designed to improve the performance of a.c. turbogenerators following a large disturbance.

Solution methods and approaches for nonlinear optimisation are outlined and their application to a single-machine power system is considered. Linear search algorithms are applied to the optimisation studies of single variable excitation control. With the aid of signal-flow graph and Bode diagram techniques, a new single state variable for feedback has been made obvious. Dynamic sensitivity method has also been used to investigate the suitability of all the feedback signals under study. The theoretical excitation control laws obtained have been confirmed on a small, but realistically scaled, laboratory-model power system.

Finally, multi-variable optimisation is applied to co-ordinated excitation and steam-flow control. Only one extra stabilising signal has been added to each of the two control loops. It has been found that substantial improvements in transient performance can be achieved by the suboptimal control laws derived, under large disturbances and different operating conditions.

A C K N O W L E D G E M E N T S

The work presented in this thesis was carried out under the supervision of Mr. A.R. Daniels, Senior Lecturer in the School of Electrical Engineering, University of Bath, England. The author wishes to express his gratitude to Mr. Daniels for his constant encouragement, interest and guidance.

The author is also indebted to Professor K.V. Diprose for his most valuable advices and enlightening discussions.

The theoretical studies have been made possible by the provision of finance from the Science Research Council to use their Interactive Computing Facilities. The guidance provided by the computing staff at UMIST is greatly appreciated.

Financial support from the University of Bath is gratefully acknowledged.

Finally, the author would like to thank Mr. H.A. Hazell, Experimental Officer, for his help in performing and recording all the experimental results.

T A B L E O F C O N T E N T S

LIST OF PRINCIPAL SYMBOLS

The principal symbols used in this thesis are listed as follows. Symbols which do not appear in the list will be defined in the text as they are introduced.

v_d, v_q	=	stator voltages in d and q axes respectively
V_{fd}	=	field voltage
V_f	=	field voltage referred to the armature circuit
i_d, i_q	=	stator currents in d and q axes respectively
i_{fd}, i_{1d}, i_{1q}	=	currents in field and d and q axis damper windings respectively
R_a	=	stator resistance in d and q axis windings
r_{fd}, r_{1d}, r_{1q}	=	resistances in field and d and q axis damper windings respectively
Ψ_d, Ψ_q	=	stator flux linkages in d and q axes respectively
Ψ_{fd}, Ψ_{1d}, Ψ_{1q}	=	flux linkages in field and d and q axis damper windings respectively
x_{ffd}, x_{11d}, x_{11q}	=	total reactances of field and d and q axis damper windings respectively
x_{ad}, x_{aq}	=	mutual reactances between any pair of d axis windings and between the q axis windings respectively

x_d, x_q = synchronous reactances in d and q axes respectively

x_d' = d axis transient reactance

x_d'', x_q'' = d and q axis subtransient reactances respectively

e_q' = q axis voltage behind transient impedance

e_d'', e_q'' = d and q axis voltage behind subtransient impedances respectively

T_{do}', T_d' = d axis transient open and short circuit time constants respectively (sec.)

T_{do}'', T_d'' = d axis subtransient open and short circuit time constants respectively (sec.)

T_{qo}'', T_q'' = q axis subtransient open and short circuit time constants respectively (sec.)

T_{qo}', T_q' = q axis transient open and short circuit time constants respectively (sec.)

P_e = electrical terminal power

T_e = air gap torque

T_m = mechanical torque

K_d = damping factor

H = inertia constant (kWs/kVA)

M = $H/\pi f_o$

w_o, f_o = rated frequency (rad/s and Hz respectively)

w = instantaneous angular velocity of rotor (rad/s)

γ = rotor slip speed (rad/s)

δ = rotor angle (rad)

V_b, V_t = voltages at infinite busbar and machine terminals respectively

R_t, X_t = transfer resistance and reactance respectively

R_l, X_l = transmission line resistance and reactance respectively

R_x, X_x = generator transformer resistance and reactance respectively

p = differential operator d/dt

s = Laplace operator

t = time (sec.)

K_i = state feedback gains, i=1,2,...,n

V_r = reference voltage to excitation regulator

V_i = state feedback signal to excitation system

V_s = derivative feedback signal of a.v.r.

T_{mo} = torque reference to governing system

T_a = accelerating torque

T_i = state feedback signal to governing system

f = objective function

I = performance index

S = sensitivity function

Δ = prefix to denote a deviation about the initial operating conditions

$\cdot$ = superscript to denote differentiation w.r.t. time, t

o = subscript to denote a steady-state value

$\_$ = subscript to denote a vector quantity

The constants T and K with appropriate subscripts denote control system time constants and gains.

CHAPTER 1 INTRODUCTION

1.1 Synchronous Stability Studies

The stability of a system of interconnected dynamic components is its ability to return to normal or stable operation after having been subjected to some form of disturbances[1,2]. The study of stability is one of the main concerns of the control engineer whose methods may be applied to electric power systems.

There are two forms of instability in power systems; the loss of synchronism between synchronous machines, and the stalling of asynchronous loads. In a power system, it is possible for either synchronous or load instability to occur. The former is more probable and hence has been given much more attention. Synchronous stability may be divided into two regimes, steady-state and transient. The steady-state stability is basically the ability of the power system when operating under given load conditions to retain synchronism when subject to small disturbances such as the continual changes in load or generation and the switching out of lines. It is most likely to result from the changes in source-to-load impedance resulting from changes in the network configuration. Transient stability is concerned with sudden and large changes in the network conditions such as those brought about by faults. The maximum power transmittable, known as the stability limit, is less than that for the corresponding steady-state

condition.

In power system practice, the operation of synchronous generators is limited by their capacity and the operating conditions[3]. Operation in the reactive-generation region (i.e. operation with lagging power factor) is usually limited by the maximum power output of the turbine and heating of the rotor and stator, while operation in the reactive-absorption region (i.e. operation with leading power factor) is restricted mainly by stability considerations. While the steady-state stability limit is quite well defined, the transient stability limit depends on the type and severity of the disturbance adopted to define the stability limit. Usually, the stability criterion adopted is the ability of the generator to withstand a 3-phase short-circuit fault of standard duration close to the generator terminals without losing synchronism.

1.2 Transient Stability Control Problem

Although steady-state stability is an important consideration, especially under leading power factor, light load conditions, transient stability is still the major consideration used for fixing the operating limit of a synchronous generator operating in the leading power factor region. It is because that with the present capacity of generation and transmission equipment, the transient stability limit is usually lower than the

steady-state stability limit.

In the UK, as the demand on the CEGB system grows, the problems of securing new sites for power station will become acute and difficult to satisfy because of suitable land scarcity and increasing stringent amenity and environmental requirements. Pressures related to the environment will have two direct effects. Firstly, there will be an incentive to try to increase the capacity on each site; this is of course augmented by the capital savings to be gained with the use of larger generating complexes. Secondly, obtaining wayleaves for new transmission lines will become more difficult and the tendency will be towards providing the minimum possible transmission from each site. One solution would be the use of ultra high voltage transmission lines, but this would involve considerable capital investment. Problems associated with the transient stability performance of power stations will therefore become more critical as the specific loading of the transmission is increased and generation concentrations become larger. They will be aggravated as unit sizes increase because the specific inertia tends to become smaller and the reactances larger, both factors being detrimental to transient stability performance. Over the past years, various methods, other than simply strengthening the transmission system, have been investigated for improving transient stability.

1.3 Practical Approaches to Transient Stability Control

Possible means of controlling stability can be classified into three basic groups:-

(a) methods involving changes in the operating systems of machines with conventional automatic voltage regulators (a.v.r.s) and governors,
(b) alterations in the transmission network, and
(c) changes in the design of conventional machines.

The first group includes fast governing[4,5], fast valving[6], and fast excitation with increased ceiling voltage[7]. Changes in the network include such techniques as braking resistors[8], series capacitor switching[9], generator dropping, load shedding, power-factor correction[10,11], phase-shift insertion[12], tie-line reactance control[13] and autoreclosing circuit breakers[14]. The last approach involves design of high short-circuit ratio machines[11], dual-excitation machines[15] and interconnected winding rotor machines[16].

With an existing system, the choice of the method of control is obviously between (a) and (b). Which method is used depends on the control objectives to be achieved and on economic considerations. Many of the control schemes proposed, especially those which exert control through changes in the network parameters have been designed entirely from the viewpoint of controlling the

generator rotor oscillations. These methods lead to an acceptable rotor transient behaviour and have the advantage in that they make use of feedback information of system states which can easily be measured. However, the system representations used with these types of control schemes have, in many cases, been simplified ones and the variations in the electrical quantities have been ignored. Furthermore, since the control action requires large and sudden variations in the electrical power flowing in the network, the problem of overvoltages may arise[17]. From the viewpoint of cost, the network parameter switching type of control schemes require a substantially higher cost as compared with the other forms of control schemes applied to the prime mover and excitation system. For example, a series capacitor switching control scheme, including the auxiliary equipment would require an initial investment which is many times that required for an excitation type of control[18].

Apart from the economic advantage in using excitation control, recent developments in solid-state excitation systems[19] with high ceiling voltages and facilities for additional signals have made this type of control more attractive to use, either on its own or in conjunction[20] with modern electro-hydraulic governing systems[21].

1.4 The Role of Excitation Control

Excitation control of a turbogenerator must be designed to meet several constraints. Firstly, the terminal voltage of the machine must be maintained within specified limits (usually $\pm 0.5\%$) over a wide range of steady operating conditions. This requires feedback of terminal voltage with a gain of the order of 200 in the forward path of the excitation control system. Secondly, the machine must have a good dynamic stability margin. For a simple proportional controller, this condition can only be met for low values of the order of ten in the forward gain. Thus for high gains, stabilising feedback must be introduced. Thirdly, the machine must have a good transient performance, following a large disturbance. The standard form of disturbance considered is a symmetrical 3-phase short-circuit at the high-voltage terminals of the generator transformer with a set fault time with the prefault impedance equal to the postfault impedance. Feedback of terminal voltage can only ever be effective in reducing the first swing in transient load angle and even this effect depends on the presence of a high value of forward gain and a high ceiling voltage. Once again, the value required (typically 50) is less than that needed to meet the steady-state regulation. If the gain is set to meet the steady-state requirement, the addition of well-designed stabilising feedback also improves the transient performance. It has now been

established that the best contribution that can be made by excitation control is to force the excitation to a positive peak immediately the fault is applied and to maintain peak excitation until the first peak in rotor angle has been reached. Since the error input voltage into the excitation system is given as the difference between a fixed voltage and terminal voltage, little subsequent control beyond the first swing in load angle is obtained.

A method of excitation control, known as 'bang-bang'[22] control, has been proposed to alleviate the effects of a generator pole-slipping during or after a major system disturbance. With normal excitation control, the swing of a machine rotor is either arrested and reversed by forced excitation or accelerated into a pole-slip. In the latter event, the speed rise is detected by the governor which reduces steam input and power output and, by throwing more load onto other machines, causes them to slow down. Such undesirable oscillations and exchanges in active power between machines can be minimised by arranging for the excitation to be removed from a machine when it starts to accelerate into a pole-slip and restoring excitation when a suitable rotor angle has been reached after a pole-slip has taken place. This bang-bang control of excitation has now become possible with the advent of fast-acting thyristor excitation control, but it is yet too early to forecast whether the overall effects on a supply system of one or more large machines

pole-slipping without excitation can be tolerated.

Another development of interest is the divided-winding[23] rotor which allows the mechanical rotor or load angle to be kept constant, irrespective of the power factor of the load. Such a development allows a machine to absorb reactive power up to the limit of its stator thermal rating without impairing its transient stability. The important feature of the divided-winding arrangement is that a change in machine reactive output does not require a corresponding change in rotor position relative to the air gap flux, i.e. there is no change in mechanical load angle. A separate cost analysis has shown that reactive power absorption of high-merit turbogenerators with divided-winding rotors is half the cost of alternative compensation equipment[24]. Against this must be set the disadvantages of an additional excitation control system with its slip rings and brushgear or rotating diodes or thyristors, and more problems associated with mechanical stresses in the rotor windings introduced by the fact that the two rotor windings carry different values of current.

In recent years, modern control theory has been widely used in the design of excitation controllers and governing systems of a.c. turbogenerators. It is now being recognised that if improvements in transient performance beyond the first swing are to be obtained, additional feedback, in the form of state feedback, must be used.

1.5 Steam-Flow Control

Traditionally, the major function of turbogenerator control is steady-state voltage and turbine speed regulation, such that both are maintained within certain specified limits throughout the loading conditions from full load to no load. In an interconnected power system, the system frequency is maintained within certain specified limits throughout changes in system load which are shared among generators in an economic manner. Machine terminal voltage regulation is achieved by excitation control while turbine speed and power-frequency regulation is achieved by steam-flow control. Under transient conditions, the excitation system helps voltage recovery after system faults. The steam governing system, on the other hand, prevents overspeed under fault and load rejection conditions.

The conventional governing system is a closed-loop control system where speed control is accomplished by speed feedback. The speed transducer used is a mechanical flyball device[25] which is driven from the turbine shaft. Turbine speed changes are sensed by the transducer and translated into control signals used to position the steam valves and adjust the turbine power output. This mechanical system, though reliable, suffers from certain functional and operational limitations. Firstly, it has inherent insensitivity produced by dead bands introduced by mechanical linkages. Secondly, the droop setting

cannot be changed on load to suit operational requirements, and thirdly, subsidiary control signals cannot easily be incorporated into the control system. The major problem amongst all is the severe wear on the teeth of the cross-shaft due to vibration giving rise to frequent governor failure. This has led to the recent installation of an electronic governor on a 500MW unit at CEGB Rugeley B power station to replace the existing mechanical system[26]. Difficulties have been experienced with mechanical governors on some sets and electronic governors have been installed as standard on all CEGB high merit units built since 1973.

Several site tests have been carried out by the CEGB to study the transient performance of turbogenerators of various ratings. Buseman and Casson[27] recorded stability tests on a 56MVA (45MW) set under various fault conditions and found that, while the voltage regulator produced beneficial effects on transient and steady-state stability, governor action was ineffective on the first rotor swing but helpful for subsequent re-synchronization. Scott et. al.[28] recorded another field test on a 200MW set equipped with a governor-controlled interceptor valve and found that, while voltage regulators contributed considerably towards the dynamic recovery of system states, the effect of the governing system depended on the severity of the fault. Governor action was found to be more significant under severe fault conditions such as 3-phase short circuit. In the Northfleet tests[29]

performed on a 120MW set equipped with governor-controlled interceptor valves, where phase-to-phase and 3-phase fault conditions were examined, it was found that the governing system made only relatively small contributions to improvements in transient stability. These test results appear to indicate that, except under the most severe fault conditions of relatively long duration, the conventional governing system only introduces relatively small improvements in transient stability.

Certain additional requirements must be met if the governing system is to make more significant contributions. The governing system, including the governor and control valves, should be fast acting, the amount of uncontrolled steam entrained in the turbine should be minimised to reduce the effective time constant of the turbine, and some form of optimal or suboptimal control be implemented. Modern turbogenerator sets with electro-hydraulic governing systems and fast-acting main and interceptor valves satisfy the first two requirements. Furthermore, the flexible nature of the electro-hydraulic governing system makes it amenable to the implementation of some form of optimal or suboptimal control.

1.6 Optimal and Suboptimal Control

Increased demand for both the quantity and reliability of electrical energy has led to the introduction of large generator units requiring a more sophisticated control

philosophy. This need has coincided with the introduction of fast and inexpensive minicomputers and microcomputers, which now allow the practical implementation of many of the techniques of modern control methods in power-system control. The application of modern control methods to the design of excitation controllers and governing systems of a.c. turbogenerators has been widely used to study the transient performance of a single-machine power system. Although there is a long list of analytical studies in this field, the number of supported experimental studies on real, although small, power-system models is far shorter[30-38].

Optimal control theory is concerned with deriving a sequence of controls, or a continuous control function of time, which, when applied to the given control system, will cause the system to operate in some optimum manner. The optimality of a control is measured by a performance index, I, which is usually a time integral of some performance measure over a specified period of time and an optimum control is defined as one which extremises the performance index. To select this optimal control function from the set of possible functions, it is necessary to know the state of the control system during that period. Should these be imperfectly known, then only approximate controls may be found. It would be very convenient if, from a knowledge of the initial state, the state equations of the system and the error index function, it were possible to derive an explicit function for the optimal

control function. Unfortunately, this is not possible, and a partial solution in the form of a set of necessary conditions for an extremum of the error index has to be accepted. In the particular case where the state equations are linear and the error measure is quadratic, a numerical solution may be obtained by numerical integration of a set of differential equations known as the Riccati equations. Generally, however, it is necessary to proceed on some systematic trial and error basis to find the extremal state and control functions. In mathematical terms, the optimal control problem is one of functional minimisation, as in the calculus of variations. It is akin to the ordinary minimisation problem in calculus, where the necessary conditions to be satisfied by the independent variables of a scalar function are established by equating to zero each of the partial derivatives of the function with respect to its arguments. In functional minimisation, rather than obtain a set of algebraic equations which are satisfied by the independent variables at the minimum of the scalar function, a set of differential equations satisfied over the control interval by the control and state variable functions of time at the extremum of the error index function is obtained instead. The functional minimisation process is further complicated by the need to satisfy the constraints existing amongst the control and state variables due to the process dynamics, as specified by the state equations.

A brief summary of the important results[39] regarding the necessary conditions to achieve the extremity of the performance index as developed by the calculus of variation, Pontryagin's Minimum Principle and dynamic programming are summarised in this section. By using variational calculus, the constrained function minimisation problem is converted to an unconstrained one through the Lagrange multipliers. This transformation results in a new performance measure, which has to satisfy certain necessary conditions for optimality. These necessary conditions, when applied to the n-th order dynamic system, usually give rise to a two-point boundary value problem (TPBVP) consisting of 2n ordinary differential equations with boundary conditions specified both at the initial and final points. The optimal control problem as formulated using the calculus of variation requires that the state equations have continuous first partial derivatives with respect to the control variables. Another drawback of this formulation is that constraints on the control variables cannot be conveniently handled.

Pontryagin formulated the optimal control problem in terms of the Hamiltonian function. Pontryagin's formulation, together with the Minimum Principle, also generally give rise to a TPBVP , but they relax the requirement of continuous partial derivatives of the state equations with respect to the control variables and unconstrained control.

An alternative to the variational procedures for deriving the optimal control is the method of dynamic programming. The corresponding necessary conditions the optimal control must satisfy is the Bellman's equation, implying that the Hamilton-Jacobi equation be satisfied. An alternative to the direct solution of the Hamilton-Jacobi equation to determine the minimum performance function is to assume a particular form which is known to be suitable, and then establish a set of ordinary nonlinear differential equations with known one-point boundary value conditions, for calculating the time coefficients in the minimum performance function.

There is yet no general solution available for Bellman's partial differential equation. However, the Hamilton-Jacobi differential equation could be solved for the important special case of a linear system with a quadratic performance measure. This constitutes the Linear Regulator Problem. The result for this linear regulator problem, as obtained by the solution of the Hamilton-Jacobi equation, is the same as that obtained by the solution of the matrix Riccati equation.

The general optimal control problem is inherently difficult to solve whether it be formulated by variational calculus, resulting in a TPBVP, which in general, can only be solved by iterative methods requiring successive integration of the state and adjoint equations or by dynamic programming, resulting in a partial differential equation for which no general solution is available. Furthermore, even when a

solution is achieved, the optimal solution is, in general, in the form of an open-loop control or a feedback control with time-variant feedback gains, except for special cases, such as the linear regulator problem with the control interval extended to infinity, where the optimal control is a constant linear feedback of all states. These optimal open-loop or variable gain state feedback controls are only applicable to systems which have fixed parameters and operating conditions, and subject to a given set of disturbance. This is hardly true of the control of turbo-generator sets in power system.

The optimum control of turbogenerators in power systems could be formulated by two approaches both of which lead to comparatively straightforward solutions and result in optimum controls amenable to practical implementation. One is to formulate the problem as a linear regulator problem, a very common method. The other approach, which is developed in this study, is to retain the nonlinearities of the system and develop some form of closed-loop linear state feedback suboptimal control. By assuming, a priori, the form of the optimum feedback control, the suboptimal control problem is transformed into one of parameter optimisation which can be solved readily by function minimisation.

1.7 System Sensitivity

1.7.1 The Significance of Sensitivity Theory

The sensitivity of a dynamic system to variations of its parameters is one of the basic aspects in the study of dynamic systems. The particular question of parameter sensitivity arises widely in those fields of engineering, where mathematical models are used for the purposes of analysis and synthesis. In order to be able to give a unique formulation of the mathematical problem, the mathematical model is usually assumed to be known exactly. This assumption is, strictly speaking, unrealistic since there is always a certain discrepancy between the actual system and its mathematical model for the following reasons. Firstly, a real system cannot be identified exactly because of the restricted accuracy of the measuring devices. Secondly, the behaviour of any real system changes with time in an often unpredictable way caused by environmental, material property, or operational influences. An additional constraint is that a theoretical concept cannot be implemented easily and, in order to even obtain the required theoretical results, the mathematical model may need to be simplified intentionally to reduce the mathematical problem or even to make the problem solvable at all.

For these reasons, the results of mathematical syntheses need not necessarily be practicable. They may even be

quite inaccurate if, for example there are considerable parameter deviations between the real system and the mathematical model and the solution is very sensitive to the parameters. Therefore, it should be part of the solution to a practical problem to know the parameter sensitivity prior to its implementation or to reduce the sensitivity if this becomes necessary.

This is of particular importance if optimisation procedures are involved, since it is in the nature of optimisation to extremise a certain performance index for the special set of parameters. Futhermore, there are many problems where sensitivity considerations are either useful or mandatory. Some examples are the application of gradient methods, adaptive and self-learning systems, the design of insensitive and suboptimal control systems, the determination of allowed tolerances in the design of networks, the calculation of optimal input signals for parameter identification, analogue and digital simulation of dynamic systems, and so forth.

1.7.2 Basic Definitions

The basis of all sensitivity considerations in the case of time-invariant parameter variations is the so-called sensitivity function $\underline{S}$. If the sensitivity function is known, it will be easy to calculate the change in the system behaviour from given parameter deviations and, conversely, to calculate allowable parameter deviations

from a given preassigned system behaviour.

The mathematical problem to be solved in sensitivity theory is the calculation of the change in the system behaviour due to the parameter variations. There are several ways to define quantities for the characterization of the parameter sensitivity of the system. The definitions commonly used[40] are summarised in this section.

Let the behaviour of the dynamic system be characterized by a quantity $\underline{x} = \underline{x}(\underline{p})$, called a system function, which, among other dependences, is a function of the parameter vector $\underline{p} = (p_1, p_2, \ldots, p_r)^T$. For example, $\underline{x}$ can represent any time domain or frequency domain property or a performance index. Let the nominal parameter vector be denoted by $\underline{p}_o = (p_{1o}, p_{2o}, \ldots, p_{ro})^T$ and the nominal function by $\underline{x}_o = \underline{x}(\underline{p}_o)$. Then, under specified continuity conditions, the following general definitions hold. The absolute sensitivity function $\underline{S}_j$ is given by

$$\underline{S}_j = \left.\frac{\partial \underline{x}(\underline{p})}{\partial p_j}\right|_{\underline{p}_o} = \underline{S}_j(\underline{p}_o) \qquad j=1,2,\ldots,r. \quad (1.1)$$

The subscript $\underline{p}_o$ indicates that the partial derivative expressed by ∂ is taken at nominal parameter values. In addition to depending on $\underline{p}_o$, $\underline{S}_j$ can also depend on other variables, such as the time or the frequency. If $\underline{S}_j$ is a function only of $\underline{p}_o$, it will be called the sensitivity for short, so that for example the term performance index sensitivity means the absolute sensitivity function of the performance index to some specified parameter changes.

The relative or logarithmic sensitivity function $\hat{\underline{S}}_j$ is given by

$$\hat{\underline{S}}_j = \left.\frac{\partial(\ln \underline{x})}{\partial(\ln p_j)}\right|_{\underline{p}_o} = \hat{\underline{S}}_j(\underline{p}_o), \quad j=1,2,\ldots,r, \tag{1.2}$$

where $(\ln \underline{x})$ means the vector of the logarithms of the elements of $\underline{x}$, so that

$$\partial(\ln \underline{x}) = (\partial x_1/x_1, \partial x_2/x_2, \ldots, \partial x_n/x_n)^T.$$

The i-th element of $\hat{\underline{S}}_j$ can be expressed by

$$\hat{S}_{ij} = \left.\frac{\partial x_i/x_i}{\partial p_j/p_j}\right|_{\underline{p}_o} = S_{ij}\frac{p_{jo}}{x_{io}}, \quad \begin{matrix} i=1,2,\ldots,n, \\ j=1,2,\ldots,r, \end{matrix} \tag{1.3}$$

where S_{ij} is the i-th element of the absolute sensitivity function $\underline{S}_j$. The semirelative or semilogarithmic sensitivity function can be expressed in the form

$$\tilde{\underline{S}}_j = \left.\frac{\partial(\ln \underline{x})}{\partial p_j}\right|_{\underline{p}_o}, \quad j=1,2,\ldots,r. \tag{1.4}$$

For the i-th components of $\tilde{\underline{S}}_j$,

$$\tilde{S}_{ij} = \left.\frac{\partial x_i/x_i}{\partial p_j}\right|_{\underline{p}_o} = \frac{1}{x_{io}}S_{ij}, \quad \begin{matrix} i=1,2,\ldots,n, \\ j=1,2,\ldots,r. \end{matrix} \tag{1.5}$$

Alternatively,

$$\underline{\tilde{S}}_j = \left.\frac{\partial \underline{x}}{\partial(\ln p_j)}\right|_{\underline{p}_o} = p_{jo}\underline{S}_j(\underline{p}_o), \quad j=1,2,\ldots,r. \tag{1.6}$$

One important application of the absolute sensitivity function is in parameter optimisation using function minimisation techniques. This form of sensitivity function is inherent in any study using gradient optimisation and is produced without extra computational cost. It also provides a basis for the comparison of the relative influence of different feedback signals on the performance of a system. The logarithmic sensitivity function is most suitable for the determination of precision levels in measurement, manufacture and setting of operational parameters because the errors involved in these processes are in proportion to the parameter values. When the comparative sensitivity of a particular variable with respect to different parameters is studied, the most suitable forms of sensitivity functions are those given by eqns. 1.2 and 1.6. Similarly, when the comparative sensitivity of different variables with respect to a particular parameter is studied, the most suitable forms are those given by eqns. 1.2 and 1.4. However, these forms of sensitivity functions may be used interchangeably, provided they are given the appropriate interpretation. Among the various forms of sensitivity functions, the absolute sensitivity function is the most convenient form to derive and evaluate and the other forms may be readily

evaluated from it. Comparison of the system sensitivities in this thesis is made by taking the integral of the absolute value of the logarithmic sensitivity functions.

CHAPTER 2 SOLUTION METHODS AND APPROACHES

2.1 Introduction

Mathematical techniques of varying degrees of complexity have been used in this study ranging from the use of the signal-flow graph and Bode diagram techniques as design tools, to the use of modern numerical methods to the solution of optimal control problems. Since the initial studies of the control of power system performance described in this dissertation are, essentially, synthesis of feedback control laws from known system outputs, the associated mathematical topics are described first. However, in later sections, the signal-flow graph and the Bode diagram are both used as basic design tools in an attempt to generate a highly appropriate system state to be used for feedback purposes. In these circumstances, a brief mention of these two techniques has been included in this chapter.

2.2 General Rules for Calculating Sensitivity Functions

It is evident from the definitions of the sensitivity functions given in Chapter 1 that they involve the calculus of partial differentiation. In order to treat the problem quite generally, consider a continuous function of the variables $x_1, x_2, \ldots, x_r$ in the general form

$$f = f(x_1, x_2, \ldots, x_r). \qquad (2.1)$$

The total differential df of f is then defined by the relationship

$$df = \frac{\partial f}{\partial x_1} dx_1 + \frac{\partial f}{\partial x_2} dx_2 + \ldots + \frac{\partial f}{\partial x_r} dx_r. \quad (2.2)$$

In the following section, several different types of the dependences among the variables x_1, x_2, ..., x_r are considered with, in all cases the continuity of all derivatives assumed.

First, suppose that x_1, x_2, ..., x_r are functions of a single variable, say a, in the form $x_1(a)$, $x_2(a)$, ..., $x_r(a)$. Then f may be considered to be a function g(a) such that

$$f = g(a), \quad (2.3)$$

with g representing the same physical quantity as f. Then from eqns. 2.2 and 2.3,

$$\frac{dg}{da} = \frac{\partial f}{\partial x_1}\frac{dx_1}{da} + \frac{\partial f}{\partial x_2}\frac{dx_2}{da} + \ldots + \frac{\partial f}{\partial x_r}\frac{dx_r}{da}. \quad (2.4)$$

In these circumstances, the variables x_i, i=1,...,r are also known as the intermediate variables.

If, however, x_1, x_2, ..., x_r are functions of another set of independent variables, say, a_1, a_2, ..., a_s then

$$\begin{aligned} x_1 &= x_1(a_1, a_2, \ldots, a_s) \\ x_2 &= x_2(a_1, a_2, \ldots, a_s) \\ &\vdots \\ x_r &= x_r(a_1, a_2, \ldots, a_s) \end{aligned} \quad (2.5)$$

The function f is then a function of a_j's such that

$$f = g(a_1, a_2, \ldots, a_s). \tag{2.6}$$

In this case, $\frac{dg}{da_j}$ j=1,...,s are no longer defined and only the partial derivatives can be taken so that

$$\begin{aligned} \frac{\partial g}{\partial a_1} &= \frac{\partial f}{\partial x_1}\frac{\partial x_1}{\partial a_1} + \frac{\partial f}{\partial x_2}\frac{\partial x_2}{\partial a_1} + \ldots + \frac{\partial f}{\partial x_r}\frac{\partial x_r}{\partial a_1} \\ &\vdots \\ \frac{\partial g}{\partial a_s} &= \frac{\partial f}{\partial x_1}\frac{\partial x_1}{\partial a_s} + \frac{\partial f}{\partial x_2}\frac{\partial x_2}{\partial a_s} + \ldots + \frac{\partial f}{\partial x_r}\frac{\partial x_r}{\partial a_s}. \end{aligned} \tag{2.7}$$

In the above differentiation, all the independent variables are considered to be constant, except that particular one with respect to which the derivative is taken.

When the variables $x_1, x_2, \ldots, x_{r-1}$ are functions of x_r it follows that

$$x_1 = x_1(x_r), \ldots, x_{r-1} = x_{r-1}(x_r). \tag{2.8}$$

Now f is a function of the intermediate variables $x_1, x_2, \ldots, x_{r-1}$ and of the independent variable x_r. If f is taken as function of x_r only

$$f = g(x_r) \tag{2.9}$$

and

$$\begin{aligned} \frac{dg}{dx_r} &= \frac{\partial f}{\partial x_1}\frac{dx_1}{dx_r} + \frac{\partial f}{\partial x_2}\frac{dx_2}{dx_r} + \ldots + \frac{\partial f}{\partial x_{r-1}}\frac{dx_{r-1}}{dx_r} \\ &\quad + \frac{\partial f}{\partial x_r} \end{aligned} \tag{2.10}$$

In the case where certain of the variables $x_1, x_2, \ldots, x_k$ are functions of the independent variables $x_{k+1}, \ldots, x_r$ it follows that

$$\begin{aligned} x_1 &= x_1(x_{k+1}, \ldots, x_r) \\ &\vdots \\ x_k &= x_k(x_{k+1}, \ldots, x_r), \end{aligned} \tag{2.11}$$

such that

$$f = g(x_{k+1}, \ldots, x_r). \tag{2.12}$$

The total derivative is not definable and in terms of the partial derivatives, eqn. 2.12 gives

$$\begin{aligned} \frac{\partial g}{\partial x_{k+1}} &= \frac{\partial f}{\partial x_1}\frac{\partial x_1}{\partial x_{k+1}} + \ldots + \frac{\partial f}{\partial x_k}\frac{\partial x_k}{\partial x_{k+1}} + \frac{\partial f}{\partial x_{k+1}} \\ &\vdots \\ \frac{\partial g}{\partial x_r} &= \frac{\partial f}{\partial x_1}\frac{\partial x_1}{\partial x_r} + \ldots + \frac{\partial f}{\partial x_k}\frac{\partial x_k}{\partial x_r} + \frac{\partial f}{\partial x_r}. \end{aligned} \tag{2.13}$$

The final case to be considered is the special case when

$$\begin{aligned} x_1 &= x_1(x_{k+1}, \ldots, x_r) \\ &\vdots \\ x_{k-1} &= x_{k-1}(x_{k+1}, \ldots, x_r) \end{aligned} \tag{2.14}$$

but

$$x_k = x_k(x_r).$$

The partial derivatives for x_{k+1}, x_{k+2}, ..., x_{r-1} can be taken as before such that, for example,

$$\frac{\partial g}{\partial x_{k+1}} = \frac{\partial f}{\partial x_1}\frac{\partial x_1}{\partial x_{k+1}} + \ldots + \frac{\partial f}{\partial x_{k+1}}, \qquad (2.15)$$

except that, for the partial derivative with respect to the independent variable x_r,

$$\frac{\partial g}{\partial x_r} = \frac{\partial f}{\partial x_1}\frac{\partial x_1}{\partial x_r} + \ldots + \frac{\partial f}{\partial x_k}\frac{dx_k}{dx_r} + \frac{\partial f}{\partial x_r}. \qquad (2.16)$$

The term $\partial x_k/\partial x_r$ of eqn. 2.13 has been replaced by the term dx_k/dx_r which is defined in the above case.

2.3 Numerical Solution

In any power system, it is important to know how the system will perform during certain transient conditions and considerable effort has gone into the development of methods to predict this performance. The main variable of interest in a synchronous machine is the rotor angle δ, since its variation as a function of time, called the swing curve, gives a direct indication of its stability.

An earlier form of the step-by-step method of solution used a network analyser to represent the conditions at any instant. From readings taken on the analyser, the setting of the analyser for the next step was determined by a manual calculation. Later on, analogue devices were developed to carry out the intermediate calculation.

The method was based on what would now be regarded as excessive simplification. With the advent of modern technology in powerful digital computers, the nonlinear system differential equations can be readily solved by a numerical step-by-step integration algorithm.

Let the system states of a power system representation be defined in a nonlinear form as

$$\dot{\underline{x}} = f(\underline{x},t) \tag{2.17}$$

Let x_n be the value of a typical variable at time t_n. The principle of the step-by-step method is that, when the value of x_n at time t_n is known, the equations can be used to calculate the derivative $\dot{x}_n$, and hence to determine the value at the succeeding instant $t_{n+1}=t_n+h$, where h is the step length. The solution values at t_{n+1} are approximated from values at the beginning of the step, possibly from values in earlier steps, and from slope evaluations which depend in form and combination on the particular method used. Errors are propagated from step to step and the error build-up depends largely on the step length. From the outset then, there is a conflict between the adequate control of error growth, on one hand, and the overall computing time required to achieve this control on the other.

A simple method is to say that

$$x_{n+1} = x_n + h\dot{x}_n \tag{2.18}$$

The method is self-starting, since the derivatives at time t=0 depend only on the values of x_o at that instant and will therefore integrate satisfactory following the discontinuity occuring at the beginning on any step. It is of first order accuracy, since it computes the slope f(x,t) only once during each step.

Any numerical integration method is, of course, only approximate, because the curve is approximated by a series of short straight lines and the accuracy obviously depends on the number of steps, i.e. the step length or time interval h. It is, therefore, advantageous to use a value of h just large enough to give the necessary accuracy and, for further reduction of computer time, to develop a higher order mathematical method of integration, which allows the use of even larger values of h. Such integration methods have been developed from the calculus of finite difference polynomials and may be classified under two headings, namely those which confine all evaluations of the algorithm to within each integration step, and those which use solution information available in previous steps. Of the two methods most frequently used in power system studies, the Runge-Kutta algorithms fall within the first group of methods, and the Predictor-Corrector algorithms into the second group.

The most commonly used version of Runge-Kutta algorithms[41] is one in which four evaluations of the slope are made within the duration of the integration step and from these, a mean weighted slope S is computed of fourth

order accuracy. The algorithm which appears in eqn. 2.19 stems from a truncated infinite series expansion of x over the interval h and eqn. 2.18 with $\dot{x}_n$ replaced by S is used to calculate x_{n+1}, such that

$$x_{n+1} = x_n + (K_1 + 2K_2 + 2K_3 + K_4)/6$$

where

$$\begin{aligned} K_1 &= h\, f(x_n, t_n) \\ K_2 &= h\, f(x_n+K_1/2, t_n+h/2) \\ K_3 &= h\, f(x_n+K_2/2, t_n+h/2) \\ K_4 &= h\, f(x_n+K_3, t_n+h) \end{aligned} \qquad (2.19)$$

Whereas the Runge-Kutta routine starts each step afresh and utilizes only slopes within each step, the predictor-corrector methods make use of the variable and its first derivative obtained in previous steps to predict at t_n the value of x_{n+1} and then uses a corrector formula to improve the accuracy of the estimate. The accuracy depends upon the number of previous values of x and $x^{\cdot}$ available and on the relative significance attached to each one.

The advantages of the Runge-Kutta methods are mainly that they are self-starting and have high accuracy. However, the disadvantage is that, as in the case of eqn. 2.19, the slope has to be computed four times within each time

step, thereby using excessive computer time. Accuracy diminishes rapidly as the step length increases and the method has limited stability. Predictor-corrector methods have the advantage of high accuracy and stability and require calculation of the slope only once per step. Their disadvantage, however, is that they cannot integrate through discontinuities.

The computer time required for a digital computation is an important factor in determining the method and the degree of simplification of the equations used. For calculations for a multi-machine system, in which each generator has a voltage regulator and a governor, the choice of computing technique is important. For the transient studies of a single-machine power system, accuracy is a more important consideration than computation time. The straightforward easily computed fourth order Runge-Kutta method has been used throughout the studies.

A flow chart for the optimisation program is shown in Fig. 2.1. The steady-state calculation is carried out using the steady-state phasor diagram as shown in Appendix A1. The total set of system and sensitivity equations is sub-divided into two groups, the differential equations and the algebraic equations. Initially, the equations are integrated over the first step using steady-state values as initial values to obtain new values for the integrable state variables. These new values are then used in the nonintegrable algebraic equations to

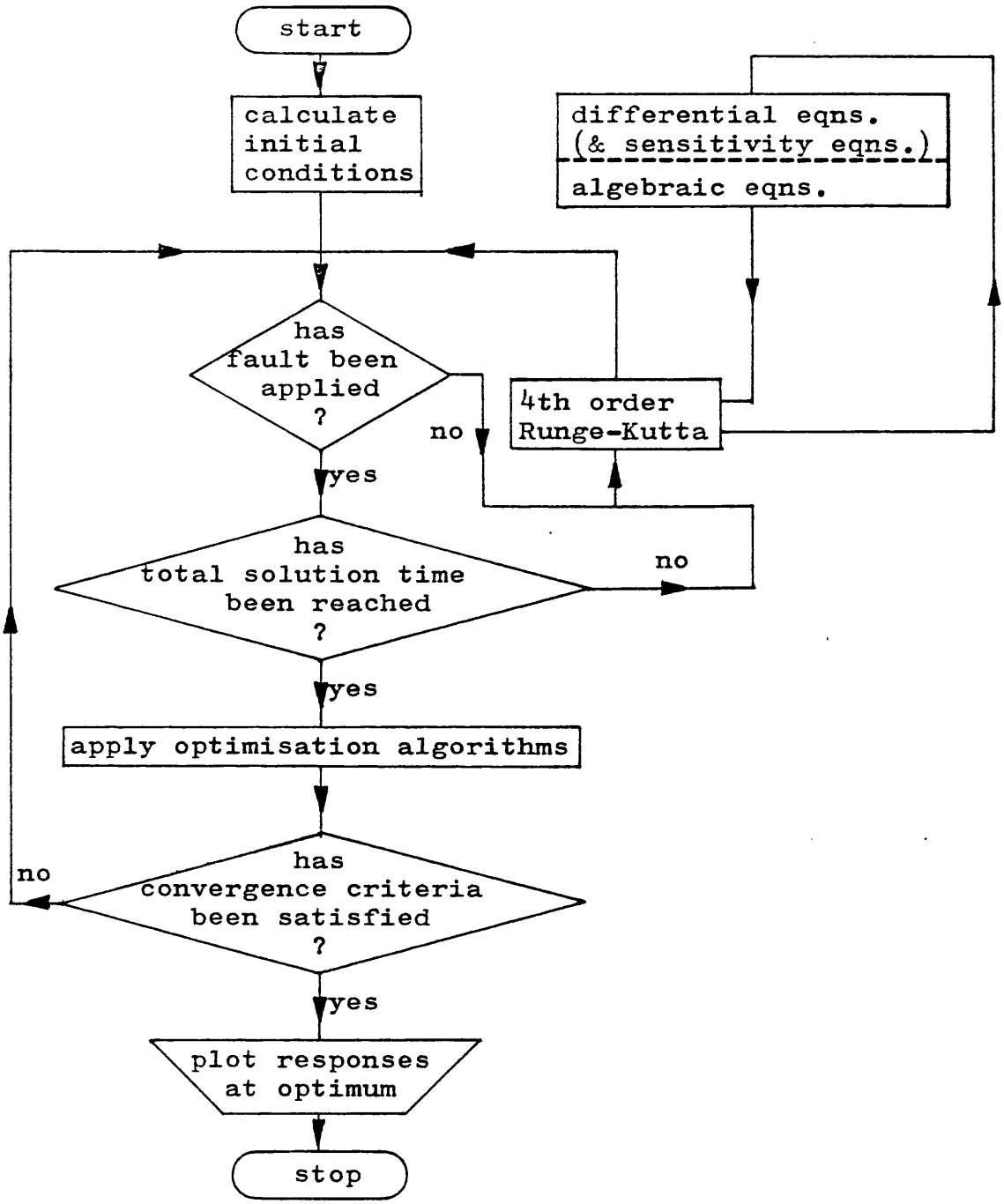

Fig. 2.1 Computer program flow chart

evaluate the auxiliary variables used in the next integration. This continues until the time interval for each required solution is reached. During each integration step, the integrable state and auxiliary variables are evaluated four times. In an attempt to save computational time, the auxiliary calculations were performed outside of the Runge-Kutta routine. However, use of this technique assumes that the values at the end of the n-th step remain constant during the (n+1)th step during which the system differential equations are being solved. Thus the solution of the algebraic equations would always be one step behind that of the differential equations, and a very small step length (in this case , 0.001s) is found to be necessary in order to maintain accuracy. When the method of solving the algebraic and differential equations simultaneously was investigated, a step length of 0.005s resulted in the same order of accuracy and this method of solution has been used. However, in practice, the accurate display of a waveform containing a 50Hz component introduced the need to use a step length of 0.001s in the derivation of transient response curves of the final optimised system.

2.4 The Problem of Numerical Optimisation

2.4.1 Problem Definition

The basic mathematical optimisation problem is to minimize a scalar quantity, known as the performance

index I, which is the value of a function of n system parameters x_1, x_2, ..., x_n. These variables must be adjusted to obtain the minimum required, i.e. to

$$\text{minimize } I = f(x_1, x_2, \ldots, x_n), \tag{2.20}$$

where $(x_1,x_2,\ldots,x_n)$ is denoted by the transpose of the n-vector $\underline{x}$, i.e. $\underline{x}^T = (x_1,x_2,\ldots,x_n)$.

The optimisation problem is formulated here as a minimisation problem. This is not restrictive since almost all problems can be put in this form. In particular, a maximum of a function can be determined by a minimisation method since

$$\text{maximum } f(\underline{x}) = -\text{minimum } [\, -f(\underline{x}) \,] \tag{2.21}$$

The value I of f embodies the design criteria of the system into a single number which is often a measure of the difference between the required performance and the actual performance obtained. The function f is referred to as the objective function whose value is the quantity to be minimised. The co-ordinates of $\underline{x}$ will take successive values as adjustments are made to their values during the optimisation process. Each set of adjustments to these variables is termed an iteration and in general, a number of iterations are required before an optimum is satisfactorily approximated. In the iterative process , a first estimate of the parameter values must be supplied as a starting point for the search for minimum.

2.4.2 Local and Global Minima

The determination of the parameters $\underline{x}_{min}$ which gives a minimum value I_{min} of the objective function f is the object in optimisation. I_{min} is the lowest possible value of I for all combinations of values of the variables $\underline{x}$. A point $\underline{x}_{min}$ which gives this lowest possible value of f is termed a global minimum. In practice, it is very difficult to determine if the minimum obtained by a numerical process is a global minimum or not. In most circumstances, it can only be said that the minimum obtained is a minimum within a local area of search. The point $\underline{x}_{min}$ is therefore termed a local minimum. A particular function may, of course, possess several local minima. One of these will be the global minimum but it is usually impossible to determine if a local minimum is also the global minimum unless all minima are found and evaluated.

2.4.3 Gradients

Some optimisation methods require gradient formulation about the objective function given by $I = f(\underline{x})$. This is obtained in the form of first and second order derivatives of f with respect to the n parameters. The Jacobian vector $\underline{g}$ is defined as the transpose of the gradient vector ∇f which is a row matrix of first order partial derivatives. The transpose of $\underline{g}$ is given by

$$\underline{g}^T = \nabla f = \left(\frac{\partial f}{\partial x_1}, \frac{\partial f}{\partial x_2}, \ldots, \frac{\partial f}{\partial x_n}\right). \qquad (2.22)$$

The nxn symmetric matrix of second order partial derivatives of f is known as the Hessian matrix and is denoted by G where

$$G = \begin{bmatrix} \frac{\partial^2 f}{\partial x_1^2} & \frac{\partial^2 f}{\partial x_1 \partial x_2} & \cdots & \frac{\partial^2 f}{\partial x_1 \partial x_n} \\ \frac{\partial^2 f}{\partial x_2 \partial x_1} & & & \vdots \\ \vdots & & & \\ \frac{\partial^2 f}{\partial x_n \partial x_1} & & & \frac{\partial^2 f}{\partial x_n^2} \end{bmatrix} \qquad (2.23)$$

The availability of the Jacobian vector and the Hessian matrix simplifies optimisation procedures and can sometimes allow solution of problems with a large number of variables. However, it is usually necessary for more general methods of optimisation to proceed without gradient information since derivatives may be uneconomic or impossible to compute, and in some cases may not even exist.

2.4.4 Conditions for a Minimum

A necessary condition for $\underline{x}$ to be an unconstrained minimum is that $\underline{g}(\underline{x}) = \underline{0}$, that is, there is no direction from $\underline{x}$ along which the function value may be decreased. A point $\underline{x}$ where $\underline{g}(\underline{x}) = \underline{0}$ is said to be a stationary point; it may be a minimum, a maximum or a saddle point.

The sufficient condition[42] for a particular stationary

point to be a minimum is that the Hessian matrix must be positive definite, that is, the curvature, or rate of change of the gradient from $\underline{x}$ must be positive. In practice, it may not be possible to confirm this but the majority of methods ensure convergence to a minimum and not a maximum by requiring that the function is reduced at each iteration.

2.4.5 Methods for One-Dimensional Problems

The selection of a lower point along a particular direction, or the linear search, as it is usually called, is usually a one-dimensional minimisation problem. This problem can also occur directly. The method of solution is to calculate the function values at specified points along the direction until the area of the minimum is located and then to fit a low order polynomial over two or three points. If derivatives are available, a cubic may be used, otherwise a quadratic is fitted. Only those coefficients of the polynomial necessary to determine its minimum point are calculated and the objective function is evaluated at this point. If the value is acceptably small, the point is taken as the linear minimum, otherwise it is used as one of the points to fit another polynomial, the worst of the original points being discarded.

2.4.6 Methods for N-Dimensional Problems

There are many ways of choosing the direction for search

in an n-dimensional problem and this choice is fundamental to the success of an algorithm. The earliest methods used the direction of steepest descent,[43] when the gradient could be calculated. Although convergence for this method can be proved, it does not perform well in practice because no account of the curvature of the function is taken in selecting the direction. Early function-only methods concentrated on using the co-ordinate directions alternatively, or on combinations of previous directions. Such methods were rarely able to deal with problems of more than three or four dimensions. A rather different approach was to compare the function values of a pattern of points spanning the space. These methods were generally very slow and often failed to converge. However, the most successful of them, the simplex method[44], where the pattern is a simplex of (n+1) points, is still useful for functions that are subject to inaccuracies.

In the region of a minimum, a function can be resonably approximated by a quadratic and the more recent minimisation algorithms are based on methods which are guranteed to converge in a finite number of steps on a quadratic function. The most straightforward of these is Newton's method. It uses both first and second derivatives to obtain a solution. The minimum of the quadratic is obtained by simply differentiating the general form of the function and equating it to zero to give the required correction to the current point $\underline{x}$. For general functions the correction is applied iteratively, that is,

$$\underline{x}_{k+1} = \underline{x}_k + \underline{p}_k, \qquad (2.24)$$

where $\underline{p}_k$ is the solution to the set of linear equations:

$$G_k \underline{p}_k = -\underline{g}_k, \qquad (2.25)$$

and $\underline{g}_k$ and G_k are the first and second derivatives of f at $\underline{x}_k$. This basic algorithm is usually modified to incorporate a linear search along $\underline{p}_k$ to prevent divergence to a maximum and to use triangular factors of G_k to overcome problems when G_k is singular. A whole class of methods which have the property of guranteed convergence on a quadratic function are the quasi-Newton methods[45]. These attempt to build up an approximation, H, to the inverse of the second derivative matrix without calculating it explicitly. An iteration of a quasi-Newton algorithm is simply to calculate $\underline{p}_k = -H_k \underline{g}_k$ the search direction, carry out a linear search along $\underline{p}_k$ to find λ_k, the approximate distance to the linear minimum, and set $\underline{x}_{k+1} = \underline{x}_k + \lambda_k \underline{p}_k$, and finally to calculate H_{k+1} from H_k and the changes made in $\underline{x}_k$ and $\underline{g}_k$. H_k is stored and updated as triangular factors to prevent conditioning problems. The different methods in the class employ different formulae in updating H_k. They all have the important property that on a quadratic function after n iterations have been applied, the approximation to the inverse of the Hessian is exact, i.e. $H_n = G^{-1}$. On general functions, after n iterations, H_n gives a fair

indication of the curvature so that subsequent progress is fast.

The directions that are generated by a quasi-Newton method have a property known as conjugacy. Conjugate directions[42] are important because it is possible to prove that, for a quadratic function, exact linear searches along a set of conjugate directions will locate the minimum of the function in the space spanned by these directions. Another class of methods that generate conjugate directions are the conjugate gradient methods[46]. The advantage of this type of method is that it requires less storage to calculate $\underline{p}_k$. The disadvantage is that after n iterations, the elements of the direction vector will be very small so that the method has to be restarted and convergence is consequently slower than the quasi-Newton methods. It is also possible to derive methods that generate conjugate directions without explicitly using gradient information. At present[47], however, algorithms for these methods do not perform as well as algorithms based on the above methods.

2.4.7 Approximating Derivatives by Differences

All of the methods discussed in the previous section (apart from Simplex) assume that some derivative information is available and it may not always be possible to provide this analytically. In such cases, numerical approximations to the derivatives can be made, based on

difference formulae. In optimisation algorithms , it is usual to use a simple, forward difference formula, for example,

$$g_j(\underline{x}) = \left(\frac{\partial f}{\partial x_j}\right)_{\underline{x}} \simeq \frac{f(\underline{x} + \delta_j \underline{e}_j) - f(\underline{x})}{\delta_j} \qquad (2.26)$$

where $\underline{e}_j$ is the jth co-ordinate direction and δ_j is a small interval for differencing. The cost of calculating g is thus n extra function evaluations.

2.5 Optimisation of System Performance

The optimal controls produced for nonlinear dynamic systems using optimal control theory are, in general, some form of open-loop controls. These controls can only be applied to systems with fixed parameters and operating conditions, and subject to the same disturbance. This form of control is not desirable for the control of turbogenerator sets in power systems.

It is well known that for a linear, time-invariant system with a quadratic performance index, the optimal control is a linear combination of all the states. This appears logical and appropriate because feedback of all the states means feedback of information that completely specifies the system. It is logical, therefore, to assume that the optimal control of a nonlinear system is also some function of all the states of the system, and that a suboptimal control could be achieved by linear feedback of all or

some of the states of the nonlinear system. With this assumption, the performance of the system can be achieved by choosing a set of optimum feedback gains. This approach converts the suboptimal control problem into a parameter optimisation problem.

The above parameter optimisation problem is formulated as a function minimisation problem as follows. Given a dynamic system described by the vector equation

$$\dot{\underline{x}} = f(\underline{x},\underline{p},t) \qquad \underline{x}(t_o) = \underline{x}_o, \qquad (2.27)$$

where $\underline{x}$ is the state n-vector and $\underline{p}$ is the vector of optimising parameters, choose $\underline{p}$ (or $\underline{p}(t)$, if $\underline{p}$ is time-variant over the interval $0 \leq t \leq t_f$) so that an objective function is minimised.

Many function minimisation methods have been developed over the years and the Gradient Methods are among the most powerful ones to date. Basically, all these methods try to locate the minimum of the objective function by performing a series of searches in the function space. The direction of search is determined using the first partial derivatives of the objective function with respect to the optimising parameters. In general, these sensitivity functions are functions of the state sensitivity functions, and they can be evaluated by solving the system sensitivity equations. The single variable optimisation by quadratic and cubic approximations are due to Powell[48] and Davidson[49] respectively while the multi-variable function minimisation subroutine

adopted is the Fortran version of the original Algol procedure based on the quasi-Newton method of Gill, Murray and Pitfield[50].

2.6 Signal-Flow Graphs

2.6.1 Introduction

A signal-flow graph is defined as an oriented linear graph on which vertices represent variables and line segments represent certain specific relationships between the vertex variables.

In one sense, a signal-flow graph is the dual representation to a block diagram, since the roles played by vertex and line segment are interchanged. There is one extremely important difference between them however, in that, on a block diagram, every kind of relationship is explicitly represented by a vertex, while on a signal-flow graph, the relationships of summation and identity are implicit in the diagram by definition. For this reason, the block diagram form of representation is more flexible and general. On the other hand, signal-flow graphs are neater and, for linear systems, are associated with a much more powerful set of manipulation and reduction rules. While it is important to realize that the use of signal-flow graphs is in no way prohibited for nonlinear systems, their greatest utility stems from the powerful reduction techniques available for linear systems. With the aid of this powerful tool, clearer

insights into the single-machine complex system are made possible. The basic signal-flow graph conventions and manipulations will now be briefly described[54].

2.6.2 Signal-Flow Graph Conventions

The line segments of a signal-flow graph represent coefficients or operators if dealing with relationships between Laplace transforms. The coefficients associated with line segments are called transmittances. The vertices of a signal-flow graph represent variables.

A vertex variable is equal to the summation of all terms associated with oriented line segments which are incident on it. For example, in the signal-flow graph of Fig. 2.2,

$$x_4 = ax_1 + bx_2 + cx_3 + dx_4 \qquad (2.28)$$

The line segment, d, originating from and incident upon vertex x_4 in Fig. 2.2 is called a self circuit or self loop.

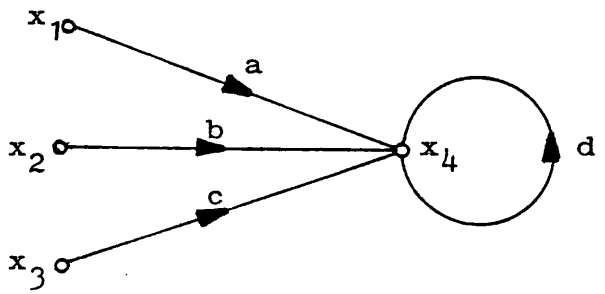

Fig. 2.2

In a signal-flow graph as shown in Fig. 2.3, the identity convention is such that

$$x_2 = ax_1 \quad x_3 = bx_1 \quad x_4 = cx_1 \tag{2.29}$$

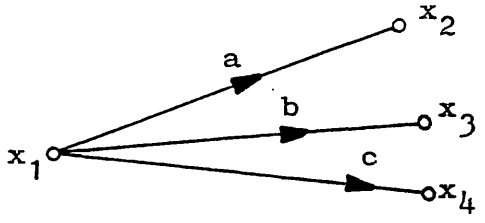

Fig. 2.3

A signal-flow graph may now be used to represent a set of linear equations. For example, the signal-flow graph of Fig. 2.4 represents the set of equations

$$\begin{aligned} x_1 &= a_{11}x_1 + a_{12}x_2 + c_1 \\ x_2 &= a_{21}x_1 + a_{22}x_2 + c_2 \end{aligned} \tag{2.30}$$

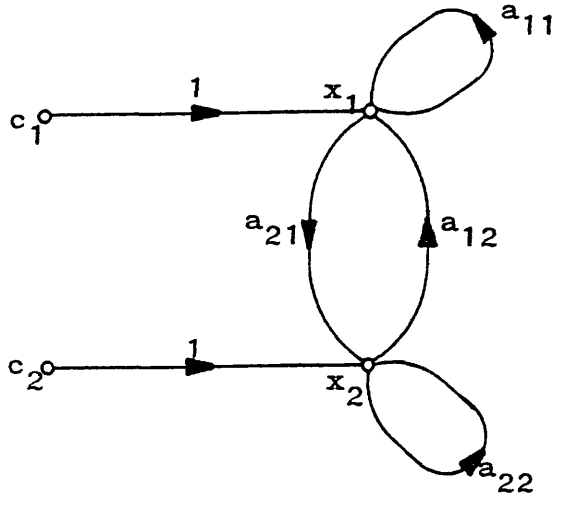

Fig. 2.4

2.6.3 Signal-Flow Graph Manipulations

Certain simple rules for the manipulation of signal-flow graphs follow directly from the previously stated definition and conventions. Consider the simple cascade arrangement of Fig. 2.5a, where

$$x_2 = a_1 x_1,\ x_3 = a_2 x_2,\ \ldots,\ x_{n+1} = a_n x_n,$$

$$\text{so that } x_{n+1} = \prod_{i=1}^{n} a_i x_1. \qquad (2.31)$$

Thus the cascade of line segments in Fig. 2.5a may be replaced by the simple equivalent line segment of Fig.2.5b.

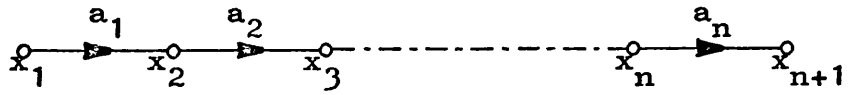

Fig. 2.5a

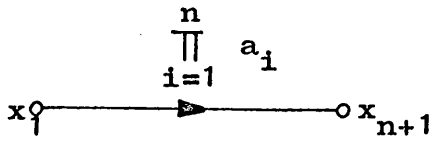

Fig. 2.5b

Consider the simple parallel arrangement of Fig. 2.6a. The relationship between x_2 and x_1 is represented by

$$x_2 = a_1x_1 + a_2x_1 + \ldots + a_nx_1$$

$$= \sum_{i=1}^{n} a_ix_1, \qquad (2.32)$$

and thus the parallel arrangement of line segments of Fig. 2.6a may be replaced by the single equivalent line segment of Fig. 2.6b.

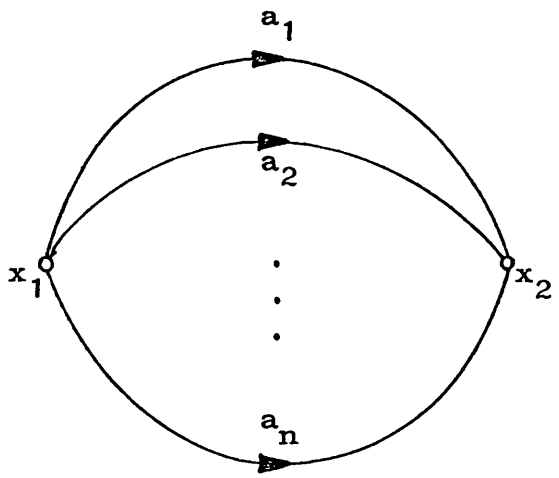

Fig. 2.6a

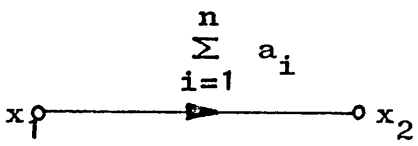

Fig. 2.6b

A rule commonly used to remove a self circuit from a vertex can be quite valuable. This rule requires that when the self circuit is removed from the vertex, all transmittances incident on that vertex are replaced by their original value divided by one minus the value of the transmittance of the self circuit removed. Application of this rule to the original flow graph of Fig. 2.4 to remove the self circuit on the vertex x_1 produces the signal-flow graph of Fig. 2.7.

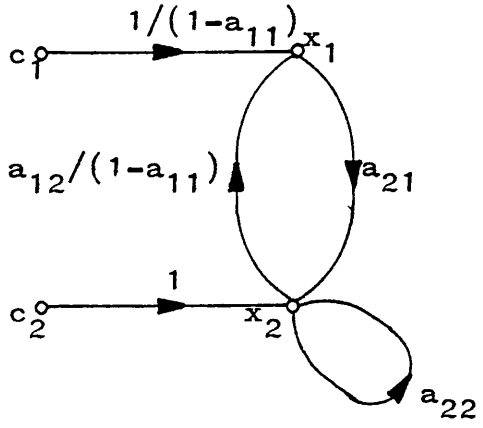

Fig. 2.7

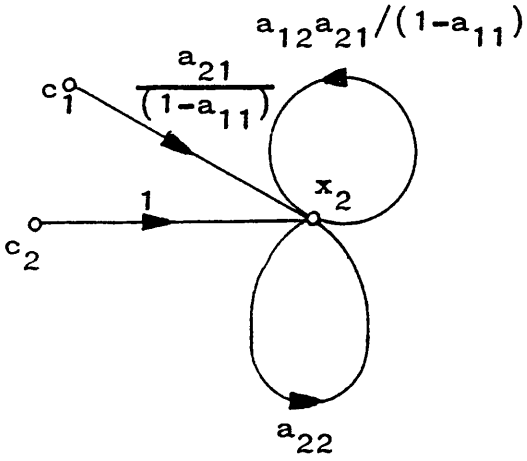

Fig. 2.8

An intermediate vertex can be removed by replacing each path between any vertices passing through that vertex to be removed by direct paths whose transmittances are the product transmittances of the line segments removed. When this rule is applied to the signal-flow graph of Fig. 2.7 to remove the vertex x_1, the resulting graph is shown in Fig. 2.8.

2.7 Bode Techniques

2.7.1 General

A number of methods are available for describing the frequency response of a circuit. One of these is the Bode diagram, named after Hendrik Bode, a Bell System research engineer, who developed the techniques. A brief summary[51] of the techniques used is described in this section.

Rapid sketching of amplitude diagrams from factorised rational transfer function is possible by making use of asymptotic approximations. For example, given a transfer function G(s) of the form

$$G(s) = \frac{K(s+a)(s+b)}{s^n(s+c)(s+d)}, \qquad (2.33)$$

the asymptotic approximation at any frequency w is given by writing (s+1) as 1 if w<1 or as w if w>1. If all poles and zeros are in the left-hand plane, the asymptotic phase shift is 90r degrees(lagging) if the amplitude approximation is K/w^r. For example, with a transfer function G(s) of the form

$$G(s) = \frac{12(s+1)}{s(s+2)(s+4)},$$

has an approximate value at w=2.5,of

$$|G(jw)| = \frac{12w}{w(w)(4)} = \frac{3}{w},$$

and can be represented by a line of slope=-1 passing through the point 3 when w=1.

2.7.2 Resonance and Quadratic Factors

The phenomena of 'resonance' is associated with systems having a quadratic factor in either the numerator or the denominator of their transfer functions. If the zeros or poles corresponding to these quadratic terms lie close to the jw axis (corresponding to a small damping ratio ζ), the frequency response of the system undergoes a pronounced dip or null in the vicinity of the zeros and a pronounced peak in the vicinity of the poles. Such systems can be referred to as resonant systems and the frequencies in the vicinity of the peaks or nulls are known as resonant frequencies. A term usually used to describe such systems is the quality factor Q, and can be defined as

$$Q = 1/2\zeta. \qquad (2.34)$$

A quadratic factor (s^2+bs+a) can be approximated to a value of a for any frequency $w>\sqrt{a}$ and to a value of w^2 for any frequency $w<\sqrt{a}$. The tangent at $w=\sqrt{a}$ is obtained by writing the factor as bw, provided that there are no other real system poles or zeros close to the quadratic form. As an example, consider a transfer function $G(s)$ of the form

$$G(s) = \frac{8(s+1)}{s^2+2s+16}$$

such that

$$|G(jw)| = 8w/16 \qquad \text{for } 1 \leq w < 4,$$

and $$|G(jw)| = 8w/w^2 \qquad \text{for } w > 4.$$

At w=4, the tangent is approximately 8w/2w and the corresponding log-log plot is sketched in Fig. 2.9. Thus from Fig. 2.9, the system has a resonant gain Q=2, with ζ, the damping ratio, equal to 0.25.

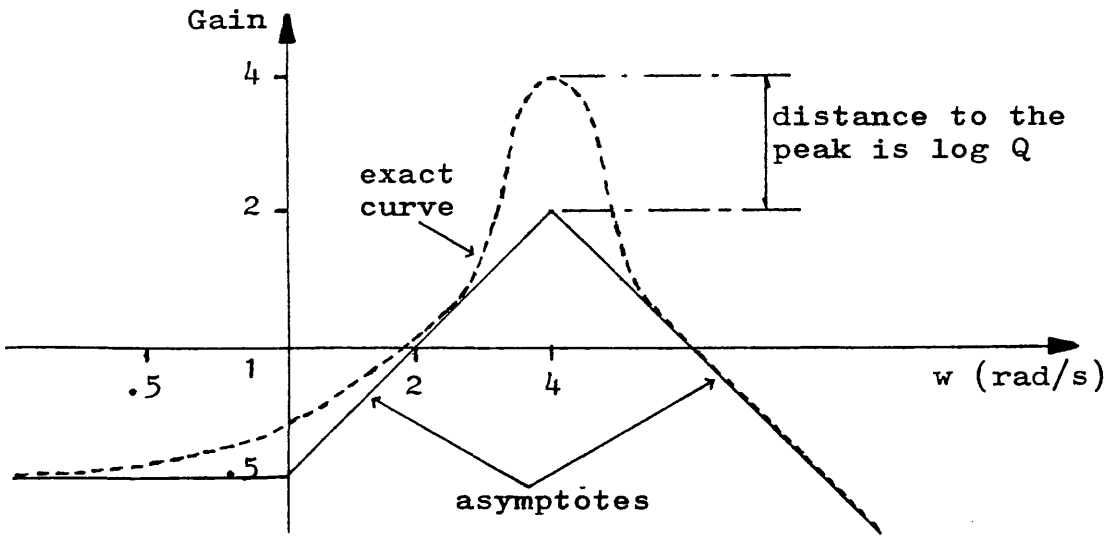

Fig. 2.9

2.7.3 Closed-loop Transfer Function

A simplified form of a closed-loop negative feedback system is shown in Fig. 2.10, where r is the reference signal, e is the actuating error signal, u is the control signal, y is the system output, C represents the controller to be introduced, G represents the plant to be controlled and H represents the feedback system to be introduced.

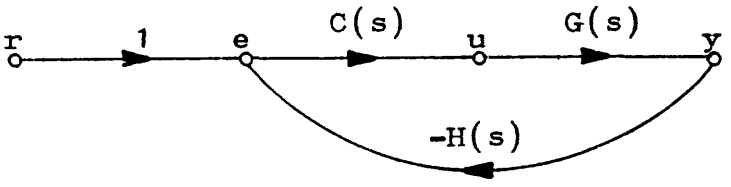

Fig. 2.10

The corresponding closed-loop transmittance T(s) of the system defined by Fig. 2.10 is given by

$$T(s) = \frac{y(s)}{r(s)} = \frac{CG(s)}{1+CGH(s)}. \qquad (2.35)$$

When CGH(s) is replaced by L(s), the loop gain function, eqn. 2.35 becomes

$$T(s) = \frac{1}{H(s)} \frac{1}{1+1/L(s)},$$

or, in terms of the frequency domain,

$$T(jw) = \frac{1}{H(jw)} \frac{1}{1+1/L(jw)}. \qquad (2.36)$$

If in eqn. 2.36 $|L(jw)| >> 1$, then $|T(jw)| \simeq |1/H(jw)|$. If, however, in eqn. 2.36 $|L(jw)| << 1$, then $|T(jw)| \simeq |CG(jw)|$. The corresponding Bode diagram can be illustrated as shown in Fig. 2.12b with A(jw) corresponds to CG(jw) and B(jw) represents H(jw). By definition, at the gain crossover, $w=w_c$, the break frequency, and $|L(jw_c)|$ =unity. The phase margin is $\pi - \angle L(jw_c)$ and

$$|T(jw_c)| = |CG(jw_c)| \; 2 \cos\left(\frac{\angle L(jw_c)}{2}\right)$$

It is then to plot CG(jw) and 1/H(jw) on the same axes, such that the spacing between them represents L(jw) and the lower envelope of the amplitude plot represents $|T(jw)|$.

2.7.4 Simple Approximations

Consider two parallel transfer functions A(s) and B(s) of Fig. 2.11a with their corresponding Bode diagram as sketched in Fig. 2.11b.

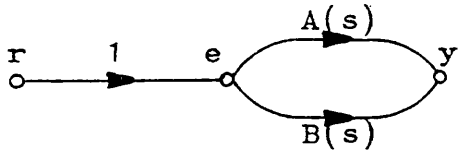

Fig. 2.11a

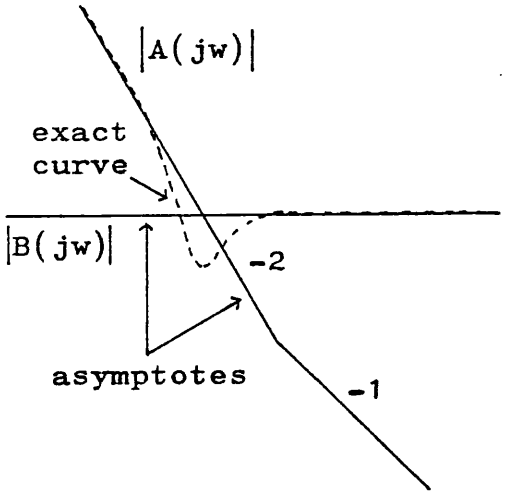

Fig. 2.11b

The transmittance T(jw) of the system is given by

$$T(jw) = \frac{y(jw)}{r(jw)} = A(jw) + B(jw). \qquad (2.37)$$

If in eqn. 2.37 $|A(jw)| \gg |B(jw)|$, then $T(jw) \simeq A(jw)$, and if $|A(jw)| \ll |B(jw)|$, then $T(jw) \simeq B(jw)$. At the gain crossover, $|A(jw_c)| = |B(jw_c)|$ such that

$$|T(jw_c)| = |A(jw_c)|\ 2\cos\left(\frac{\angle A(jw_c) - \angle B(jw_c)}{2}\right),$$

and

$$\angle T(jw_c) = \frac{\angle A(jw_c) + \angle B(jw_c)}{2}$$

If, however, the transmittance paths of the transfer functions A(s) and B(s) are such that as indicated in Fig. 2.12a, their corresponding Bode diagram will be as given in Fig. 2.12b.

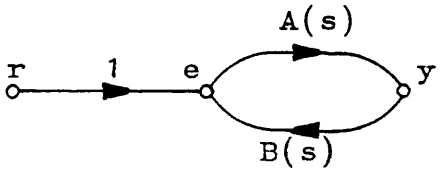

Fig. 2.12a

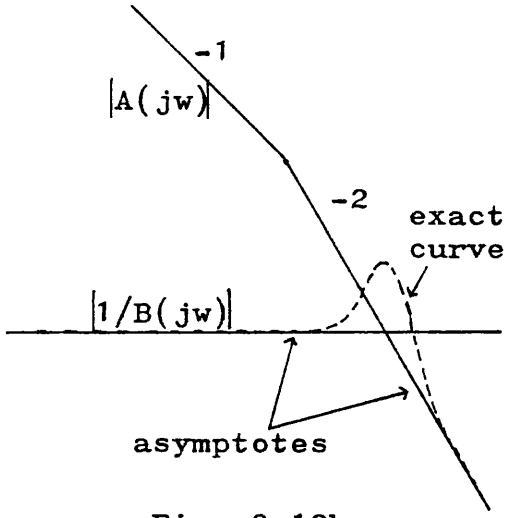

Fig. 2.12b

The transmittance T(jw) of the system is then given by

$$T(jw) = \frac{A(jw)}{1 + AB(jw)} = A(jw) \,//\, 1/B(jw) \qquad (2.38)$$

If in eqn. 2.38 $|A(jw)| \gg |1/B(jw)|$, then $T(jw) \simeq 1/B(jw)$; and if $|A(jw)| \ll |1/B(jw)|$, then $T(jw) \simeq A(jw)$. At the gain crossover, $|A(jw_c)| = |1/B(jw_c)|$, such that

$$|T(jw_c)| = \frac{|A(jw_c)|}{2\cos\left(\frac{\angle A(jw_c) - \angle B(jw_c)}{2}\right)},$$

and

$$\angle T(jw_c) = \frac{\angle A(jw_c) + \angle B(jw_c)}{2}.$$

2.7.5 Compensation

Since a loop-gain slope of -2 corresponds to an asymptotic phase lag of at least 180°, the aim of a designer must be to arrange that the $|CG(jw)|$ and $|1/H(jw)|$ curves cross with a slope between 0 and -2, while maintaining all the specification objectives as far as possible. This is done by variations of gain or the addition of poles or zeros into the controller transfer function C(s), or the feedback transfer function H(s) of Fig. 2.10.

The general methods of the application of Bode techniques to the design of closed-loop control systems are well established[53] and only the particular application to the design of an excitation system of a turbogenerator has been described in any detail.

CHAPTER 3 FORMULATION OF THE SUBOPTIMAL CONTROL PROBLEM

3.1 System Studied

The system under study consists of a single turbogenerator connected through a transformer and a double circuit transmission network to an infinite busbar in the general manner described by the schematic diagram of Fig. 3.1.

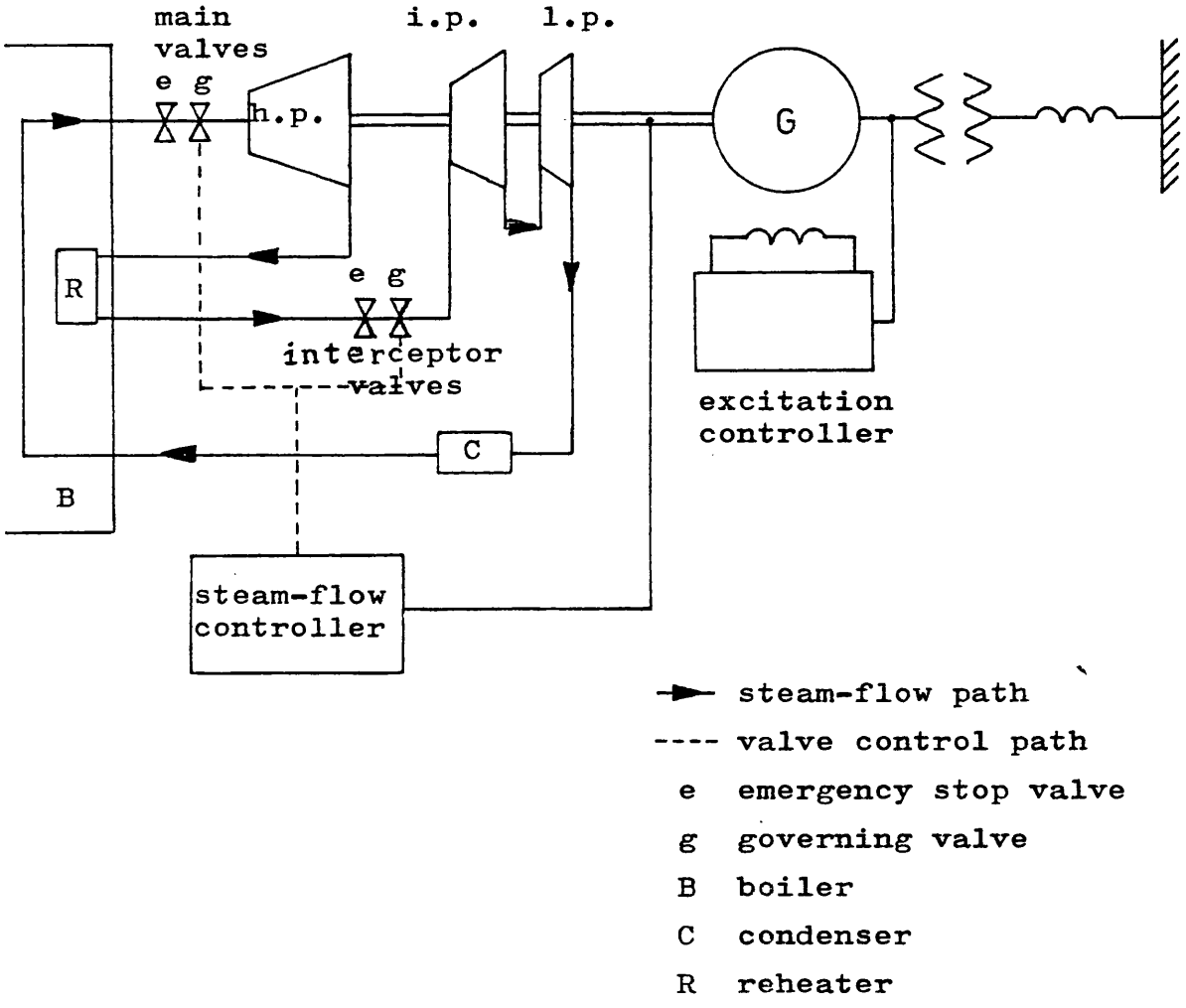

Fig. 3.1 General system arrangement

The relevant machine and system data is based on the Pembroke power station in South Wales and is given in Appendix A2. The fault condition is assumed to be a symmetric 3-phase short circuit at the high-voltage terminals of the generator transformer with the prefault impedance equal to the postfault impedance. Fault durations of 0.22s and 0.14s have been considered in this study. Initially, the machine is assumed to be delivering 0.85p.u. power with unity power factor at the busbar with the terminal voltage set at 1.0p.u.

3.2 Synchronous Machine Representation

The model used to simulate the generator is based on a set of two-axis equations for an idealised synchronous machine, which are obtained by applying an axis transformation to the original 3-phase equations. This transformation, known as Park's transformation[55-60], resolves the stator quantities into components along the pole and interpole axes, known as the direct and quadrature axes repectively and a component relating to the zero-sequence effects. The latter will not be represented in the ensuing analysis because the operations considered do not involve zero-sequence quantities. The current paths in the rotor iron and in the damper windings are represented by one additional closed winding in the rotor on each axis. The idealised machine is subject to the following assumptions[60]. Firstly, a

current in any winding is assumed to set up a m.m.f. wave which is sinusoidally distributed in space around the air gap. Secondly, the effects of hysteresis may be neglected. Finally, a component of m.m.f. acting along the direct axis is assumed to produce a sinusoidally distributed flux wave in the direct axis only and a quadrature axis m.m.f. produces a sinusoidally distributed flux wave in the quadrature axis only.

The direct- and quadrature-axis flux linkage and voltage equations for the generator can be derived from the schematic layout of the 3-phase windings shown in Fig. 3.2. The algebraic signs correspond to generator action.

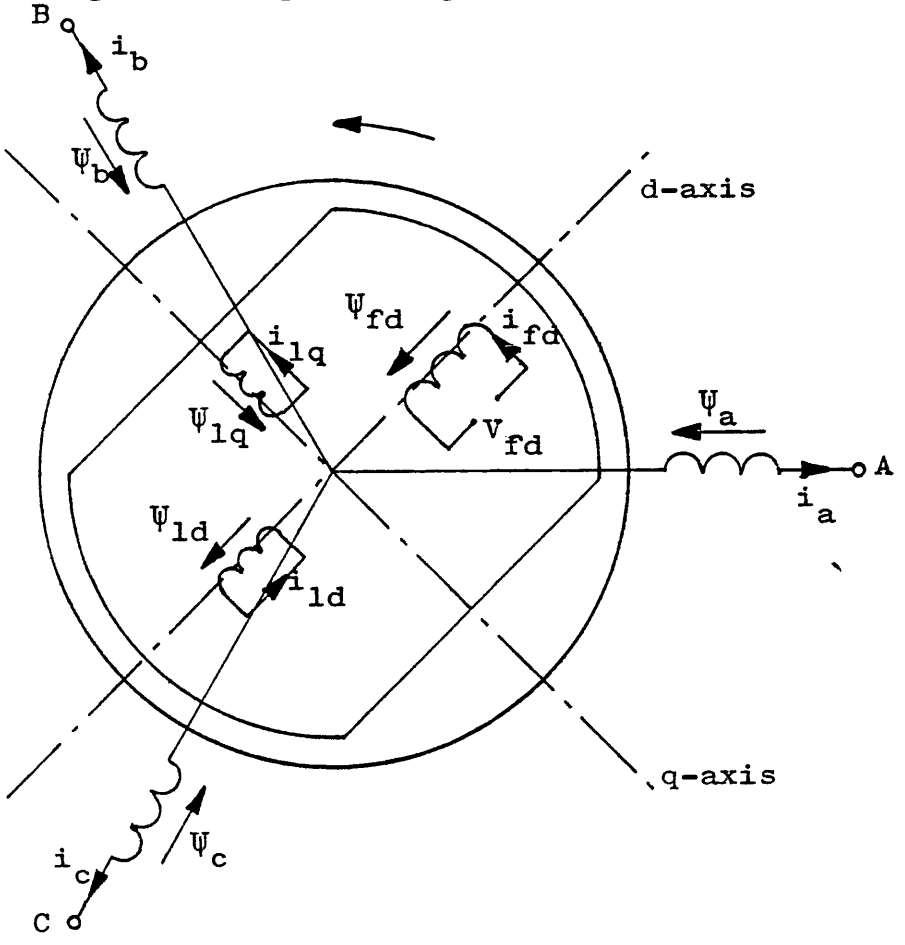

Fig. 3.2 Schematic arrangement of generator windings

The following sets of equations are all in per unit form with the flux linkage equations given by

$$\Psi_{fd} = x_{ffd}i_{fd} - x_{ad}i_d + x_{ad}i_{1d} \tag{3.1}$$

$$\Psi_d = x_{ad}i_{fd} - x_d i_d + x_{ad}i_{1d} \tag{3.2}$$

$$\Psi_{1d} = x_{ad}i_{fd} - x_{ad}i_d + x_{11d}i_{1d} \tag{3.3}$$

$$\Psi_q = -x_q i_q + x_{aq}i_q \tag{3.4}$$

$$\Psi_{1q} = -x_{aq}i_q + x_{11q}i_{1q} \tag{3.5}$$

The corresponding voltage equations take the form

$$V_{fd} = p\Psi_{fd}/w_o + r_{fd}i_{fd} \tag{3.6}$$

$$v_d = p\Psi_d/w_o - w\Psi_q/w_o - r_a i_d \tag{3.7}$$

$$0 = p\Psi_{1d}/w_o + r_{1d}i_{1d} \tag{3.8}$$

$$v_q = p\Psi_q/w_o + w\Psi_d/w_o - r_a i_q \tag{3.9}$$

$$0 = p\Psi_{1q}/w_o + r_{1q}i_{1q} \tag{3.10}$$

$$V_t = \sqrt{(v_d^2 + v_q^2)} \tag{3.11}$$

The equations for the air gap torque and the motion of the rotor are

$$T_e = \Psi_d i_q - \Psi_q i_d \tag{3.12}$$

and

$$Mp^2\delta = T_m - T_e - K_d p\delta/w_o \tag{3.13}$$

respectively. Saturation in the machine may be modelled

by taking the machine reactances as a function of the conditions of magnetisation in the iron circuits of the machine[59]. However, it has been shown[61] that saturation has little effect on the transient stability of the machine. Saturation effects are therefore neglected in this investigation. The damping coefficient K_d in the swing equation is assumed to be constant. Although a value for K_d can be estimated[62,63], there is some uncertainty as to the best value of K_d to be used because of a lack of reliable values for some machine parameters and because of the presence of turbine damping.

The above seventh order model takes account of the decay of the stator flux linkages which gives rise to power frequency oscillations in the machine axis voltages and currents. It also accounts for the initial braking torque which is responsible for the rotor back swing observed in site tests[29]. The drawback of this model is that state variables, which are required as feedback signals, are not readily measurable. These equations can be combined into operational forms by eliminating the rotor currents, and through some algebraic manipulations, the following equations are obtained[64]:

$$pe_d'' = ((x_q - x_q'')i_q - e_d'')/T_{qo}'' \qquad (3.14)$$

$$pe_q' = (V_f - (x_d - x_d'')i_d - e_q'')/T_{do}' \qquad (3.15)$$

$$pe_q'' = (e_q' - (x_d' - x_d'')i_d + e_q'' - (T_1(e_q'' - x_d''i_d) + T_2x_di_d - T_{kd}V_f)/T_{do}')/T_{do}'' \qquad (3.16)$$

$$v_d = p(e_q"-x_d"i_d)/w_o + w(e_d"+x_q"i_q)/w_o - r_a i_d \quad (3.17)$$

$$v_q = p(-e_d"-x_q"i_q)/w_o + w(e_q"-x_d"i_d)/w_o - r_a i_q \quad (3.18)$$

By neglecting the decay of stator linkages, the speed variation and the less significant terms, the fifth order machine model is obtained in the form:

$$pe_d" = ((x_q-x_q")i_q - e_d")/T_{qo}" \quad (3.19)$$

$$pe_q' = (V_f - (x_d-x_d')i_d - e_q')/T_{do}' \quad (3.20)$$

$$pe_q" = (e_q' - (x_d'-x_d")i_d - e_q")/T_{do}" \quad (3.21)$$

$$e_d" = v_d + r_a i_d - x_q"i_q \quad (3.22)$$

$$e_q" = v_q + r_a i_q + x_d"i_d \quad (3.23)$$

$$T_e = e_d"i_d + e_q"i_q - (x_d"-x_q")i_d i_q \quad (3.24)$$

The fifth order machine model can be further simplified into the third order machine model by neglecting the effects of the damper windings as:

$$pe_q' = (V_f - (x_d-x_d')i_d - e_q')/T_{do}' \quad (3.25)$$

$$0 = v_d + r_a i_d - x_q i_q \quad (3.26)$$

$$e_q' = v_q + r_a i_q + x_d'i_d \quad (3.27)$$

$$T_e = e_q'i_q - (x_d'-x_q)i_d i_q \quad (3.28)$$

The seventh order model has been used in all the optimisation and sensitivity studies while the third order model is the basis for Bode design.

3.3 Transmission System

The equations for the transmission system between the generator terminals and the infinite busbar are formulated with the assumption that the transformer magnetising and line charging currents can be neglected. The transformer and the transmission line are represented by lumped series inductance and resistance. By applying Park's transformation to the 3-phase equations for the transmission system, the following equations in the d-q axes of the generator are obtained:

$$v_d = V_b \sin\delta + X_t p i_d/w_o + R_t i_d - w X_t i_q/w_o \qquad (3.29)$$

$$v_q = V_b \cos\delta + X_t p i_q/w_o + R_t i_q + w X_t i_d/w_o \qquad (3.30)$$

3.4 Excitation System

Three types of excitation systems are in common use today[65], namely, the a.c. exciter with static rectifier, the rotating a.c. exciter with rotating rectifier(Brush-less exciter) and the static thyristor exciter. The main structural difference between a.c. exciters and thyristor exciters is the power amplification element. The power amplification element of a thyristor exciter is a thyristor converter while that of an a.c. exciter is an a.c. generator. The thyristor converter is basically an inertialess system and the speed of response is very fast compared with the a.c. exciter. Another major operational

difference between them is the control of the output voltage. While 4-quadrant operation is possible for the thyristor, voltage reversal is not possible in the a.c. exciters because of the presence of uncontrolled rectifiers.

The basic structure of an excitation system with an a.c. exciter is shown schematically in Fig. 3.3.

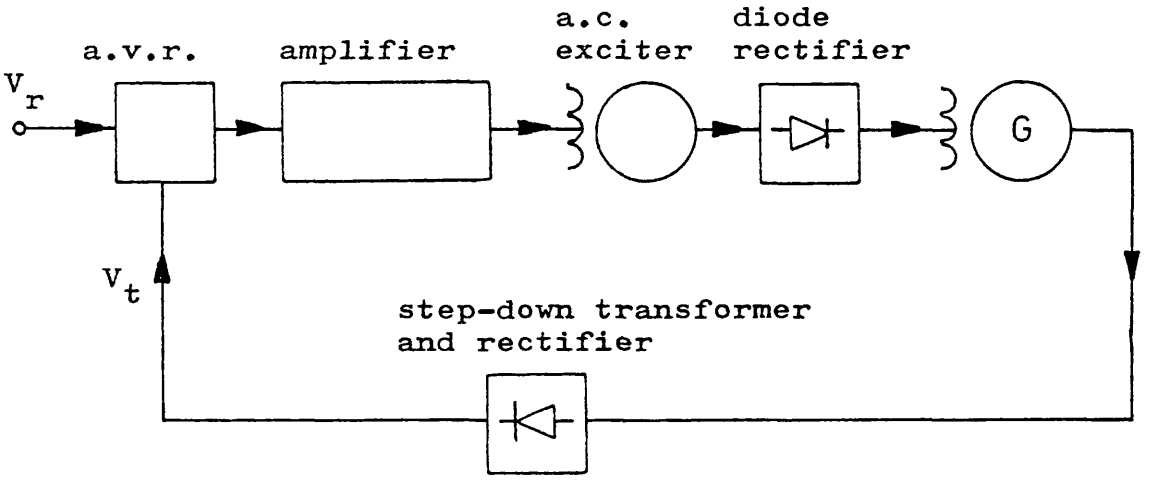

Fig. 3.3 Excitation system with a.c. exciter

The machine terminal voltage is derived from the machine terminals through a step-down transformer and rectifier. The control signal produced by the automatic voltage regulator(a.v.r.) is amplified, either by cascade magnetic amplifiers as in earlier designs, or by a thyristor amplifier. The amplified control signal feeds the field winding of the a.c. exciter, where output is restricted by diode rectifiers to supply the excitation to the turbo-generator. Two types of rectifiers are commonly used, namely, static and rotating diode rectifiers. The latter is also called a brushless exciter because both the

exciter armature and the diode rectifier of such exciters are housed on the generator shaft, thus dispensing with slip rings and brushes.

The basic structure of a thyristor excitation system is illustrated in Fig. 3.4.

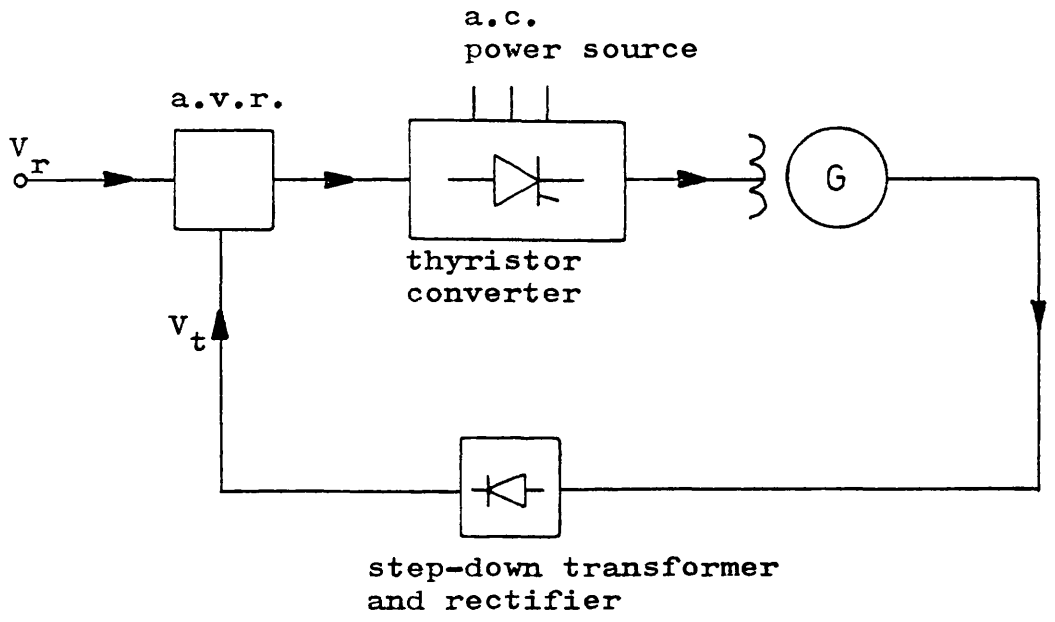

Fig. 3.4 Excitation system with thyristor exciter

The control signal produced by the a.v.r. is used to control the thyristor converter which supplies the excitation for the turbogenerator. Power input to the thyristor converter can be obtained either from the generator terminals or from a separate source such as an a.c. exciter mounted on the generator shaft. The latter arrangement is usually preferred because full field forcing would still be possible under fault conditions when the generator terminal voltage collapses. A new arrangement still under development is the rotating

thyristor exciter in which the thyristor converter and the armature of the exciter are housed on the generator shaft, thus forming a brushless thyristor exciter.

The excitation system in the present investigation is assumed to be capable of reversal of field voltage with an extra feedback signal V_i available at the input summing junction as shown in Fig. 3.5.

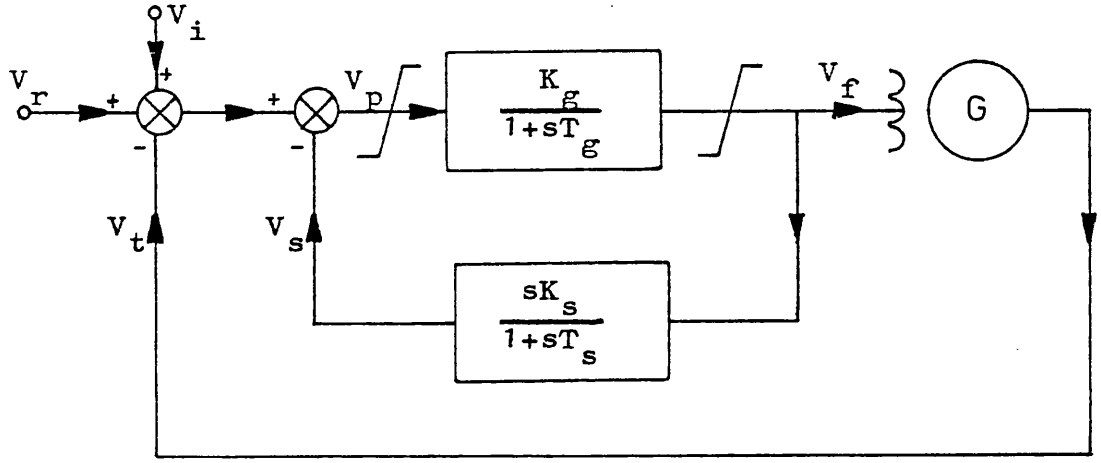

Fig. 3.5 Generalised excitation system

The modelling of the excitation system is based on the assumption[60] that the parameters of the excitation system remain unaltered throughout any transient change. Further, the characteristics of the rectifiers and thyristor converters are assumed to be linear, and saturation in the excitation system is represented by limits on the output voltages. The effect is such that as soon as V_f is limited to its limiting value VFMAX, V_p will be clamped down immediately to a value of VPMAX/K_g. Finally, the reactive-power limit control is neglected. The block diagram representation as shown in Fig. 3.5 may

represent systems with thyristor exciters or a.c. exciters depending on the values used for the various time constants in the model. The regulator time constant T_g of excitation systems with thyristor exciters will be much smaller than that of systems with a.c. exciters. The forward transfer function represents the main regulator and exciter and the feedback transfer function represents the stabilising derivative feedback which is required if high regulator gain is used to achieve satisfactory steady-state voltage regulation. Again, the time lags introduced by the transducers are neglected.

3.5 Governor System and Turbine

Mechanical Watt-type governors with fixed droop characteristics have operated reliably on turbogenerators since the invention of the steam turbine. In due course, the problems of dead band in the control problem became appreciated and were largely solved by forms of electrical speed measurement. Later, increased torque-to-inertia ratios for large machines necessitated an improved valve response, which led towards the adoption of high pressure electro-hydraulic control for the steam valve. Probably the most significant advance, however, lay in the scope and flexibility of control engendered by a basically electrical approach which enhances the control capabilities far beyond the concept of simple speed regulation. Thus the electro-hydraulic governor in its current form incorporates the capability for interfacing with computer

or other overall automatic control schemes.

Functionally, an eletric governor is the same as a conventional mechanical governor with the speed transducer and signal transmission system replaced by their electrical equivalents. The main hydraulic power amplifier which activates the steam-flow control valves remains the same. By using electrical transmission of signals, the dead bands caused by mechanical linkages in the mechanical transmission system can be eliminated and the electrical speed-error signal can readily be mixed with other subsidiary control signals to achieve optimal or suboptimal control. Furthermore, variable droop setting can be achieved by variation of the speed transducer gain.

Various forms of speed transducers can be used. The most direct approach is to use a d.c. tachogenerator coupled to the turbine shaft, which generates a voltage proportional to speed. Another approach is to derive a frequency modulated signal(1 to 10 KHz are typical) which is then processed by a frequency sensitive circuit to produce the speed error signal. The modulated signal may be derived using a magnetic toothed wheel or a light emitting element mounted on the shaft and a stationary transducer which detects the movement of the rotating elements.

The detailed representation of the electro-hydraulic governing system is fairly complex. However, test results[66] showed that the overall response of the valve position control loop is relatively simple in form once

the system has been satisfactorily stabilised. A relatively simple model which still represents the pertinent characteristics of the system is adopted. The assumptions made to simplify the model are as follows. Firstly, the time lags of the signal transducers are neglected, since they are small comparing with time constants of the rest of the system. Secondly, the steam flow is taken to be a linear function of the control signal over the whole range of operating conditions. Finally, the valve opening and closing speeds are assumed to be the same. With these assumptions, the governor system may be represented by a single time-lag transfer function:

$$\frac{y}{u} = \frac{1}{1 + sT_1} \qquad (3.31)$$

where u is the control signal and y is the valve opening.

The turbine considered is a modern three-stage reheat turbine as shown in Fig. 3.1. High pressure steam from the boiler is fed through two sets of main steam valves into the high-pressure(h.p.) cylinder. The first set of valves are the emergency stop valves which are normally fully open and close only under emergency conditions such as total loss of load or excessive overspeed. The second set is the main governing valves which are continuously controlled. Thermal-mechanical energy conversion takes place in the h.p. cylinder, which accounts for about a quarter of the total mechanical output of the turbine in steady state. The exhaust steam from the h.p. cylinder is fed back to the boiler into the reheater where more

thermal energy is added to the steam. It is then piped through a set of emergency stop valves and a set of interceptor valves into the intermediate pressure(i.p.) and low pressure(l.p.) cylinders where the energy conversion is completed. The steam is condensed in the condenser and fed back into the boiler as feed water, thus completing the heat cycle.

The steam-flow dynamics in the turbine system is very complex and a fairly detailed representation of the nonlinear system flow dynamics gives rise to an objectionally complicated model. However, test results[66] showed that the overall response of the system is relatively simple in form. A simple representation which adequately represents the overall relationship between the governor valve motion and turbine power output is sought. The following first order transfer function is adopted:

$$\frac{T_m}{y} = \frac{1}{1 + sT_2} \qquad (3.32)$$

where T_m is the turbine power output and y is the valve opening. Such an approximation implicitly makes the following assumptions. Firstly, the boiler is assumed to be an infinite steam source, i.e. it supplies steam at constant temperature and pressure. Secondly, the high pressure and interceptor valves are assumed to travel in unison. Thirdly, the difference in pressures in reheater and condenser is neglected. Fourthly, the turbine power output is taken to be a linear function of valve displacement over the whole range of operating conditions.

Finally, the efficiency of the turbine is assumed to be constant over the speed range considered. The prime mover system is therefore represented by the second order system as shown in Fig. 3.6.

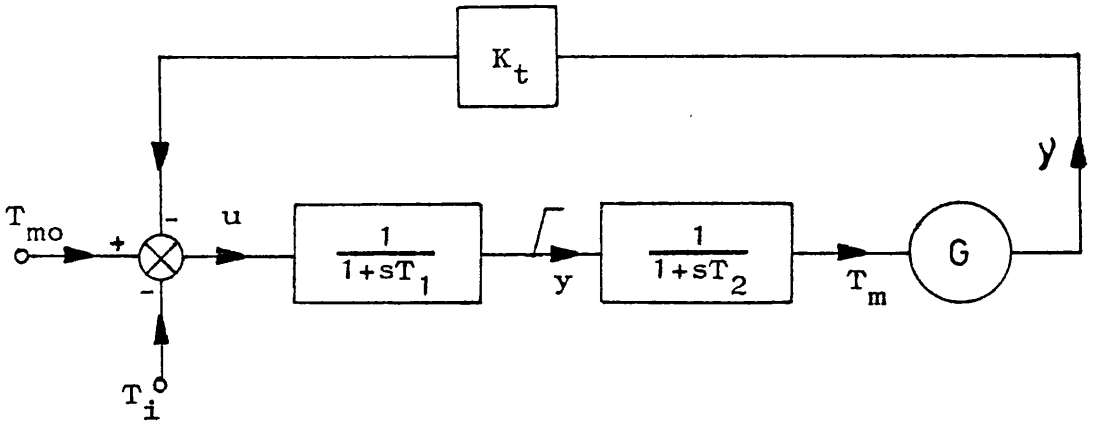

Fig. 3.6 Block diagram of prime mover system

The value of the feedback gain K_t is set to give the standard 4% speed regulation. T_{mo} is the reference signal and T_i is the extra feedback signal available with modern electro-hydraulic governors.

3.6 Choice of Performance Index

The optimum control is one which minimises a particular performance index. It is therefore vitally important that such a performance index adequately represents the required performance of the system being optimised. As far as the turbogenerator is concerned, there are three basic requirements that an optimum control should fulfil, namely, quick recovery of the machine terminal voltage after a severe fault, high first swing stability margin and

effective damping of subsequent oscillations. Several forms of functions have been considered. Different forms are found to be necessary for excitation control only and co-ordinated control.

3.7 Dynamic Sensitivity Equations

Consider a dynamic system given by the nonlinear vector equation

$$\dot{\underline{x}} = f(\underline{x},\underline{u},p,t) \tag{3.33}$$

where $\underline{x}$ is the state n-vector, $\underline{u}$ is the control m-vector and p is the parameter for which the sensitivity function is required. Differentiating equation 3.33 with respect to p and assuming that the control variables are independent of the parameter, the general sensitivity function equation is obtained in the form

$$\dot{\underline{z}} = G\underline{z} + \frac{\partial f}{\partial p} \tag{3.34}$$

where $\underline{z}$ is the sensitivity vector $(z_1,z_2,\ldots,z_n)^T$, $\dot{\underline{z}}$ is the time derivative of the sensitivity vector $(\dot{z}_1,\dot{z}_2,\ldots,\dot{z}_n)^T$; $z_i = \frac{\partial x_i}{\partial p}$, $\dot{z}_i = \frac{d}{dt}\frac{\partial x_i}{\partial p}$, $i=1,2,\ldots,n$, and G is the Jacobian matrix given by

$$G = [g_{ij}] = [\frac{\partial f_i}{\partial x_j}].$$

The initial condition for eqn. 3.34 is $z_i=0$ at $t=0$, $i=1,2,\ldots,n$ if p is not a system initial condition and if p is the initial condition for x_j, $z_i=0$ at $t=0$, $i=1,2,\ldots,j-1,j+1,\ldots,n$ and $z_j=1$. The sensitivity

equation 3.34 is linear and of order n. In general, for a system of order n containing k parameters for which sensitivity functions are required, k sets of sensitivity equations each of order n are introduced. These k sets of sensitivity equations plus the system equations making a total of (n+1)k equations, must be solved together to obtain the system states and the sensitivity functions.

CHAPTER 4 EXCITATION CONTROL STUDIES USING NONLINEAR SINGLE VARIABLE OPTIMISATION

4.1 Introduction

Attempts to improve the transient performance of an a.c. turbogenerator when subjected to a large disturbance usually involve feedback of additional system states into the excitation system. When, however, the proposed extra feedback signals are specified system states, a form of optimisation can be used to synthesise the required control law. It is now proposed to use only one extra feedback signal into the excitation system in additional to the terminal voltage feedback in an attempt to improve the response in rotor angle following a large disturbance, without degenerating the terminal voltage response. Such a synthesis method involves the single variable optimisation of a nonlinear system model and incorporates successive approximations of a nonlinear polynomial. When the relative suitability of different proposed signals is to be considered, dynamic sensitivity methods can be used to compare the optimised system performance produced by each of the extra feedback signals.

4.2 Power System Stabiliser

Until quite recently, it has been common practice for automatic voltage regulators used to control the

excitation of large turbogenerators to be designed by the machine manufacturer using classical control methods. The general approach used in the UK[21] has been to set the parameters of the a.v.r. on site, using only terminal voltage feedback. It has however, now been established that the use of power system stabilisers[67] can lead to an improvement in the transient response of the power system. A power system stabiliser is an element or group of elements which provides an additional input to the regulator to improve power system dynamic performance. A number of different quantities may be used as inputs to the power system stabiliser. These extra feedback quantities are termed supplementary signals, or more commonly, stabilising signals.

The presence of long lines and weak transmission links on the North American Continent has led to the increasing use of thyristor excitation systems for which the use of supplementary stabilising feedback signals has been found necessary. In practice, these extra feedback signals have been derived from a number of sources, including shaft speed[68], terminal power[69], accelerating power[70,71] and frequency deviation[72].

Many analytical studies of the application of modern control methods to improve, or even optimise, the transient performance of a turbogenerator have been reported in recent years but there are few reported experimental studies in this area. Some of the most recent experimental studies have incorporated direct

digital control of excitation using both minicomputer[34,35] and microprocessor installations[36]. In some cases, the required control law has been obtained using linearised system equations, while, in other cases, certain of the system nonlinearities have been taken into account, to produce so-called suboptimal controllers[73] which produce a closed-loop controller giving an acceptable transient performance for a wide range of initial and final system operating conditions. Such optimal or suboptimal controllers theoretically require feedback of all the system states, which is not likely to be possible in practice. A suboptimal controller incorporating feedback of three system states has previously been described[74], and,more recently, a report of an attempt to reduce the number of extra system states to two has been published[75].

In these previous studies[74,75], the use of dynamic sensitivity analysis, using a gradient technique to produce a suboptimal excitation controller, has been described. Although such a technique allows sensitivity curves for each individual stabilising signal to be obtained, it does not readily allow an investigation of making the obvious step of producing a closed-loop excitation control law in the presence of only one feedback signal. The single variable optimisation technique using a linear search method described provides a concise and systematic solution to this problem.

4.3 Single Variable Optimisation

Most numerical methods for determining the optimum value of a given nonlinear objective function are iterative and proceed by generating a sequence of new estimates, each improving on the previous one. The different procedures available are characterised by the strategy used to produce this series of improving approximations. However, the problem of minimising a function of a single variable often occurs in the associated algorithms developed to minimise a function of n variables. It is common to determine a parameter, say λ, which either minimise or reduces $f_\lambda = f(\underline{x}(\lambda))$ with each iteration, such that, for the kth iteration, a direction of search $\underline{p}_k$ is determined and a scalar λ_k is determined which minimises $f(\underline{x}_k+\lambda\underline{p}_k)$ with respect to λ. Then

$$\underline{x}_{k+1} = \underline{x}_k + \lambda_k \underline{p}_k \qquad (4.1)$$

The process is illustrated in Fig. 4.1.

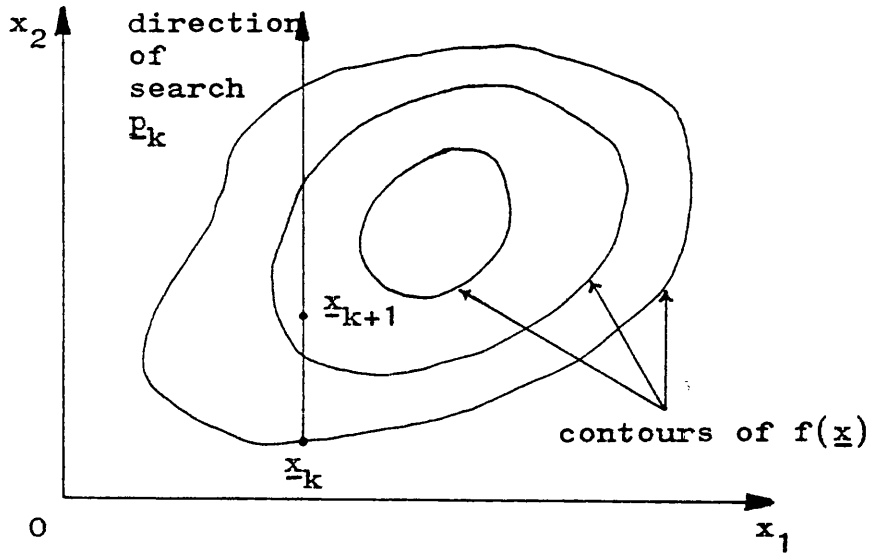

Fig. 4.1 Linear search

The procedure for finding a minimum of $f(\underline{x})$ along $\underline{p}_k$ is usually referred to as a linear search and there are two basic approaches to the problem of performing such a linear search.

The first method is that of function comparison in which function values are only used in comparison tests. Such methods(Fibonacci, Bisection and Golden Section etc) fail to utilize all the information available in that they disregard the quantity by which the function values differ at the various points.

The second method, that of function approximation, utilizes this additional information and is based on the assumption that $f(\underline{x})$ approximates to a quadratic or cubic polynomial. The minimum value of a quadratic or cubic can readily be determined. A simple algorithm for determining the minimising value of the parameter λ for a quadratic approximation has been described by Powell[48] and is illustrated in Fig. 4.2. The flow chart is self-explanatory. The corresponding algorithm for a cubic approximation, reported by Davidson[49], makes use of the values of the function and its derivative at two points and is described in Fig. 4.3. The procedure of 'boxing in' of the minimum is demonstrated by Fig. 4.3a of the flow chart while the 'polynomial fit' starts in Fig. 4.3b. The derivation of the basic formulations used are described in Appendices A3 and A4. Both the quadratic and cubic approximations are used in the single variable optimisation studies.

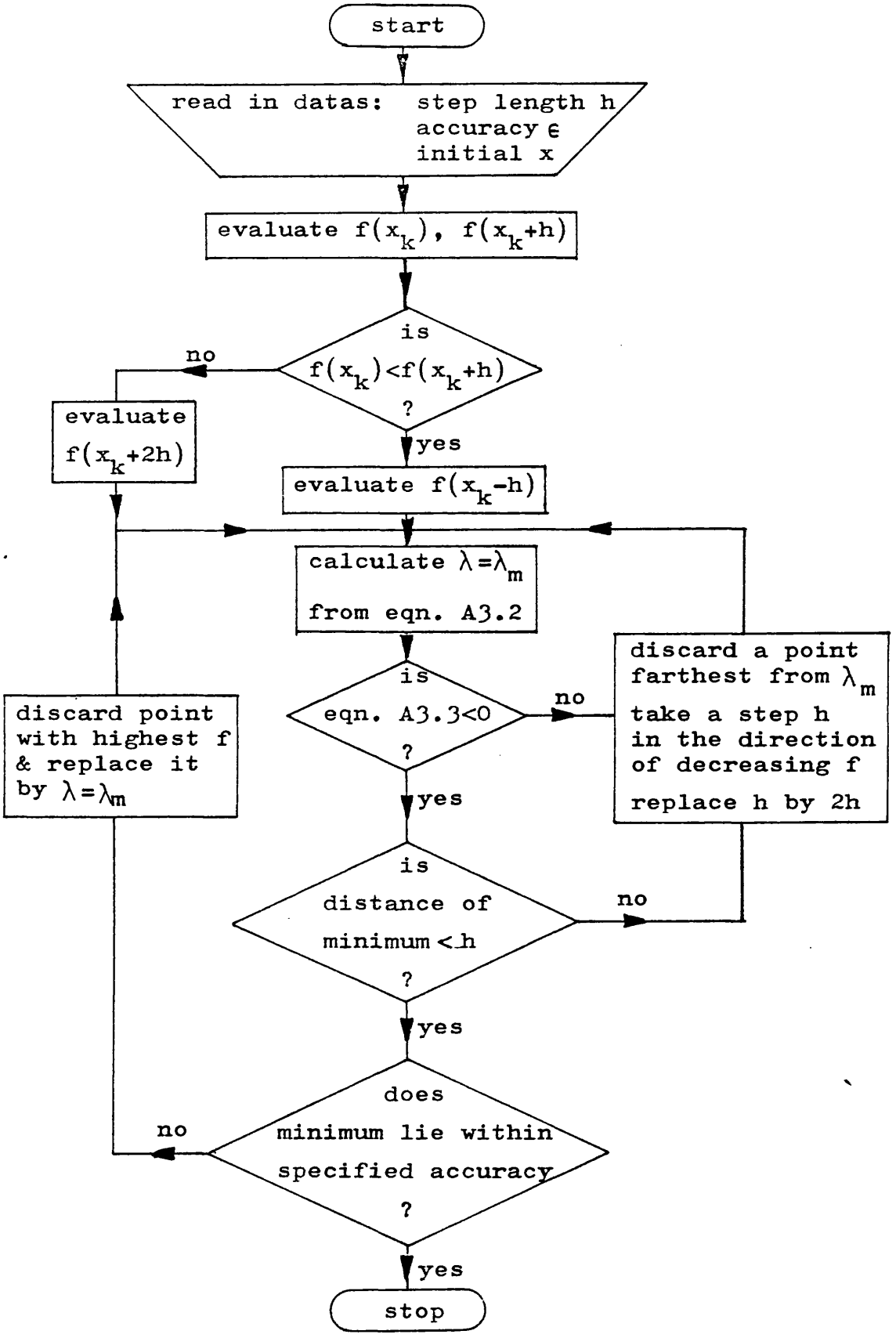

Fig. 4.2 Flow chart for quadratic approximation

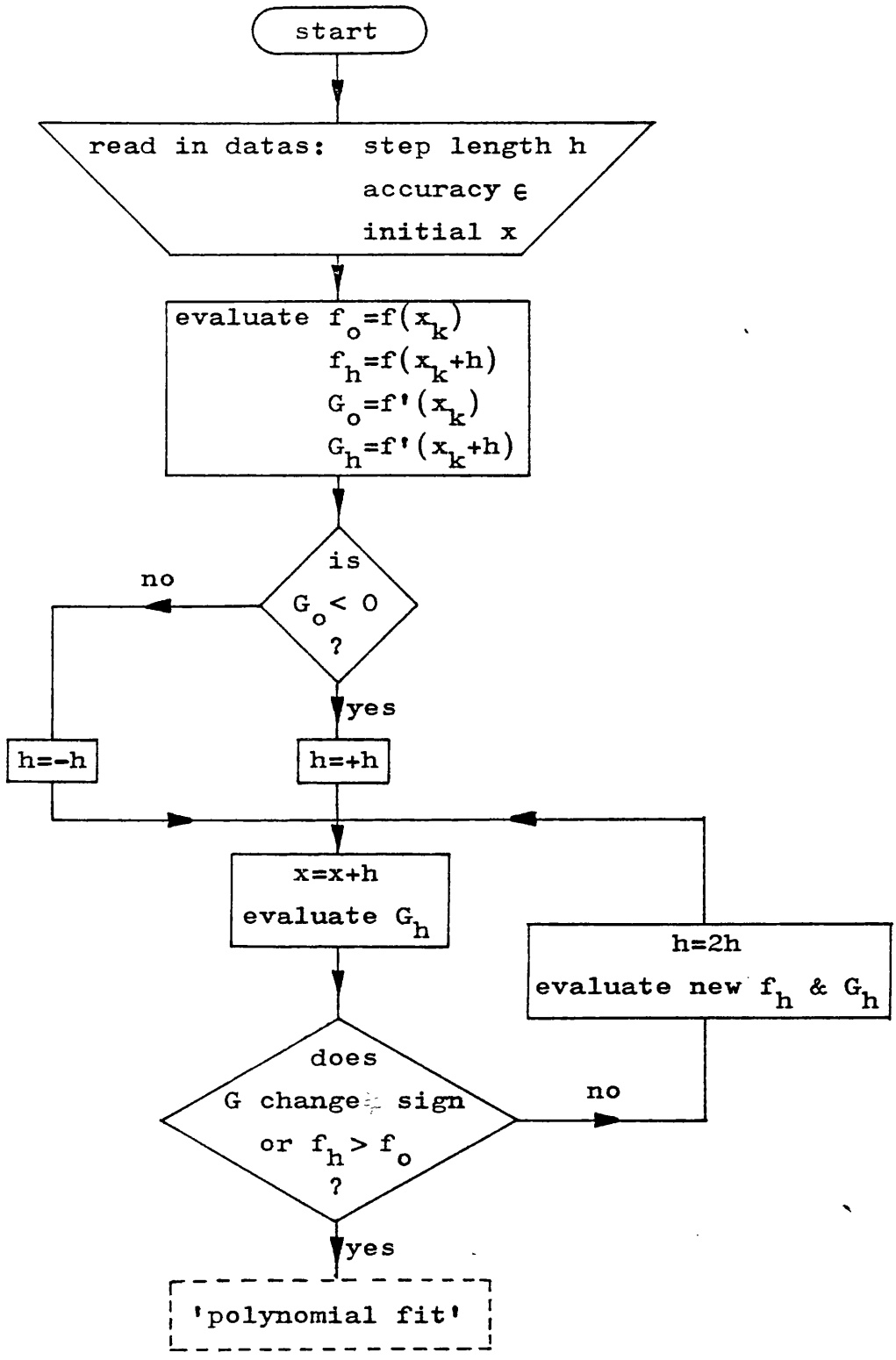

Fig. 4.3a Flow chart for cubic approximation:-

'boxing in'

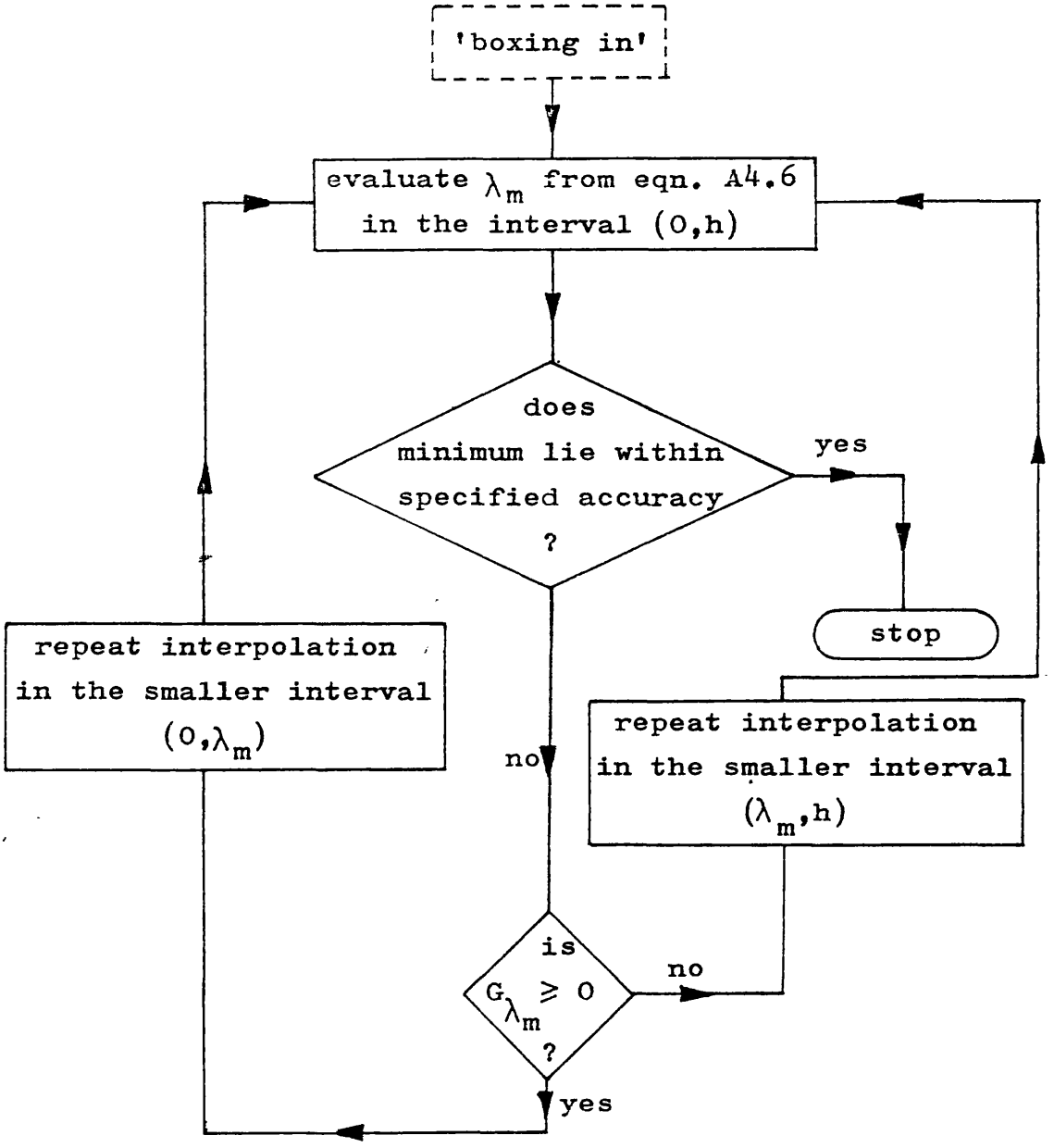

Fig. 4.3b Flow chart for cubic approximation:- 'polynomial fit' .

4.4 System Formulation

4.4.1 Power System Model

The system under consideration consists of a single turbo-generator connected through a transformer and a double circuit transmission network to an infinite busbar in the general manner described by Fig. 4.4.

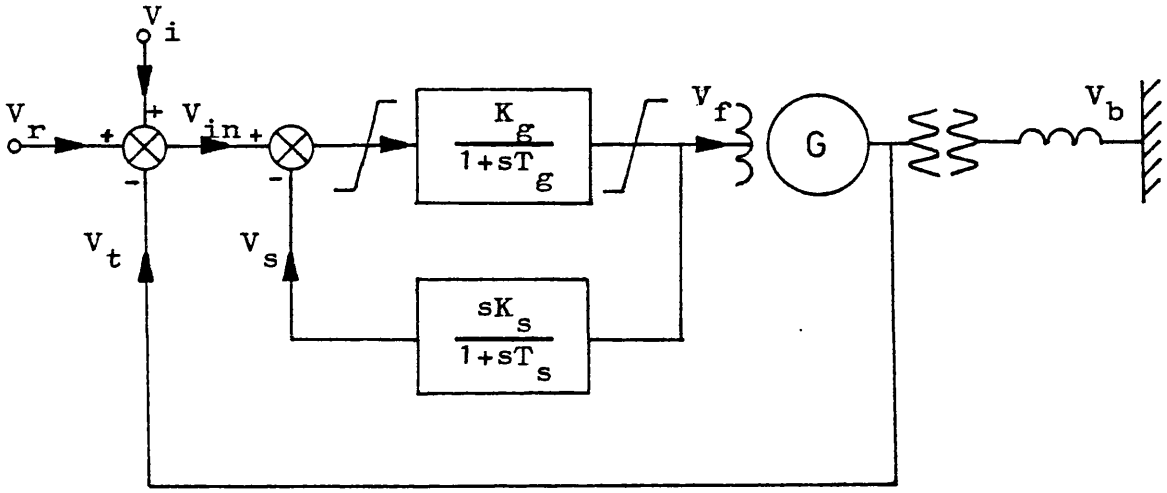

Fig. 4.4 General system arrangement

The system configuration and operating conditions have been previously described in section 3.1, except that the effect of prime mover control has been neglected in this study. A seventh order set of differential equations has been used to represent the machine with derived equations used to take account of the decay of stator flux linkages, speed variations and transients in the transmission system. The excitation control system shown in Fig. 4.4 is assumed to be of thyristor type, and hence is capable of reversal of field voltage.

4.4.2 Optimisation of System Performance

In general, it can be assumed that a suboptimal controller for a nonlinear system is some function of some of the system states. In the present study, the extra feedback signal, V_i, of Fig. 4.4, is a linear function of only one state variable, x, such that

$$V_i = K \Delta x \tag{4.2}$$

where Δx is the change in the proposed system state, x, and K is the optimising parameter. Suboptimal control is obtained by a suitable choice of the optimising parameter, K, thereby converting the problem into a function minimisation problem. The function, or performance index I, to be minimised has been chosen to have the form

$$I = \int_o^T (A_1 \Delta V_t^2 + \frac{A_2}{0.1+t} \Delta \delta^2) dt \tag{4.3}$$

where V_t is the terminal voltage, δ is the operating load angle, A_1 and A_2 are weighting factors. A reduction of this form of error squared integral over the transient period T following a system disturbance implies a reduction in the terminal voltage and load angle transients. By adjusting the weighting factors A_1 and A_2, either the terminal voltage or the load angle can be allowed to assume more weight. The inverse time factor in the load angle term represents an emphasis on the initial swings.

4.4.3 Derivation of Sensitivity Equations

The sensitivity equations are derived by differentiating the system equations with respect to the feedback gain constant as described in section 3.7. Before the differentiation, the algebraic system equations are re-arranged to a form suitable for the numerical solution of the system equations. The system equations are

$$pe_d'' = ((x_q - x_q'')i_q - e_d'')/T_{qo}'' \tag{4.4}$$

$$pe_q' = (V_f - (x_d - x_d'')i_d - e_q'')/T_{do}' \tag{4.5}$$

$$pe_q'' = (e_q' - (x_d' - x_d'')i_d - e_q'' - (T_1(e_q'' - x_d''i_d) + T_2 x_d i_d - T_{kd}V_f)/T_{do}')/T_{do}'' \tag{4.6}$$

$$p\delta = y \tag{4.7}$$

$$py = (T_m - T_e - K_{dd}y)/M \tag{4.8}$$

$$pV_f = ((V_r - V_t + V_i - V_s)K_g - V_f)/T_g \tag{4.9}$$

$$pV_s = (K_s pV_f - V_s)/T_s \tag{4.10}$$

$$pI = A_1(\Delta V_t)^2 + \frac{A_2}{0.1+t}(\Delta\delta)^2 \tag{4.11}$$

$$pi_d = (pe_q'' - w_o(V_b \sin\delta + (R_t+R_a)i_d) + w(e_d'' + (x_q''+X_t)i_q))/(X_t+x_d'') \tag{4.12}$$

$$pi_q = (-pe_d'' + w(e_q'' - (X_t+x_d'')i_d) - w_o(V_b\cos\delta + (R_t+R_a)i_q))/(X_t+x_q'') \tag{4.13}$$

The auxiliary equations are given by

$$V_i = K\Delta x \tag{4.14}$$

$$T_e = e_d"i_d + e_q"i_q - (x_d"-x_q")i_di_q \tag{4.15}$$

$$w = w_o + y \tag{4.16}$$

$$v_d = V_b\sin\delta + X_tpi_d/w_o + R_ti_d - wX_ti_q/w_o \tag{4.17}$$

$$v_q = V_b\cos\delta + X_tpi_q/w_o + R_ti_q + wX_ti_d/w_o \tag{4.18}$$

$$V_t = \sqrt{(v_d^2 + v_q^2)} \tag{4.19}$$

where $K_{dd} = K_d/w_o$.

The sensitivity equations with respect to the single state feedback gain K are as follows:

$$p(\frac{\partial e_d"}{\partial K}) = ((x_q-x_q")\frac{\partial i_q}{\partial K} - \frac{\partial e_d"}{\partial K})/T_{qo}" \tag{4.20}$$

$$p(\frac{\partial e_q'}{\partial K}) = (\frac{\partial V_f}{\partial K} - (x_d-x_d")\frac{\partial i_d}{\partial K} - \frac{\partial e_q"}{\partial K})/T_{do}' \tag{4.21}$$

$$p(\frac{\partial e_q"}{\partial K}) = (\frac{\partial e_q'}{\partial K} - (x_d'-x_d")\frac{\partial i_d}{\partial K} - \frac{\partial e_q"}{\partial K} - (T_1(\frac{\partial e_q"}{\partial K}-x_d"\frac{\partial i_d}{\partial K}) + T_2x_d\frac{\partial i_d}{\partial K} - T_{kd}\frac{\partial V_f}{\partial K})/T_{do}')/T_{do}" \tag{4.22}$$

$$p(\frac{\partial \delta}{\partial K}) = \frac{\partial y}{\partial K} \tag{4.23}$$

$$p(\frac{\partial y}{\partial K}) = (-\frac{\partial T_e}{\partial K} - K_{dd}\frac{\partial y}{\partial K})/M \tag{4.24}$$

$$p(\frac{\partial V_f}{\partial K}) = ((-\frac{\partial V_t}{\partial K} + \frac{\partial V_i}{\partial K} - \frac{\partial V_s}{\partial K})K_g - \frac{\partial V_f}{\partial K})/T_g \tag{4.25}$$

$$p(\frac{\partial V_s}{\partial K}) = (K_sp(\frac{\partial V_f}{\partial K}) - \frac{\partial V_s}{\partial K})/T_s \tag{4.26}$$

$$p(\frac{\partial I}{\partial K}) = 2.0\ (A_1\Delta V_t\frac{\partial V_t}{\partial K} + A_2\Delta\delta\frac{\partial \delta}{\partial K}/(0.1+t)) \tag{4.27}$$

$$p\left(\frac{\partial i_d}{\partial K}\right) = \left(p\left(\frac{\partial e_q''}{\partial K}\right) - w_o\left(V_b\cos\delta\frac{\partial \delta}{\partial K} + (R_t+R_a)\frac{\partial i_d}{\partial K}\right)\right.$$

$$+ w\left(\frac{\partial e_d''}{\partial K} + (x_q''+X_t)\frac{\partial i_q}{\partial K}\right)$$

$$\left. + \left(e_d'' + (X_t+x_q'')i_q\right)\frac{\partial w}{\partial K}\right)/(X_t+x_d'') \qquad (4.28)$$

$$p\left(\frac{\partial i_q}{\partial K}\right) = \left(-p\left(\frac{\partial e_d''}{\partial K}\right) + w\left(\frac{\partial e_q''}{\partial K} - (X_t+x_d'')\frac{\partial i_d}{\partial K}\right)\right.$$

$$+ \left(e_q'' - (X_t+x_d'')\right)\frac{\partial w}{\partial K}$$

$$\left. - w_o\left(-V_b\sin\delta\frac{\partial \delta}{\partial K} + (R_t+R_a)\frac{\partial i_q}{\partial K}\right)\right)/(X_t+x_q'') \qquad (4.29)$$

The auxiliary sensitivity equations are described by

$$\frac{\partial V_i}{\partial K} = K\frac{\partial x}{\partial K} + \Delta x \qquad (4.30)$$

$$\frac{\partial T_e}{\partial K} = \frac{\partial e_d''}{\partial K}i_d + \frac{\partial i_d}{\partial K}e_d'' + \frac{\partial e_q''}{\partial K}i_q + \frac{\partial i_q}{\partial K}e_q''$$

$$- (x_d''-x_q'')\left(i_d\frac{\partial i_q}{\partial K} + i_q\frac{\partial i_d}{\partial K}\right) \qquad (4.31)$$

$$\frac{\partial w}{\partial K} = \frac{\partial \gamma}{\partial K} \qquad (4.32)$$

$$\frac{\partial V_t}{\partial K} = \left(v_d\frac{\partial v_d}{\partial K} + v_q\frac{\partial v_q}{\partial K}\right)/V_t$$

$$= \left(v_d\left(V_b\cos\delta\frac{\partial \delta}{\partial K} + X_t p\left(\frac{\partial i_d}{\partial K}\right)/w_o + R_t\frac{\partial i_d}{\partial K} - wX_t\frac{\partial i_q}{\partial K}/w_o\right.\right.$$

$$\left. - X_t i_q\frac{\partial w}{\partial K}/w_o\right) + v_q\left(-V_b\sin\delta\frac{\partial \delta}{\partial K} + X_t p\left(\frac{\partial i_q}{\partial K}\right)/w_o\right.$$

$$\left.\left. + R_t\frac{\partial i_q}{\partial K} + wX_t\frac{\partial i_d}{\partial K}/w_o + X_t i_d\frac{\partial w}{\partial K}/w_o\right)\right)/V_t \qquad (4.33)$$

4.4.4 System Sensitivity

The application of dynamic sensitivity methods to the optimisation of nonlinear power system models has been previously reported[74]. Of the four sensitivity functions in common use, that based on the logarithmic function is

used in the present application, such that the sensitivity S_{p_o} of some system state, x, to some system parameter, p, is given by

$$S_{p_o} = \left.\frac{\partial(\ln x)}{\partial(\ln p)}\right|_{p_o} = \left.\frac{\partial x}{\partial p}\frac{p}{x}\right|_{p_o} \qquad (4.34)$$

where p_o is the nominal parameter value. The derivative term of eqn. 4.34 is inherent in any study based on the cubic approximation.

Comparison of the system sensitivities for different parameters is made by taking the integral of the absolute value of the logarithmic sensitivity function.

This sensitivity approach allows the inclusion of sensitivity functions for the terminal voltage, V_t, and the load angle, δ, to be included in the performance index. This can result in a reduction in the sensitivity of these states to parameter changes at a very small sacrifice in performance[76].

System optimality, which is defined in terms of a performance index, is arbitrary. However, it is possible to obtain some correlation between the sensitivity and optimality of a system. The performance index chosen in this study is very closely related to system stability and such a correlation should exist. Results obtained in later sections confirm this view.

4.5 Optimisation Studies

4.5.1 General

In order to assess the relative effects of several different additional feedback signals, a large number of optimisation studies have been performed with different values of step length h and specified accuracy ϵ. Weighting factors of $A_1 = 1$ and $A_2 = 5$ in eqn. 4.3 have been used with the integral of eqn. 4.3 evaluated over 3.5s in attempts to find the optimised value of the parameter K of eqn. 4.2. The convergence criterion has been assumed to be satisfied when $|K(\text{last}) - K(\text{current})| < \epsilon$, the specified accuracy. Both the quadratic and cubic approximation have been fully investigated.

The choice of extra signals into the excitation system has been limited to four particular signals, all of which have previously been used by various authors and all of which have been previously used in reported experimental studies. These four signals are $\Delta\delta$, the change in operating load angle, δ, Δw the change in rotor velocity from synchronous speed, $p^2\delta$, the transient rotor acceleration and ΔP_e the transient electrical output power.

4.5.2 Minimisation using the Quadratic Approximation

Table 4.1 shows the results of the optimisation study when the machine is subjected to a 0.22s fault duration.

Control Number	Feedback Signal	Initial Value of Gain	Accuracy ϵ = 0.001			Accuracy ϵ = 0.00001		
			Final Gain	Value of PI	Iteration Number	Final Gain	Value of PI	Iteration Number
Q1	$\Delta\delta$	0	-0.0597	4.4966	8	-0.0595	4.4966	10
Q2	Δw	0	0.0519	4.3254	16	0.0524	4.3250	26
Q3	$p^2\delta$	0	0.0122	3.5622	14	0.0118	3.5602	18
Q4	ΔP_e	0	0.4096	3.5273	8	0.4093	3.5273	10
Q5	$\Delta\delta$	-0.3407	-0.3438	3.4724	18	-0.3448	3.4723	29

Table 4.1 Optimisation studies with quadratic approximation and 0.5 step length

Control Number	Feedback Signal	Initial Value of Gain	Accuracy ϵ = 0.001			Accuracy ϵ = 0.00001		
			Final Gain	Value of PI	Iteration Number	Final Gain	Value of PI	Iteration Number
Q6	$\Delta\delta$	0	-0.0595	4.4966	13	-0.0595	4.4966	16
Q7	Δw	0	0.0524	4.3251	19	0.0529	4.3247	27
Q8	$p^2\delta$	0	0.0178	3.8740	16	0.0118	3.5602	21
Q9	ΔP_e	0	0.4092	3.5273	14	0.4093	3.5273	16
Q10	$\Delta\delta$	-0.3418	-0.3443	3.4723	13	-0.3448	3.4748	23

Table 4.2 Optimisation studies with quadratic approximation and 5.0 step length

The step length chosen initially was 0.5, and the results for two specified accuracies, $\epsilon = 0.001$ and $\epsilon = 0.00001$ are shown in Table 4.1. The computation takes an average of 8s of CPU time per iteration on the PDP10 computer at UMIST. In order to cover a wide range of parameter space and to test the convergence of the algorithms, the optimisation was repeated for a larger step length, 5.0, and the results of this study are shown in Table 4.2. Comparison of Table 4.1 and 4.2 shows that the final gains arrived at are nearly identical but that the increase in step length increases the number of iterations required. The minimum value of the performance index obtained for either $\Delta\delta$ or Δw feedback is higher than that obtained for either $p^2\delta$ or ΔP_e feedback.

A similar pattern emerged when corresponding results were obtained for a fault duration of 0.14s. However, in this case, the performance index obtained with $\Delta\delta$ feedback appeared to be close to the values obtained with $p^2\delta$ and ΔP_e feedback. It can be concluded that, although the change in fault duration results in a change in the entire system configuration, this local minimum did exist but was missed by the search in the 0.22s fault study. This was confirmed by using the optimised feedback constant of 0.34066 for $\Delta\delta$ for the 0.14s fault study, with a step length of 0.5, as an initial starting point for the optimisation for the 0.22s fault study. The result of this reoptimisation is shown as control Q5 in Table 4.1 and confirms that such a local minimum did, in fact, exist.

The corresponding performance index is now the best obtained as compared with the original value of 4.4966 which is close to the value of 4.5225 obtained without any additional feedback corresponding to the action of terminal voltage feedback acting alone.

Although the chosen value of step length and the specified accuracy do affect the rate of convergence, a poor estimate does not stop the process, based on the quadratic approximation, from converging to give close agreement between values of feedback constants obtained for widely differing step lengths. This general effect is illustrated in Table 4.3 in the particular case of feedback of transient electrical power, ΔP_e. It can be seen from Table 4.3 that in spite of a 5000:1 ratio in step lengths, the value of the feedback constant only ranges from 0.4077 to 0.4105 with the performance index constant at 3.5273.

Step Length	Final Gain	Value of PI	Iteration Number
0.01	0.4077		13
0.10	0.4105		8
0.50	0.4096	3.5273	8
5.00	0.4092		14
50.00	0.4093		21

Table 4.3 Effect of change in step length

It can, therefore, be concluded that the quadratic approximation produces convergence for a wide range in step lengths, although it is possible to miss an important

local minimum in the value of the performance index by an inappropriate choice of step length.

4.5.3 Minimisation using the Cubic Approximation

Although the cubic approximation described in Appendix A4 does allow a gradient criterion to be used in the minimisation routine, an initial comparison of the algorithms has been made without this information. The result of this study using a step length of 0.5 and an accuracy of 0.00001 is given in Table 4.4. The average computational time for each iteration is 13s of CPU time which is 5s more than that for the quadratic approximation. Table 4.4 includes the initial and final values of the gradient.

Control Number	Feedback Signal	Initial Gradient	Final Gain	Final Gradient	Value of PI	Iteration Number
C1	$\Delta\delta$	0.967	-0.3429	0.497	3.4730	6
C2	Δw	-4.65	0.0553	1.29	4.3278	5
C3	$p^2\delta$	-57.1	0.0	-57.1	4.5225	2
C4	ΔP_e	-1.71	0.4395	0.567	3.5343	4

Table 4.4 Optimisation studies with cubic approximation and 0.5 step length

It can be seen from a comparison of Table 4.1 and 4.4 that the use of the cubic approximation seems to offer a faster rate of convergence but at the expense of more CPU time per iteration. Table 4.4 also shows that the use of the cubic

approximation has found the local minimum for $\Delta\delta$ feedback initially missed using the quadratic approximation. However, it can be seen from Table 4.4 that, in the particular case of $p^2\delta$ feedback, the algorithm has not converged to an optimum. This effect was even more obvious with the optimisation performed using a step length of 5.0 when only the particular feedback associated with $\Delta\delta$ converged to an optimum.

This major disadvantage can readily be overcome by using the available information on gradient from one iteration to restart the optimisation. It has been found that the chosen value of accuracy has little effect under these conditions but that the choice of a suitable step length is critical. Use of the technique incorporating gradient values is illustrated in Table 4.5, for the particular case of $p^2\delta$ feedback with a specified accuracy of 0.00001.

Control Number	Step Length	Iteration Count	Feedback Gain	Gradient Value	Value of PI
CG1	0.5	1	0.0	-57.1	4.5225
		2	0.5	0.23	5.9892
CG2	0.1	1	0.0	-57.1	4.5225
		2	0.1	5.01	5.4486
		3	0.0261	24.3	4.2989
		4	0.0146	56.4	3.6375
CG3	0.001	1	0.0146	56.4	3.6375
		2	0.0136	38.4	3.5924
		3	0.0166	-4.93	3.5609

Table 4.5 Optimisation studies with cubic approximation using gradient values

The initial optimisation, CG1, of Table 4.5, has been performed with a step length of 0.5 and there is a change in the sign of the gradient between the first and second iteration corresponding to feedback constants of 0.0 and 0.5 respectively. This shows that the optimum value of feedback constant is between 0.0 and 0.5 and the optimisation is repeated as CG2 in Table 4.5 with a shorter step length of 0.1.

Four further iterations are now necessary to locate the required value of gain constant as being between 0.0 and 0.0146. In the third optimisation, CG3 of Table 4.5, the step length is further reduced to 0.001 and the required minimum value of performance index is located by three further iterations to give the feedback constant as being between 0.0116 and 0.0136. The total number of iterations is now seven at 13s of CPU time per iteration and the corresponding performance index has a value of 3.59242.

This process can, if necessary, be further repeated by successive reductions in the step length. However, the corresponding value of this feedback constant, obtained using the quadratic approximation, is shown as control Q3 of Table 4.2 as 0.0118 with a corresponding performance index of 3.5602, which was obtained after 18 iterations at 8s of CPU time per iteration.

Use of the cubic approximation produces a faster rate of convergence when the local minimum is known to lie within a specific range. However, the choice of step length used is critical and must be chosen from an initial estimate.

4.6 Theoretical Results of Optimisation Studies

4.6.1 Transient Response Curves

The results of the optimisation studies given in the previous section have been applied to give the field voltage, load angle and terminal voltage transient response curves of the single machine system with one additional signal fed into the excitation system. A full range of operating conditions has been investigated with different fault durations with the results obtained using the seventh order nonlinear machine model. Typical results are given in Fig. 4.5 and 4.6 for a fault duration of 0.22s with results plotted for 5.0s. The high frequency components on the terminal voltage curves, Fig. 4.5b and 4.6b, do not appear clearly on this time scale and have, therefore, been erased from the plots. Figure 4.5 shows the results obtained for feedback of either transient electrical power, ΔP_e, or transient velocity, Δw, while Fig. 4.6 shows the corresponding results for feedback of either transient load angle δ or acceleration $p^2\delta$. The result obtained using terminal voltage feedback acting alone has been included in both Figs. 4.5 and 4.6 for comparison purposes.

The input control law is shown as the field voltage response curves of Figs. 4.5c and 4.6c and clearly shows the effect of the additional single feedback signal in forcing the field voltage away from its positive ceiling

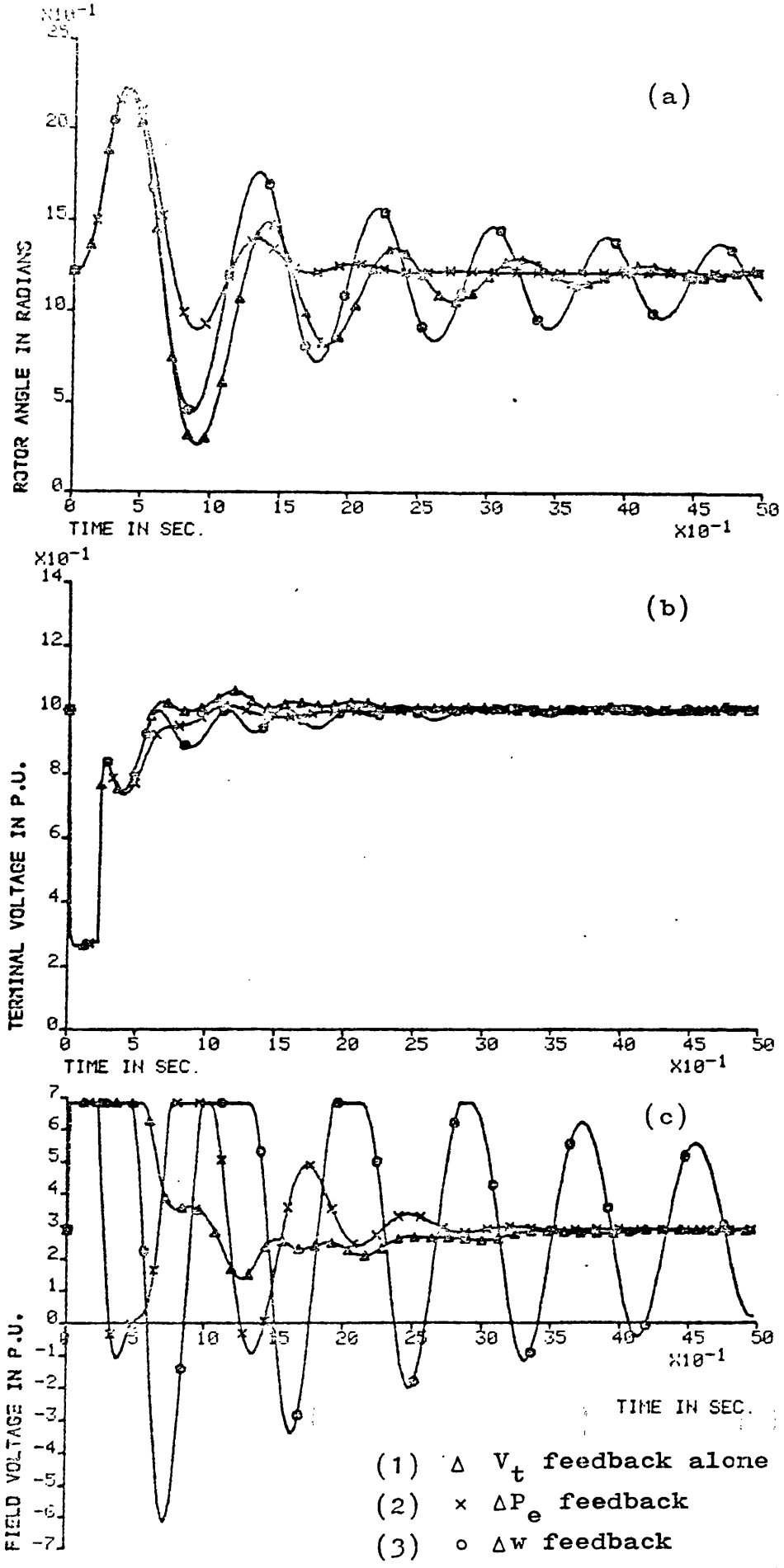

Fig. 4.5 Theoretical response curves

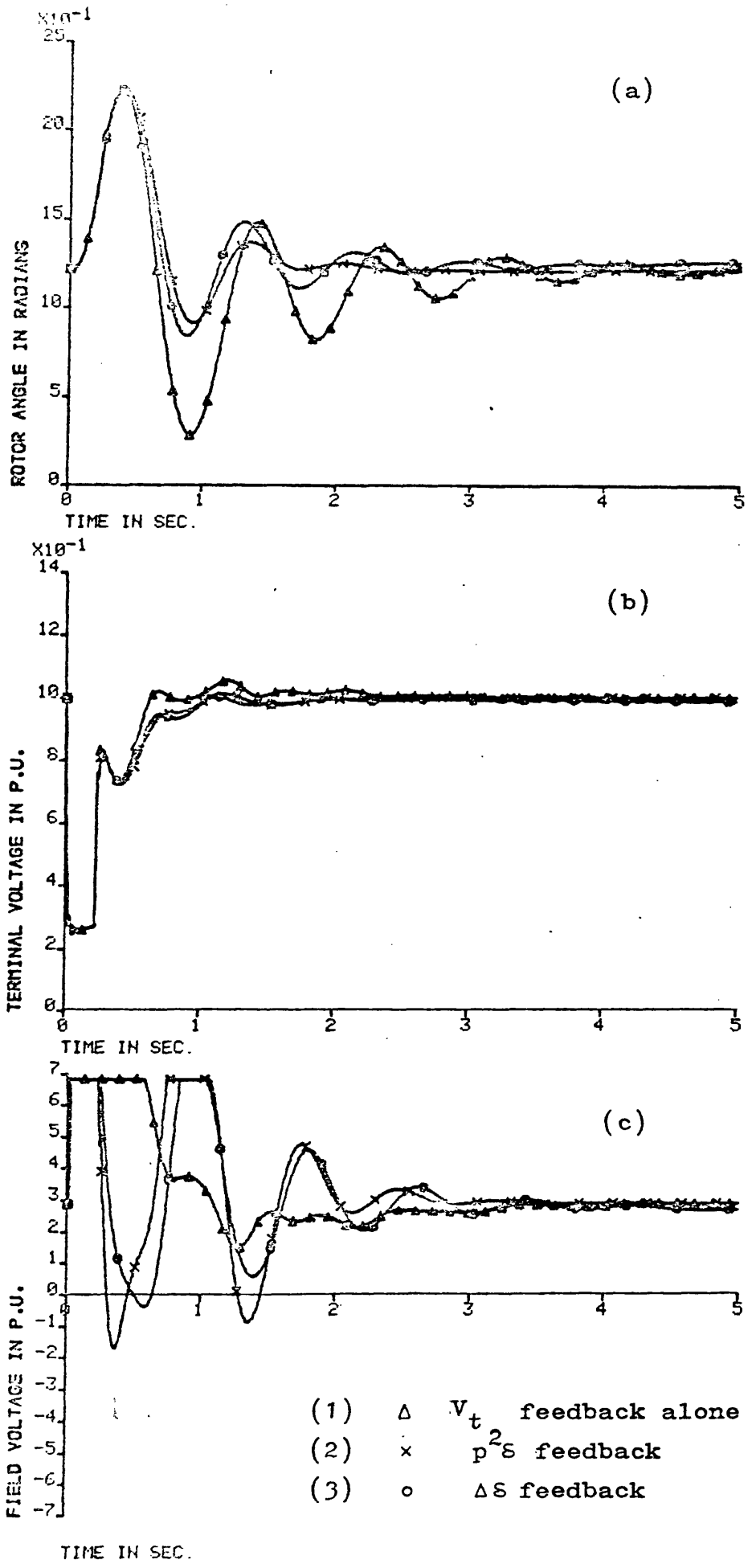

Fig. 4.6 Theoretical response curves

value earlier than that obtained with terminal voltage feedback acting alone. In all cases, except that of Δw feedback, there is a short excursion into negative field voltage. The rapid decrease in field voltage and its subsequent reversal are, of course, only possible with the modern excitation system described in Fig. 4.4 and are not possible with existing rotating diode excitation systems.

Inspection of the load angle curves of Figs. 4.5a and 4.6a show that, in all cases, when one extra control signal is fed back into the excitation system, an improvement in the damping in rotor oscillations after the first peak, is obtained. Since all the excitation controllers considered force the excitation to the same positive ceiling value they all give the well established result of the same value in the first peak in rotor angle. However, the load angle response curve obtained with Δw feedback is clearly inferior to that obtained with any one of the other three extra feedback signals, although the corresponding value of the feedback constant was obtained from an optimisation study. This particular point will be borne out by the corresponding sensitivity studies to be discussed later. The results obtained with either $p^2\delta$ or ΔP_e feedback are, of course, very similar, since governor action has been neglected in this study. The result obtained for $\Delta\delta$ feedback is better than that obtained for Δw feedback but inferior to those obtained for either $p^2\delta$ or ΔP_e feedback.

Because the prime object of feedback of terminal voltage alone is to regulate terminal voltage, the terminal voltage response curves of Fig. 4.5b and 4.6b confirm this fact. However, the terminal voltage responses obtained with feedback of either ΔP_e or $p^2\delta$ are very acceptable. Some further deterioration in terminal voltage response with $\Delta\delta$ feedback is shown by Fig. 4.6b while the corresponding response with Δw feedback shown in Fig. 4.5b is probably unacceptable.

Corresponding results obtained for a fault duration of 0.14s confirmed the general points made above for the 0.22s fault duration time.

4.6.2 Sensitivity Curves

A study of the variation in the value of the given performance index with changes in the feedback gains from their calculated nominal values, for all four systems under consideration, is shown in Fig. 4.7, which also includes the value of the performance index with feedback of terminal voltage acting alone. It can be seen from Fig. 4.7 that, although the value of the performance index obtained with Δw feedback remains effectively constant for large changes in the corresponding feedback constant from its nominal value, the actual value of the performance index is very close to the value obtained without extra feedback. In these circumstances, Fig. 4.7 indicates that Δw feedback is not very effective and confirms the results given in Fig. 4.5. The minimum

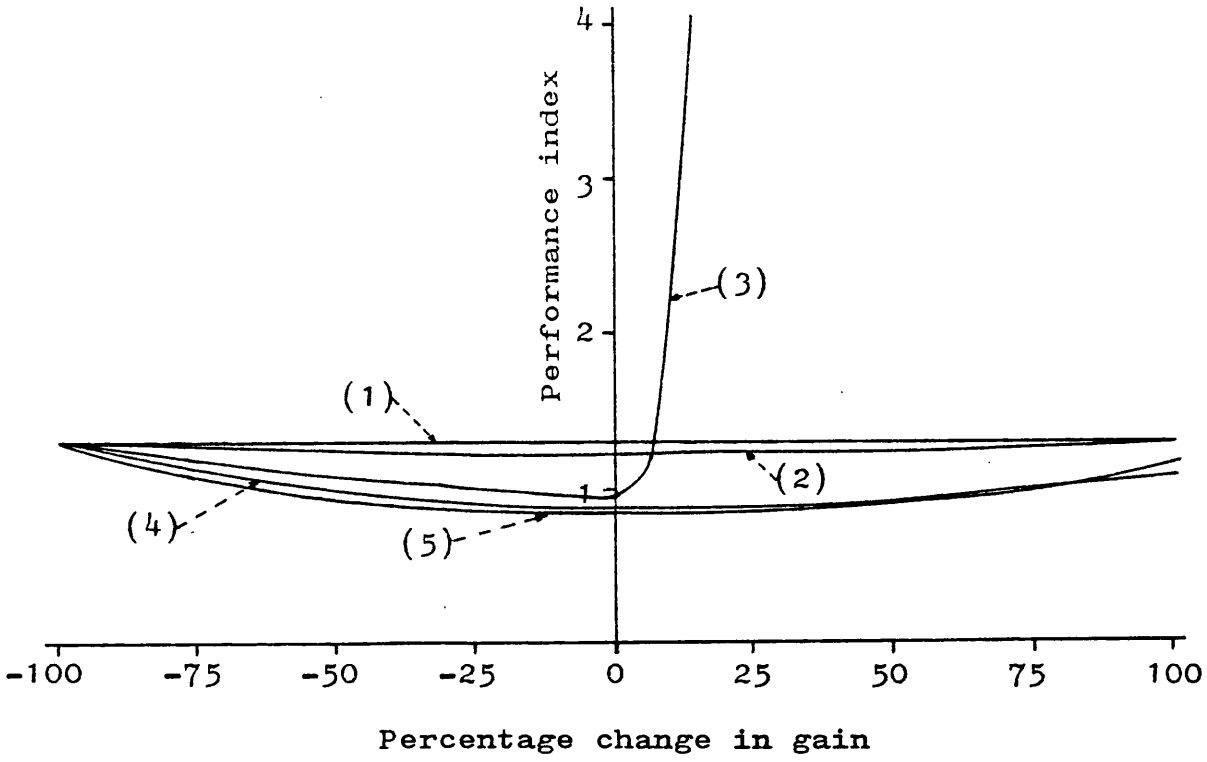

Fig. 4.7 Variation of performance index with change in feedback gain

(1) terminal voltage feedback alone
(2) Δw feedback
(3) $\Delta\delta$ feedback
(4) $p^2\delta$ feedback
(5) ΔP_e feedback

value of performance index obtained with $\Delta\delta$ feedback is close to those obtained with either $p^2\delta$ or ΔP_e feedback. However, it is clearly shown in Fig. 4.7 that the system with $\Delta\delta$ feedback is, in fact, highly sensitive to changes in the feedback constant, particularly when a increase in the value of this constant is introduced. This effect is confirmed by Fig. 4.8, which shows the effect of a 20% decrease and a 5% increase in the feedback constant associated with $\Delta\delta$, on the transient rotor angle sensitivity curve and the corresponding rotor angle response

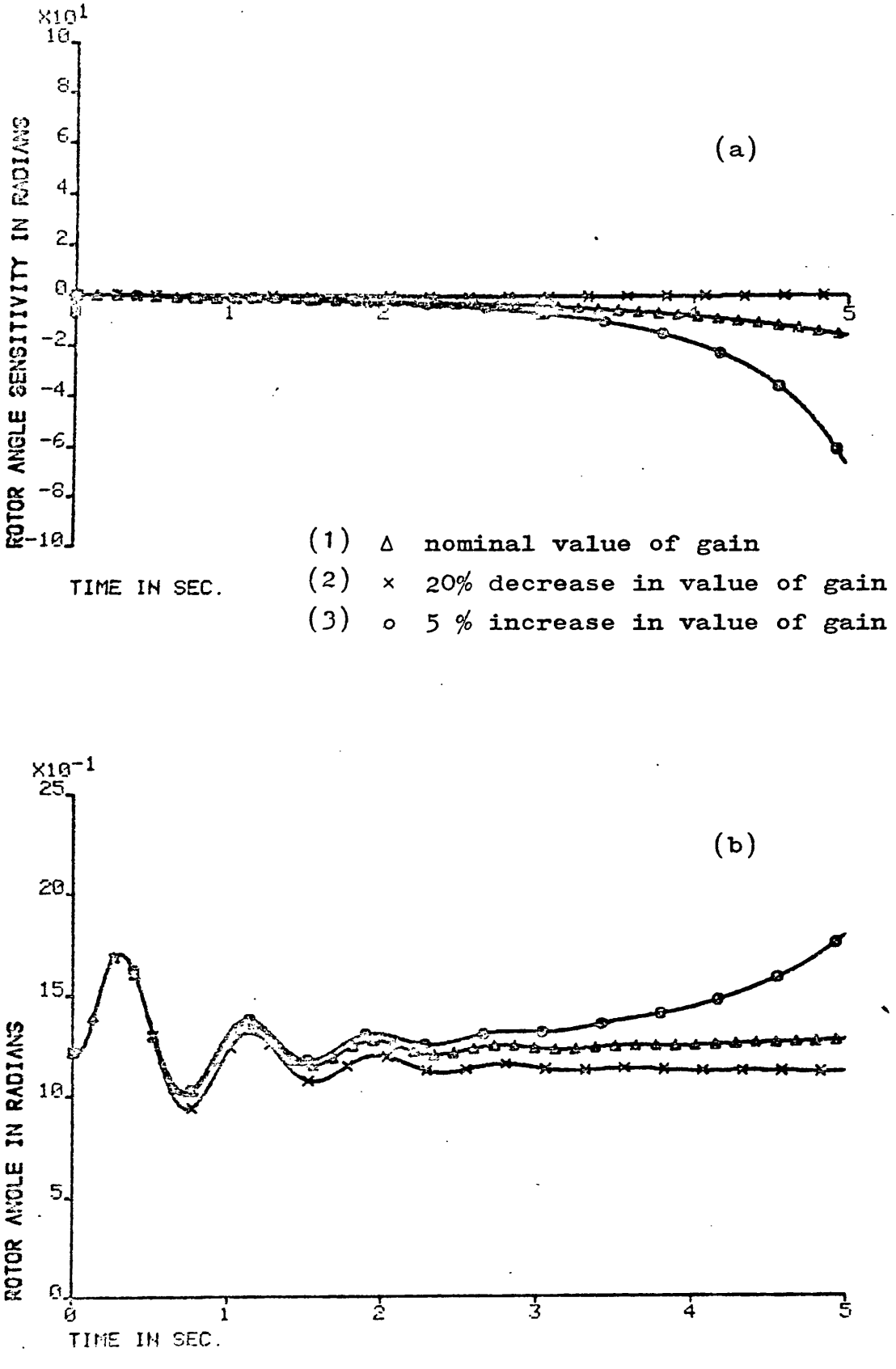

Fig. 4.8 Theoretical sensitivity curves for $\Delta\delta$ feedback

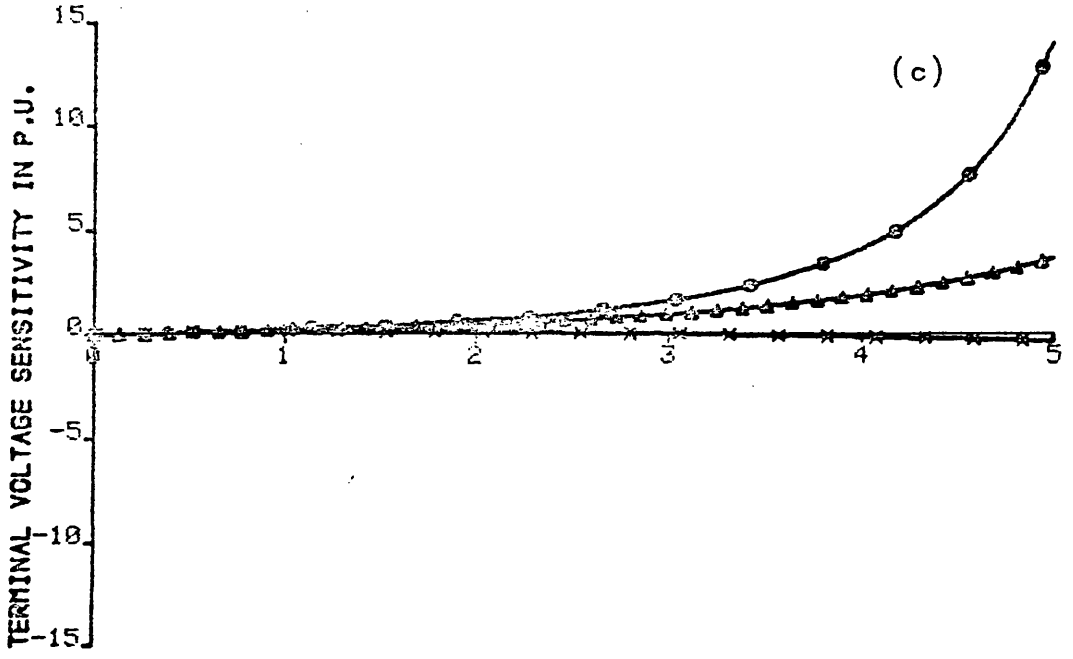

(1) Δ nominal value of gain

(2) × 20% decrease in value of gain

(3) o 5% increase in value of gain

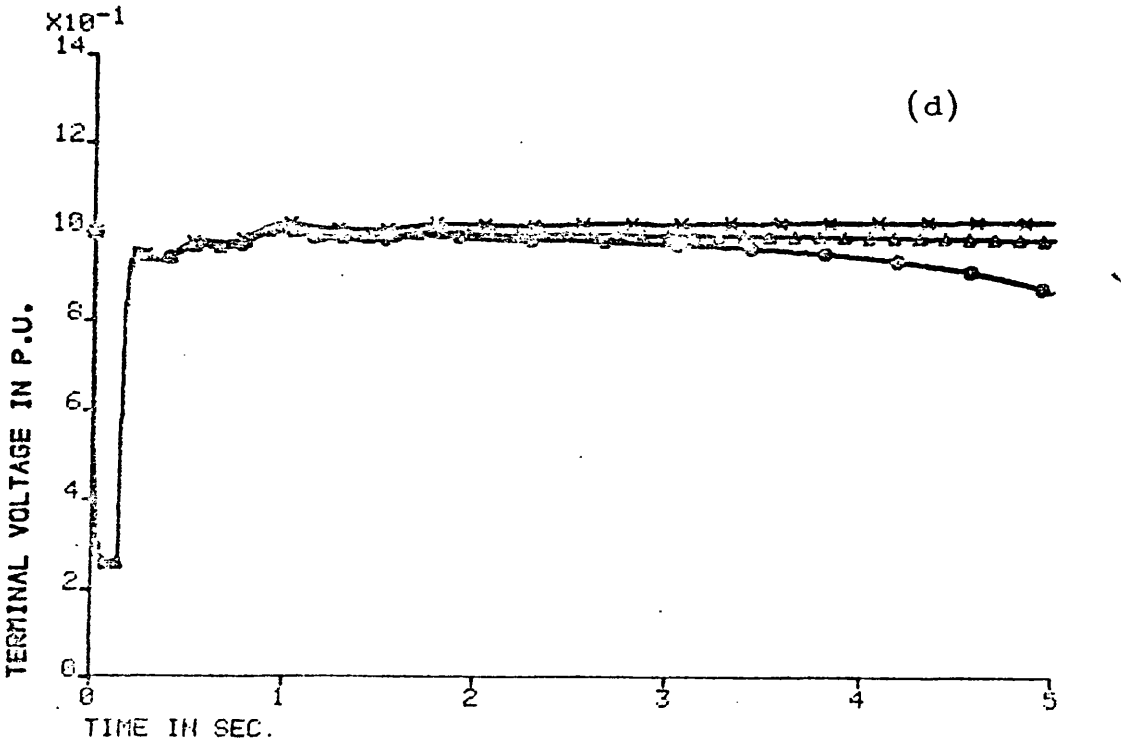

Fig. 4.8 Theoretical sensitivity curves for $\Delta\delta$ feedback

curve. The sensitivity curves are divergent with time such that a small parameter variation can, eventually, have a very significant effect on the system, a result confirmed by the rotor angle responses of Fig. 4.8b. This very important information can be disguised in the transient response curves and this fact is confirmed by the result obtained with the nominal value of feedback constant, K_o, shown as curve (1) in Fig. 4.8. It can be concluded that in any optimal study involving feedback of one extra signal, sensitivity curves must play an important part in the synthesis of a given system.

Figure 4.7 also shows that the variation in performance index with changes in the feedback constant is very similar for both $p^2\delta$ and ΔP_e feedback. Both feedback systems are quite insensitive to relatively large changes in the feedback constant and this result is confirmed for the particular case of ΔP_e feedback by the sensitivity curves shown in Fig. 4.9. The three curves of Fig. 4.9 are shown for terminal voltage feedback alone, for the nominal value, K_o, of the feedback constant with ΔP_e feedback incorporated and for a 50% increase in the value of that feedback constant. Figure 4.9a gives the corresponding rotor angle sensitivity curves and clearly shows that the system angle response is quite insensitive to the large change in feedback constant. The corresponding curves for terminal voltage sensitivity and response are given in Figs. 4.9c and 4.9d respectively. Since the prime object of terminal voltage feedback

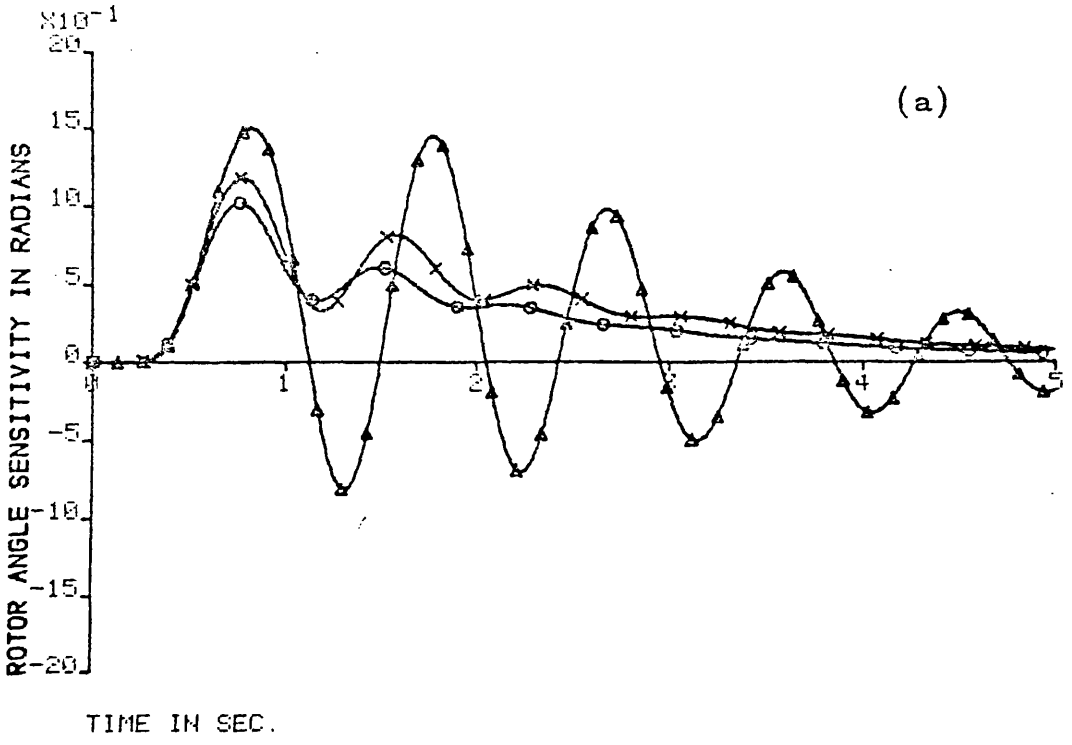

(1) Δ V_t feedback

(2) × ΔP_e feedback with nominal gain

(3) ○ ΔP_e feedback with 50% increase in gain

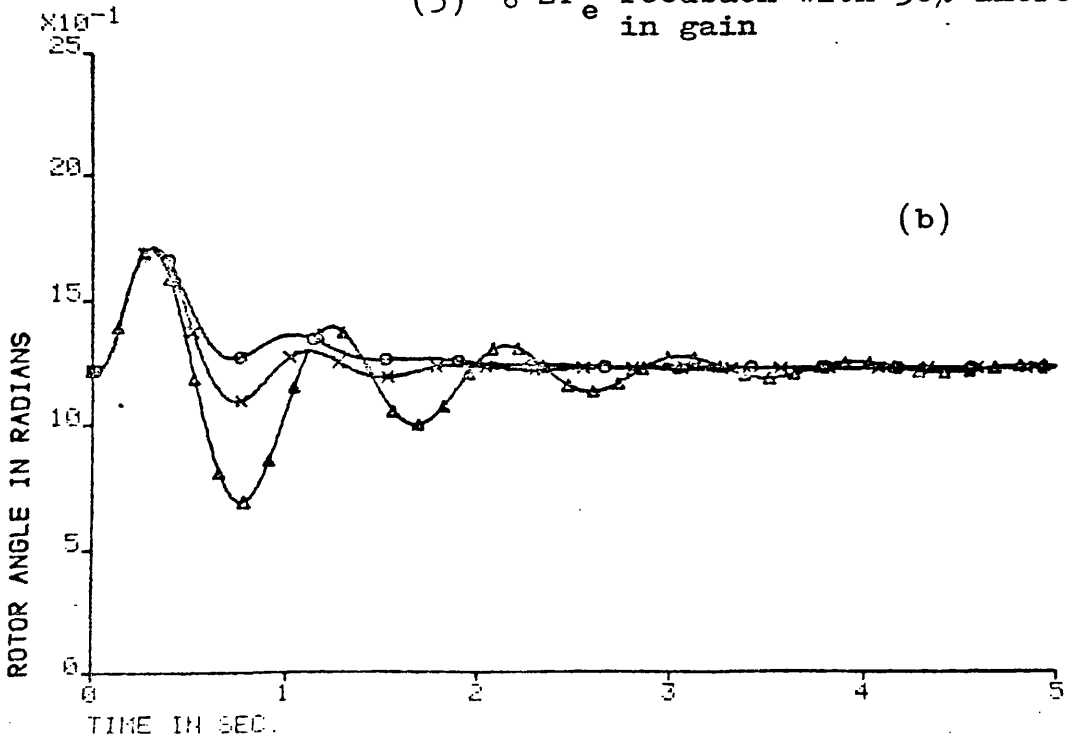

Fig. 4.9 Theoretical sensitivity curves for ΔP_e feedback

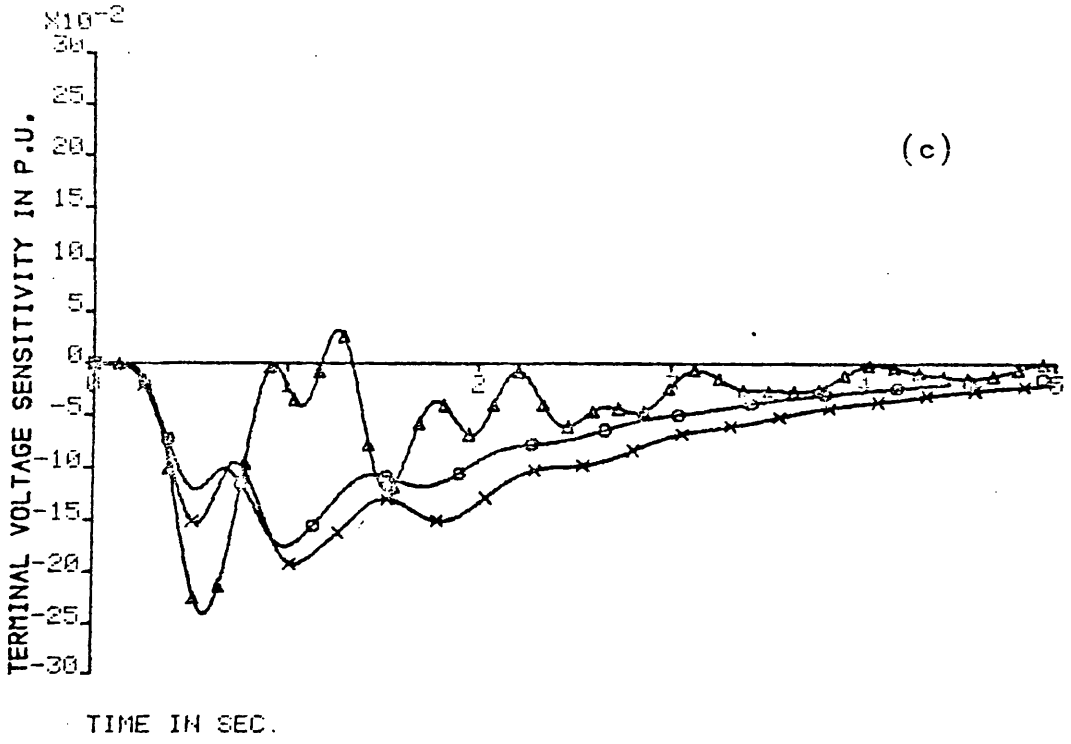

(1) Δ V_t feedback

(2) × ΔP_e feedback with nominal gain

(3) o ΔP_e feedback with 50% increase in gain

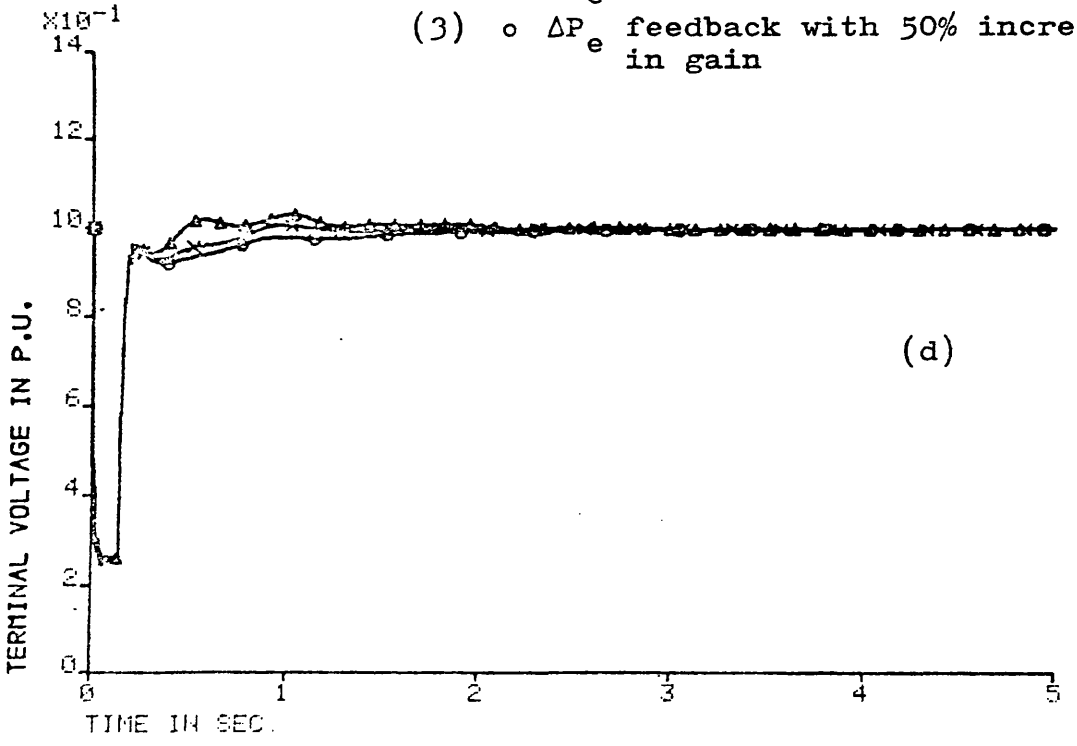

Fig. 4.9 Theoretical sensitivity curves for ΔP_e feedback

acting alone is to control the terminal voltage, the corresponding terminal voltage, sensitivity and response curves, shown as curve (1) in Figs. 4.9c and d confirm this point. However, inspection of the sensitivity curves of Fig. 4.9c shows that the use of ΔP_e feedback maintains a high degree of terminal voltage insensitivity to a large change in the associated feedback constant.

Corresponding curves obtained for feedback of $p^2\delta$ confirmed that the same general trends in system performance and sensitivity as those obtained for ΔP_e feedback did, in fact, exist.

A final comparison of the sensitivity of the load angle response for all four feedback systems is given in Table 4.6 which shows the comparative sensitivity S as the integral of the logarithmic sensitivity function, integrated over 5.0s with a standard fault condition and a fault duration of 0.14s. The corresponding value of

Feedback Signal	Integral of logarithmic sensitivity function	Value of PI
$\Delta\delta$	0.0286	0.86654
Δw	0.00166	1.24224
$p^2\delta$	0.00232	0.84662
ΔP_e	0.00245	0.84273

Table 4.6 Comparison of load angle sensitivities

performance index must be included if sensible comparisons are to be made. Larger values of the sensitivity

function S are inherently associated with reductions in system stability and larger values of the performance index obviously reduce the effectiveness of the presence of the extra feedback signal. Although the use of Δw feedback results in the lowest value of the logarithmic sensitivity function in Table 4.6, it also results in the highest value of the performance index. Feedback of $\Delta\delta$ produces a high value of the sensitivity S with a reasonable value for the performance index. Both ΔP_e and $p^2\delta$ feedback result in acceptable values for both sensitivity and performance index.

4.7 Discussion of Results

The method of single variable optimisation, based on a nonlinear mathematical model of a single-machine power system, has been successfully applied to the problem of the synthesis of a suboptimal excitation controller for a turbogenerator. Such a controller incorporates feedback of only one extra control signal, in additional to conventional terminal voltage feedback and the optimisation technique has been applied as a powerful method used to synthesise a control law based on the existence of a given single system state, available for feedback purposes. Many such signals have, in the past, been proposed for such a purpose and the use of four such signals has been fully investigated.

An application of dynamic sensitivity methods has brought

out several interesting phenomena about the relative suitability of these four particular signals. It is suggested that the extra information obtained by the use of sensitivity methods, which is obtained at a relatively low cost in extra computation, should always be used to assess the suitability of a particular feedback signal.

When the extra signal was taken as the change in the load angle during the disturbance, the corresponding output responses were found to be highly sensitive to parameter changes.

The relatively poor damping in oscillations in both the load angle and terminal voltage responses, obtained with transient rotor velocity feedback, were unacceptable and confirm the well established fact that phase compensation should be used with this signal.

Since governor action has been neglected, the system responses with feedback of either acceleration or transient electrical power are very similar. Both produced satisfactory transient responses and both are highly insensitive to parameter changes. However, in practice, transient electrical power can more readily be obtained as a control signal.

CHAPTER 5 OPTIMISATION OF EXCITATION CONTROL USING CLASSICAL BODE TECHNIQUES

5.1 Introduction

The classical methods of analysis, synthesis, and design of closed-loop control systems originated by Nyquist, Bode, Evans and many others, were originally developed at times when many arithmetical calculations were made by hand. Such methods have two basic functions. The first and more important function is to provide insight into the design procedure, particularly in cases where an adequate design may not exist, let alone be unique. The second function was to provide simple and, usually, approximate methods of analysis by the use of correlations between time-, frequency- and s-domain system responses. Although the advent of large digital computers tends to make the second function obsolete, it cannot fulfil the basic design function required. However, the development of powerful interactive graphics facilities now allows the system designer to interact effectively with the digital computer.

During the last decade, the design of an excitation control system for an a.c. turbogenerator has attracted much attention. Analyses of such a system have been performed, which are based on small disturbance system behaviour using Routh's criterion[77], the Nyquist plots[78], Root-locus diagrams[79,80], phase plane techniques[81] and synchronising torque concepts[82]. Design techniques such

as pole-zero cancellation[83], root contour methods[84] and multi-variable frequency response methods[85,86] have all been applied to the problem. However, in order to determine the general applicability of these synthesised compensators, the system behaviour when subjected to a large disturbance should also be assessed, together with an investigation of the usefulness of the given compensator for different sets of system parameters and operating conditions. In a recent publication[87], which is a result of the previous chapter, examples of the syntheses of various stabilisers based on nonlinear optimisation have been demonstrated but no attempt has been made to complete the excitation control design. Such a method of synthesis can sometimes be used as an ingradient of design but has limited power by itself.

The general open-ended design technique to be described is based on an application of Bode techniques to obtain a suitable basic form of compensation with accurate values determined precisely by nonlinear optimisation techniques carried out on an interactive graphics terminal.

5.2 System Configuration

The system under study consists of a single machine connected to an infinite busbar through a step-up transformer and a double circuit transmission line in the general manner described by Fig. 4.4. A set of seventh order derived voltage equations is used to represent the system during the nonlinear optimisation study. Simplified third

order equations obtained by neglecting the decay of stator flux linkages and the presence of damper windings form the basis for Bode design. The system performance has been assessed for a large disturbance in the form of a symmetrical 3-phase short circuit, at the high-voltage terminals of the transformer, of set duration with system initial conditions of 0.85p.u. power, unity power factor at the busbar and 1.0p.u. terminal voltage. Only excitation control is considered with the mechanical input power assumed to be constant.

5.3 The Basic Design Method

5.3.1 General

In an initial attempt to establish the relative influences of the various feedback paths on the model of an uncontrolled synchronous machine, a classical control approach based on the concepts of Bode techniques has been used. This is made possible with the aid of signal-flow graph representation of the linearised third order machine differential equations with all the system resistances being neglected. The system initial conditions corresponding to the specified operating conditions are

$$V_b = 0.95415 \text{ p.u.}$$
$$\delta_o = 1.21721 \text{ rad.}$$
$$v_{do} = 0.83243 \text{ p.u.}$$
$$v_{qo} = 0.55414 \text{ p.u.}$$
$$i_{do} = 0.83573 \text{ p.u.}$$
$$i_{qo} = 0.30847 \text{ p.u.}$$

5.3.2 System Equations Manipulation

The set of equations representing the nonlinear third order model of the machine system which neglects system resistances can be obtained from equations in section 3.2 in the general form:

$$pe_q' = (V_f - (x_d - x_d')i_d - e_q')/T_{do}' \quad (5.1)$$

$$p\delta = \gamma \quad (5.2)$$

$$p\gamma = (T_m - T_e - K_d\gamma/w_o)/M \quad (5.3)$$

$$0 = v_d - x_q i_q \quad (5.4)$$

$$e_q' = v_q + x_d' i_d \quad (5.5)$$

$$v_d = V_b \sin\delta - X_t i_q \quad (5.6)$$

$$v_q = V_b \cos\delta + X_t i_d \quad (5.7)$$

$$V_t = \sqrt{(v_d^2 + v_q^2)} \quad (5.8)$$

$$T_e = v_d i_d + v_q i_q \quad (5.9)$$

By applying the theory of small perturbations to the above set of equations, the following linearised equations are obtained:

$$p(\Delta e_q') = (\Delta V_f - (x_d - x_d')\Delta i_d - \Delta e_q')/T_{do}' \quad (5.10)$$

$$p(\Delta\delta) = \Delta\gamma \quad (5.11)$$

$$p(\Delta\gamma) = (\Delta T_m - \Delta T_e - K_d\Delta\gamma/w_o)/M \quad (5.12)$$

$$\Delta i_q = \Delta v_d/x_q \quad (5.13)$$

$$\Delta i_d = (\Delta e_q' - \Delta v_q)/x_d' \quad (5.14)$$

$$\Delta v_d = V_b \cos\delta_o \Delta\delta - X_t \Delta i_q = \frac{V_b \cos\delta_o \Delta\delta}{1 + X_t/x_q} \quad (5.15)$$

$$\Delta v_q = -V_b \sin\delta_o \Delta\delta + X_t \Delta i_d \quad (5.16)$$

$$\Delta V_t = (v_{do}\Delta v_d + v_{qo}\Delta v_q)/ V_{to} \quad (5.17)$$

$$\Delta T_e = v_{do}\Delta i_d + i_{do}\Delta v_d + v_{qo}\Delta i_q + i_{qo}\Delta v_q \quad (5.18)$$

where suffix o represents initial condition before the disturbance and prefix Δ shows the change in the system parameters during the disturbance. If, for example, the mechanical torque is assumed to be constant during the disturbance, it follows that the term ΔT_m in eqn. 5.12 is zero.

This set of equations can then be Laplace transformed, and, with minor rearrangements, can be represented by the following finalised form:

$$\Delta e_q' = \frac{x_d - x_d'}{1+T_{do}'s} \Delta i_d + \frac{1}{1+T_{do}'} \Delta V_f \quad (5.19)$$

$$\Delta\delta = \frac{1}{s} \Delta\omega \quad (5.20)$$

$$\Delta\omega = \frac{1}{Ms+K_d/w_o} (\Delta T_m - \Delta T_e) \quad (5.21)$$

$$\Delta v_d = V_b \cos\delta_o \Delta\delta - X_t \Delta i_q \quad (5.22)$$

$$\Delta v_q = -V_b \sin\delta_o \Delta\delta + X_t \Delta i_d \quad (5.23)$$

$$\Delta V_t = \frac{V_b}{V_{to}} \left(\frac{v_{do}\cos\delta_o}{1+X_t/x_q} - v_{qo}\sin\delta_o\right)\Delta\delta + X_t v_{qo}/V_{to}\, \Delta i_d \quad (5.24)$$

$$\Delta T_e = v_{do}\Delta i_d + i_{do}\Delta v_d + v_{qo}\Delta i_q + i_{qo}\Delta v_q \quad (5.25)$$

Equation 5.24 has been obtained by substituting eqns. 5.15 and 5.16 into eqn. 5.17.

Since the main object of excitation control is to maintain the terminal voltage within specified limits for a wide range of steady operating conditions, a high forward path gain is required and the typical form of the excitation system is illustrated in Fig. 4.4, such that, by simple block diagram manipulation

$$E(s) = \frac{K_g(1+sT_s)}{(1+sT_g)(1+sT_s) + sK_gK_s} \qquad (5.26)$$

with, typically, $K_g = 200$, $K_s = 0.035$, $T_g = 0.5$, $0.5 \leq T_s \leq 2.0$. The saturation effect of the excitation system described in section 3.4 should be noted.

5.3.3 Signal-Flow Graph Representation

The corresponding signal-flow graph representation of eqns. 5.19-5.25 is given in Fig. 5.1. For simplicity in presentation, both the Δ prefix and the do' suffix for the time constant have been deleted in this and all the following signal-flow graphs.

The basic flow diagram can be simplified by standard signal-flow graph manipulations as demonstrated in Appendix A5. The resulting flow diagram is given in Fig. 5.2, where

$$G(s) = \frac{1}{Ms^2 + K_d/w_o s} \qquad (5.27)$$

$$H_1 = \frac{V_b \cos\delta_o (v_{qo} + x_q i_{do})}{x_q + X_t} - V_b \sin\delta_o \, i_{qo} \qquad (5.28)$$

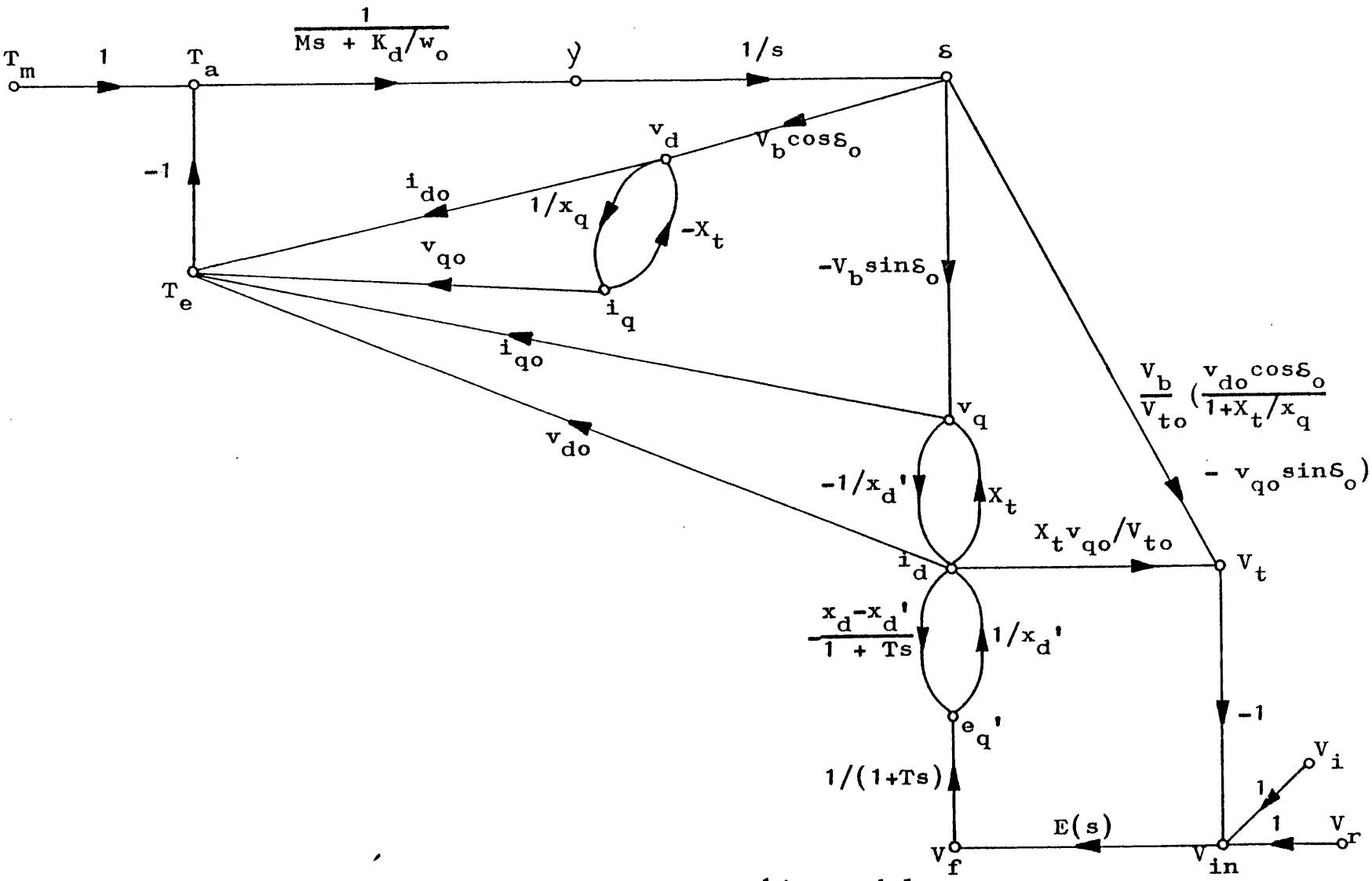

Fig. 5.1 Signal-flow graph of third order machine model

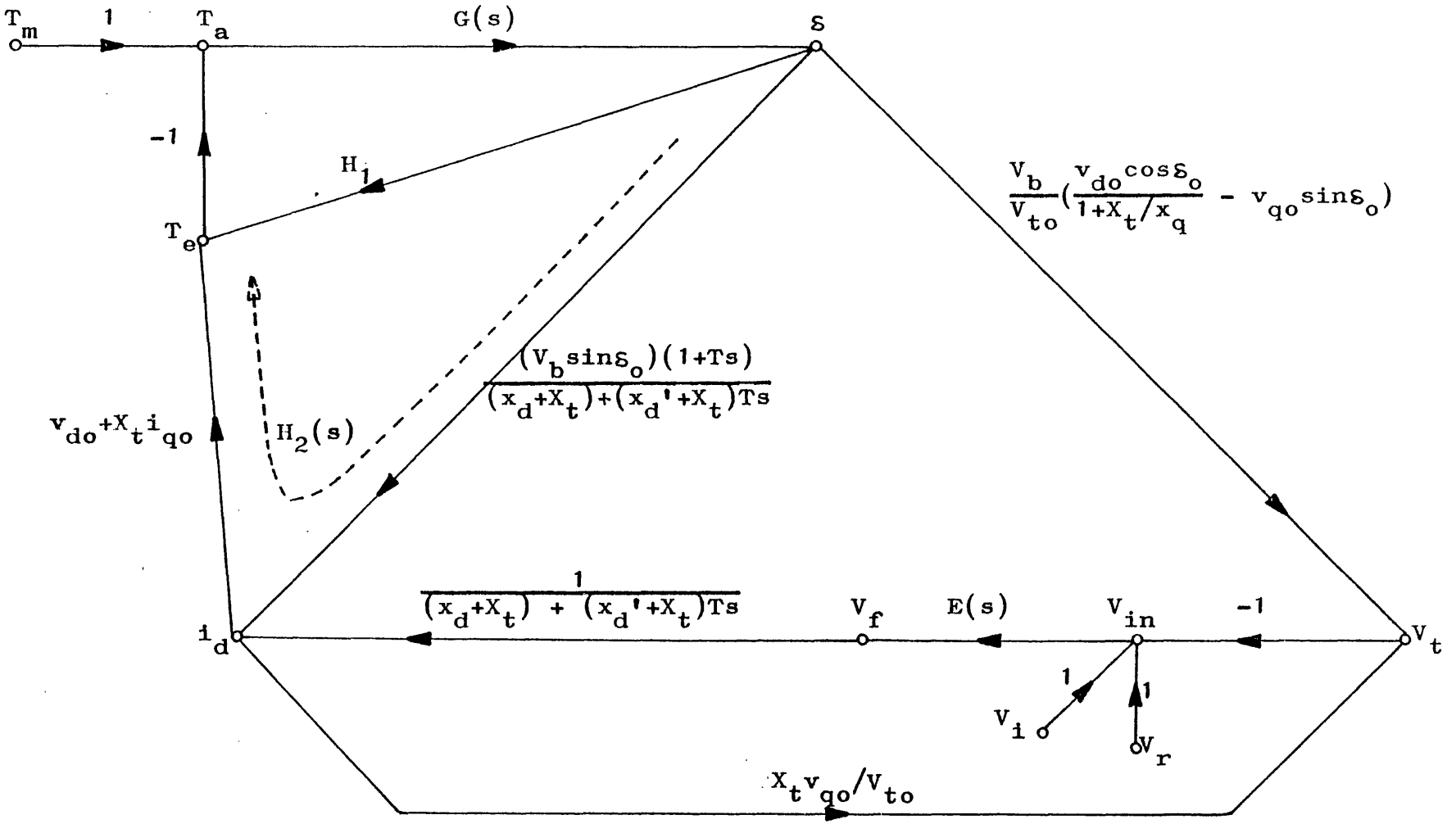

Fig. 5.2 Simplified signal-flow graph

When the values of system parameters listed in Appendix A2 and the given initial conditions of section 5.3.1 are substituted into the transmittances of Fig. 5.2, the following simplified diagram of Fig. 5.3 is obtained.

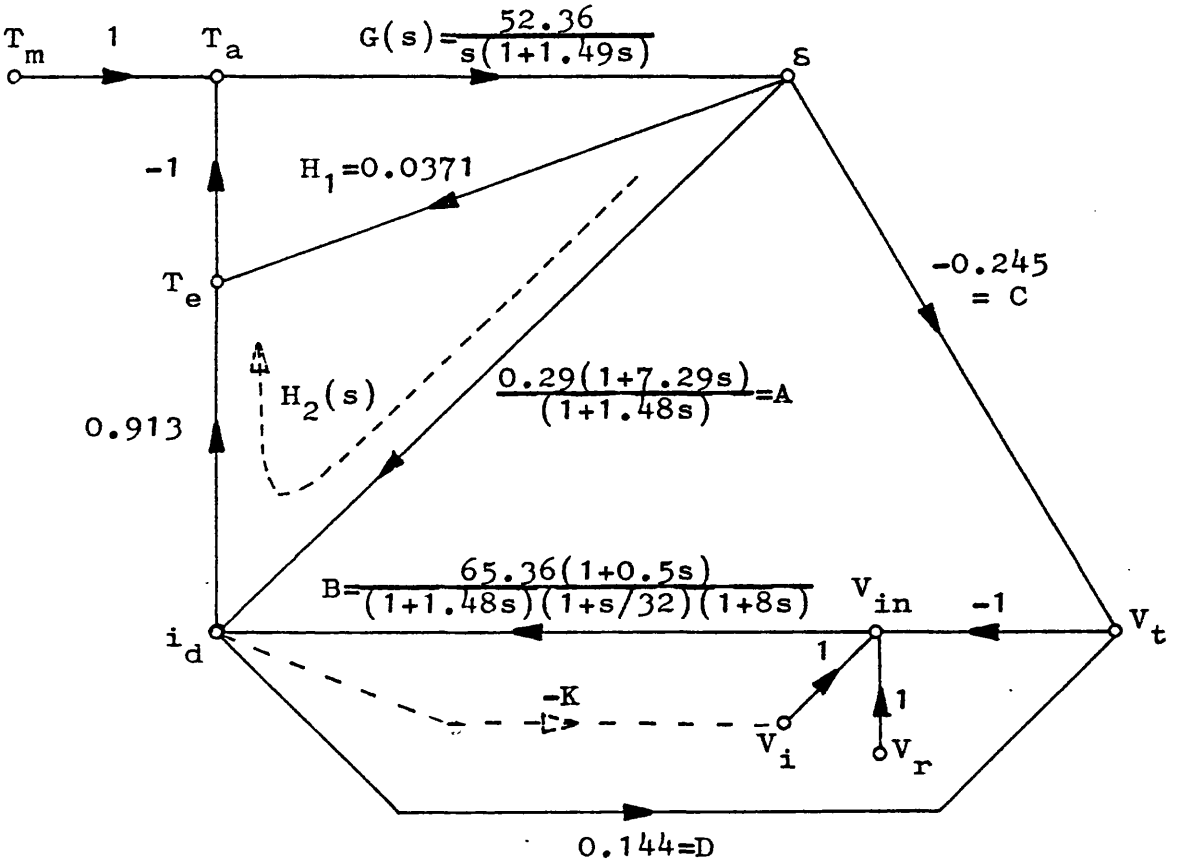

Fig. 5.3 Simplified signal-flow graph

5.3.4 Feedback of Direct-Axis Current

It can immediately be seen from Fig. 5.3 that the system quantity, direct-axis current i_d, is at the 'crossroad' of all transmittances to the electrical torque T_e, except the frequency-independent path H_1 from δ to T_e. It can readily be seen later from the log modulus plots that at

the operating conditions considered, H_1 is negligible compared with the transmittance via i_d, which is called $H_2(s)$.

Any feedback to the input V_i of the system must suffer a phase shift introduced by the presence of the transfer function E(s) of the excitation system as well as that introduced by the presence of the time constant T. One obvious way to reduce these lags is to close the loop from i_d to V_i.

5.3.5 Bode Design

For simplicity in representation, only the asymptotic approximations are shown in the log modulus plots. Consider the overall transfer function characteristic from δ to i_d, where

$$i_d = \frac{A+BC}{1+BD}\,\delta \qquad (5.29)$$

Using the Bode techniques described in section 2.7, log modulus plots of $|A+BC|$ and $|1+BD|$ are easily derived as shown in Fig. 5.4. The division process of $|(A+BC)/(1+BD)|$ is seen to be approximately, as $|BC/BD|$ before 0.67rad/s, and, as $|A|$ after 0.67rad/s. The resulting log modulus of i_d/δ is a flat straight line to a close approximation.

Suppose a negative feedback path with a fixed gain K from i_d to V_i is introduced, which is equivalent to a positive feedback path from i_d to V_t, the new transmittance

from i_d to V_t becomes

$$D' = D + K \tag{5.30}$$

In the particular case when K=0.3, the resulting log modulus diagram is modified with the transmittance D being replaced by D' as indicated in Fig. 5.4. This modification does not qualify for V_t calculation, and is adopted here only for the ease of manipulation of transfer functions.

Figure 5.5 shows the log magnitude characteristic of δ/T_m. For the a.v.r. system, the transmittance A from δ to i_d is approximately a frequency independent constant value of 1.6 as indicated in Fig. 5.4. Since H_2 is the transmittance from δ to T_e via i_d, H_2 for a.v.r. is simply given as

$$H_2 = 1.6 \times 0.913 \tag{5.31}$$

at all frequencies. Similarly, with proportional i_d feedback, the modified H_2 becomes

$$H_2'(s) = \frac{i_d}{\delta}(D') \times 0.913 \tag{5.32}$$

The log magnitude plots corresponding to $|G(jw)|$, $|1/H_1|$, $|1/H_2|$ and $|1/H_2'(jw)|$ are given in Fig. 5.5. Although there are in fact two feedback paths H_1 and H_2 in this simplified system, it is apparent from an inspection of Fig. 5.5 that the system is dominated by the feedback path H_2 such that, by application of simple Bode techniques, the closed-loop system has a resonant

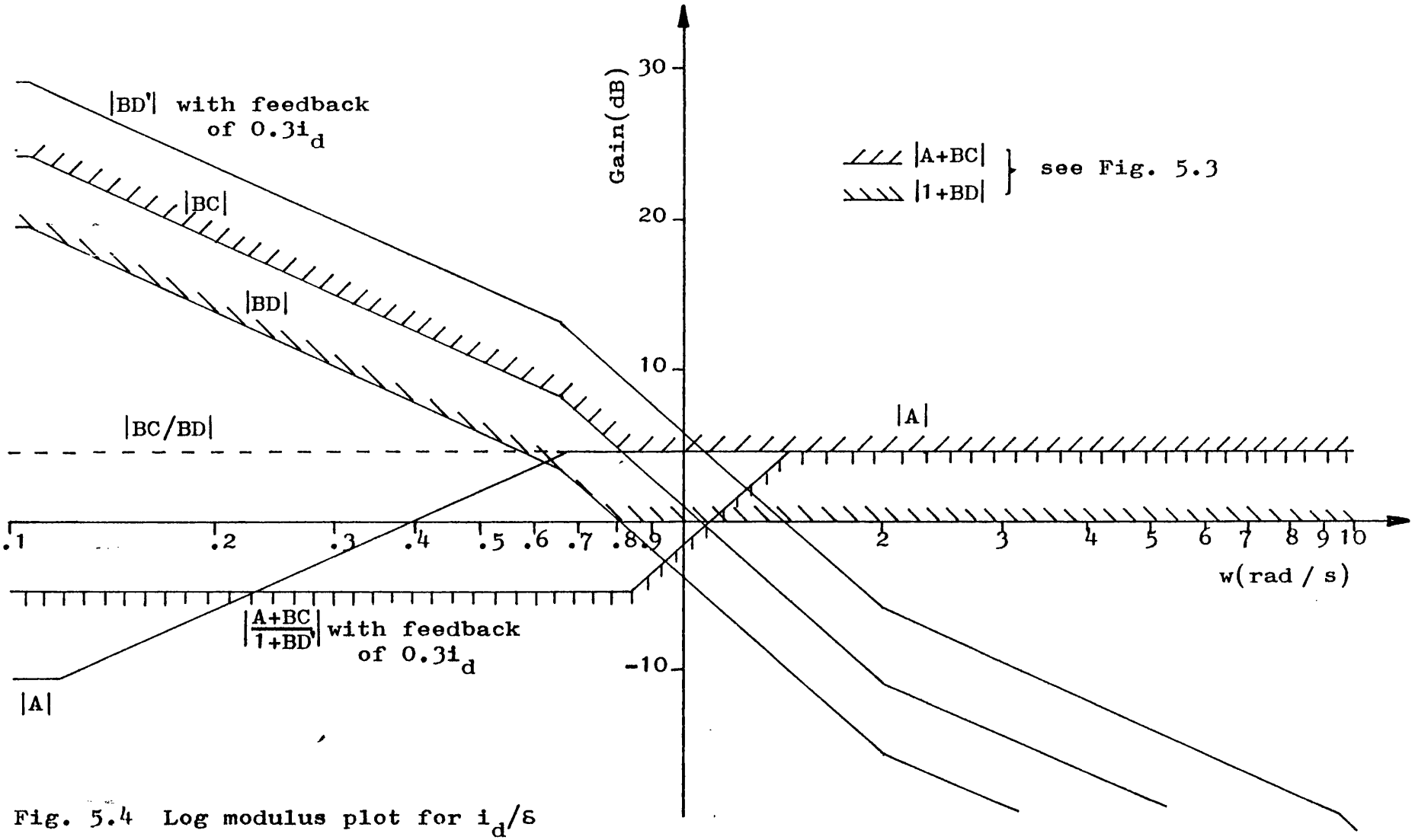

Fig. 5.4 Log modulus plot for i_d/δ

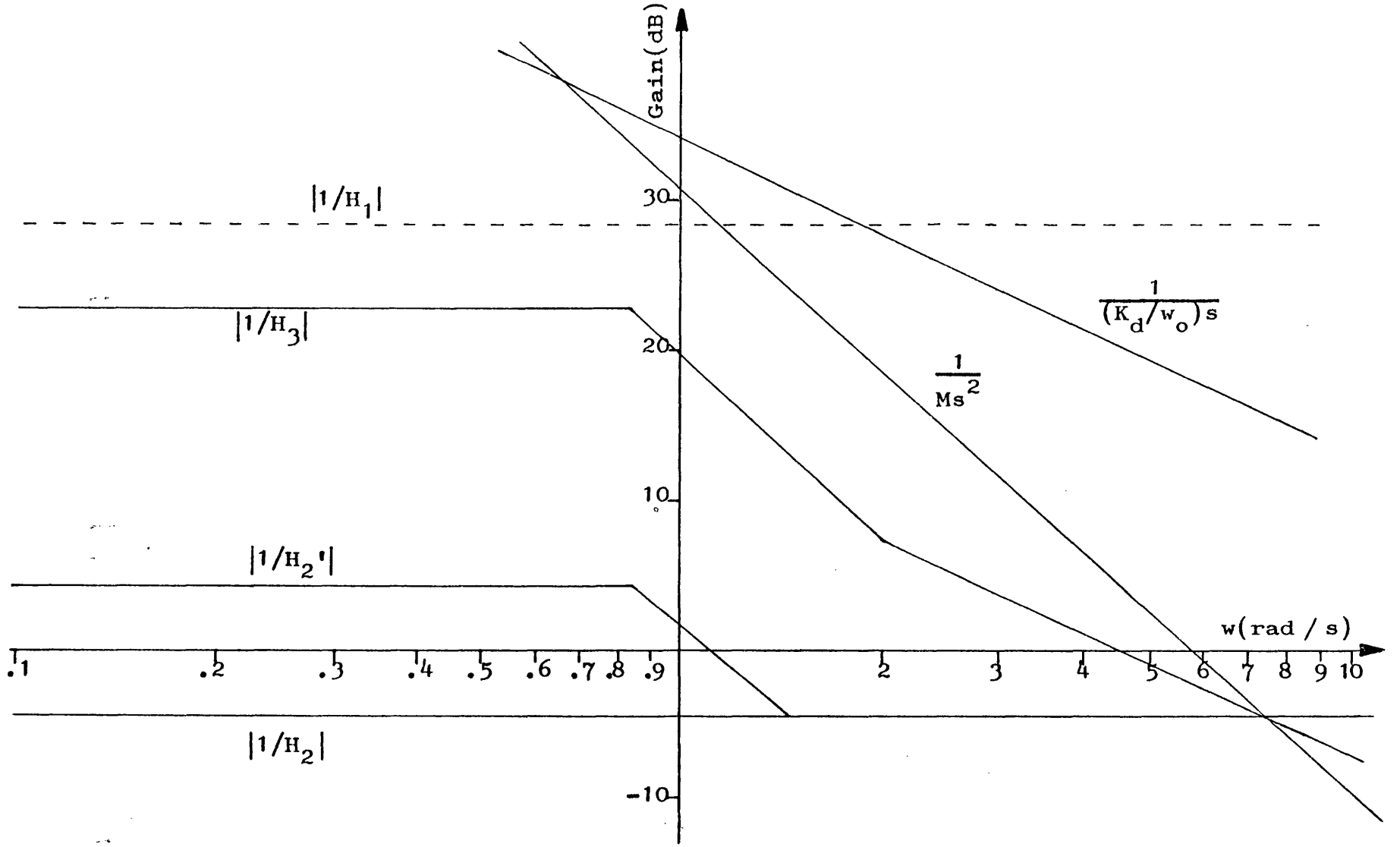

Fig. 5.5 Log modulus plot for ε/T_m

pole pair at w = 7.5rad/s. For the a.v.r. system, the flat characteristic of H_2 does not give any additional damping other than the natural mechanical damping K_d. With the closure of the loop round i_d to V_i, almost all the damping comes from the phase advance of $H_2'(jw)$.

One obvious way to increase system damping is to increase the i_d feedback gain constant K to a value such that, the phase advance zero of $1/H_2'(jw)$ is now at the resonant frequency, giving 50% of critical damping, indicated as $|1/H_3(jw)|$ in Fig. 5.5. However, this increase in the gain constant will probably reduce the total outer loop gain at low frequencies to such a value that the primary voltage control will be severely degraded. Furthermore, the neglected frequency-independent feedback path of H_1 has to be taken into account when the gain constant K is being pushed up.

At this stage, the classical design approach seems to clearly indicate that the use of feedback of the direct-axis current into the excitation system with a suitable value of gain constant could improve the transient response in the operating load angle without deteriorating the terminal voltage response. This classical approach has been used as a design method to show which system quantities could be used to improve the total system performance. The resulting synthesis to obtain appropriate values for the feedback constant K, and the subsequent sensitivity studies of the system may

therefore be performed using a more elaborate simulation of the nonlinear system model in conjunction with some form of optimal control method.

5.4 Nonlinear Single Variable Optimisation

5.4.1 General

Nonlinear single variable optimisation using both quadratic and cubic approximation algorithms have been described in the previous chapter. A search procedure making use of both algorithms has been adopted here as shown in the flow chart of Fig. 5.6. In this way, a local optimum can be guranteed without a deliberate initial choice of step length and accuracy specification.

In the present study, the extra feedback signal V_i of Fig. 4.4 is defined as

$$V_i = K \Delta i_d \tag{5.33}$$

where K is the optimising parameter and Δi_d is the change in the proposed feedback signal, the direct-axis current. The performance index is defined as

$$I = \int_o^T (A_1 \Delta V_t^2 + \frac{A_2}{0.1+t} \Delta \delta^2) dt \tag{5.34}$$

where V_t is the machine terminal voltage, δ is the operating load angle. Weighting factors A_1 and A_2 have been chosen to be 1 and 5 respectively with the integral

of eqn. 5.34 evaluated over 3.5s in attempts to find the optimised value of the parameter K of eqn. 5.33. The convergence criterion has been assumed to be satisfied when $|K(\text{last})-K(\text{current})| < 0.001$, the specified accuracy ϵ.

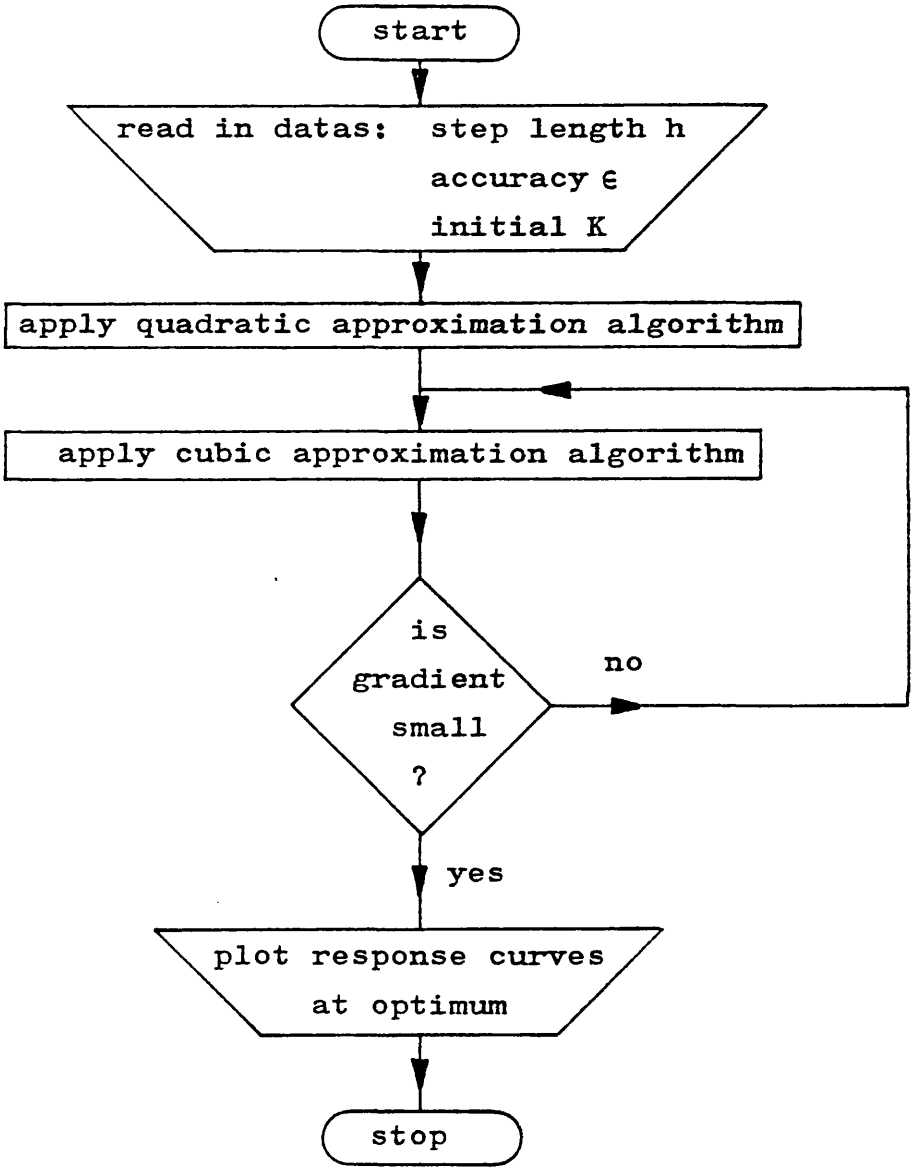

Fig. 5.6 Flow chart for optimisation studies

5.4.2 Optimisation Studies

It has previously been noted in Chapter 4 that step length is critical in the cubic approximation while the quadratic approximation may miss a local minimum. However, use of the flow chart as shown in Fig. 5.6 will safeguard against such discrepancies. A demonstrative example is listed in detail in Table 5.1 to show the procedure.

Control Number	Step Length	Iteration Count	Feedback Gain	Gradient Value	Value of PI
Q11	0.5	1	0.0	/	4.7107
		9	-0.3522	/	3.5169
C12	0.01	1	-0.3522	-0.00726	3.5169
		2	-0.3422	0.6499	3.5439
C13	0.001	1	-0.3452	0.62	3.5423
		2	-0.346	0.047	3.5171

Table 5.1 Optimisation studies with T_s=0.5, fault duration=0.22s

The computational time for the quadratic approximation is about 8s CPU time per iteration on the PDP10 computer at UMIST and 13s for the gradient optimisation. The total CPU time for Table 5.1 is about 2min and the local minimum has been exactly located to lie between -0.346 and -0.3522, the values arrived at the eleventh and the last iteration respectively.

Control Number	T_s	Fault duration	Value of PI (K=0)	Final Gain	Gradient Value	Total Iteration Count	Value of PI
QC2	1	0.22	4.5566	-.315	-.0062	10	3.4423
QC3	1	0.14	1.2111	-.346	.1432	15	.8383
QC4	2	0.14	1.2485	-.309	-.0116	17	.8102

Table 5.2 Optimisation studies with defferent T_s and fault durations

Table 5.2 listed above shows the result of the optimisation studies when the machine is subjected to different fault durations and different excitation system stabilising feedback time constants T_s. The step length, h, for each of the initial quadratic approximation optimisation is fixed to be 0.5. This is then appropriately adjusted for the subsequent cubic approximation optimisation. An optimum is arrived at the point where the gradient is finally reduced to near zero.

One general conclusion can be made from the results of Tables 5.1 and 5.2. Although there are differences in the fault durations applied and system parameters, the order of magnitude of the optimum feedback gains is not changed. This suggests that the proposed feedback control system will not be sensitive to these variations.

It is interesting to note that feedback of $K\Delta i_d$ is equivalent to feedback of $Kf(\Delta\delta,\Delta e_q')$. From the manipulation of the signal-flow graph as shown in Appendix A6, it can be found that

$$K\Delta i_d = K\Delta e_q'/(x_d'+X_t) + K\Delta\delta V_b \sin\delta_o/(x_d'+X_t) \quad (5.35)$$

Burrows and Daniels[36] suggested feedback combination of

$$- 0.564 \Delta e_q' - 0.4613 \Delta\delta$$

which is roughly equivalent to feedback of $- 0.34 \Delta i_d$.

5.4.3 Transient Response and Sensitivity Curves

The results of the optimisation studies given in the previous section have been applied to give the field voltage, load angle and terminal voltage transient response curves of the single-machine system with transient direct-axis current as the additional signal fed into the excitation system. A full range of operating conditions has been investigated with the results obtained using the seventh order nonlinear machine model. Typical results are given in Figs. 5.7 and 5.8 for fault durations of 0.14s and 0.22s respectively with results plotted for 5s. Curve (2) of both figures show the results obtained for feedback of Δi_d with nominal gain values. Curve (3) of Fig. 5.7 corresponds to a 30% increase while curve (3) of Fig. 5.8 corresponds to a 30% decrease in the value of the nominal gain constant. The results obtained using terminal voltage feedback acting alone has been included in both figures for comparison purposes.

The input control law is shown as the field voltage response curves of Figs. 5.7c and 5.8c and clearly shows the effect of the additional single feedback signal in forcing the field voltage away from its positive ceiling value earlier than that obtained with terminal voltage

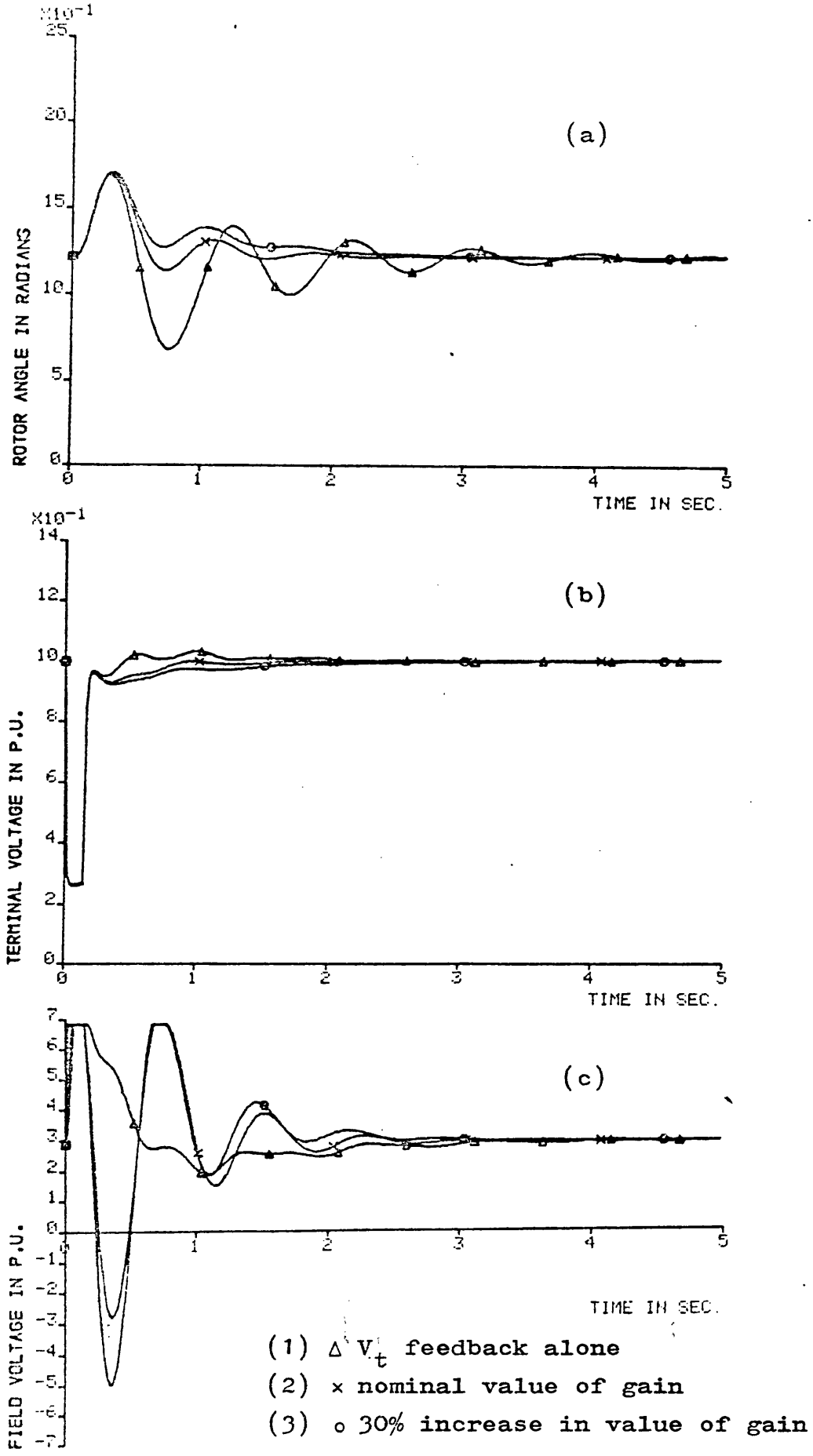

Fig. 5.7 Theoretical response curves for Δi_d feedback

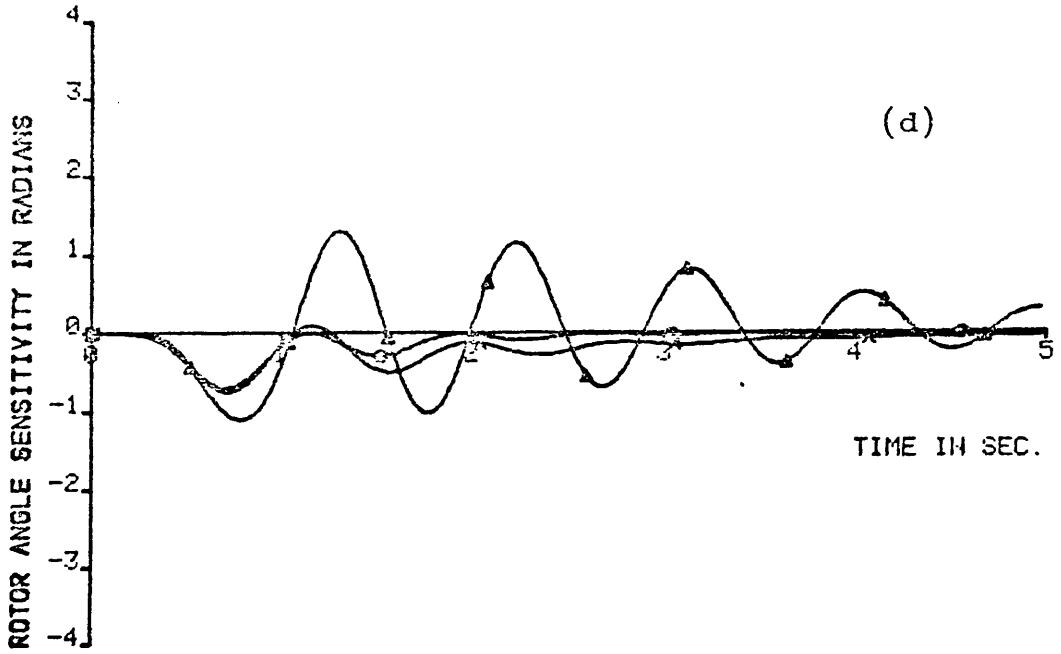

(1) Δ V_t feedback alone
(2) × nominal value of gain
(3) ∘ 30% increase in value of gain

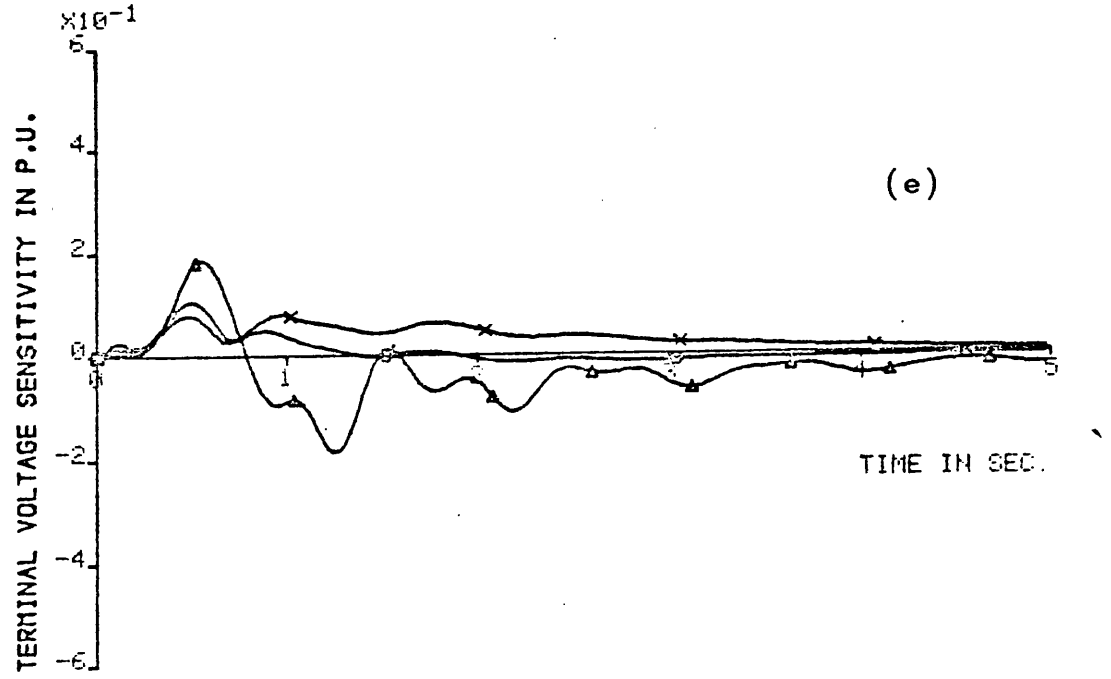

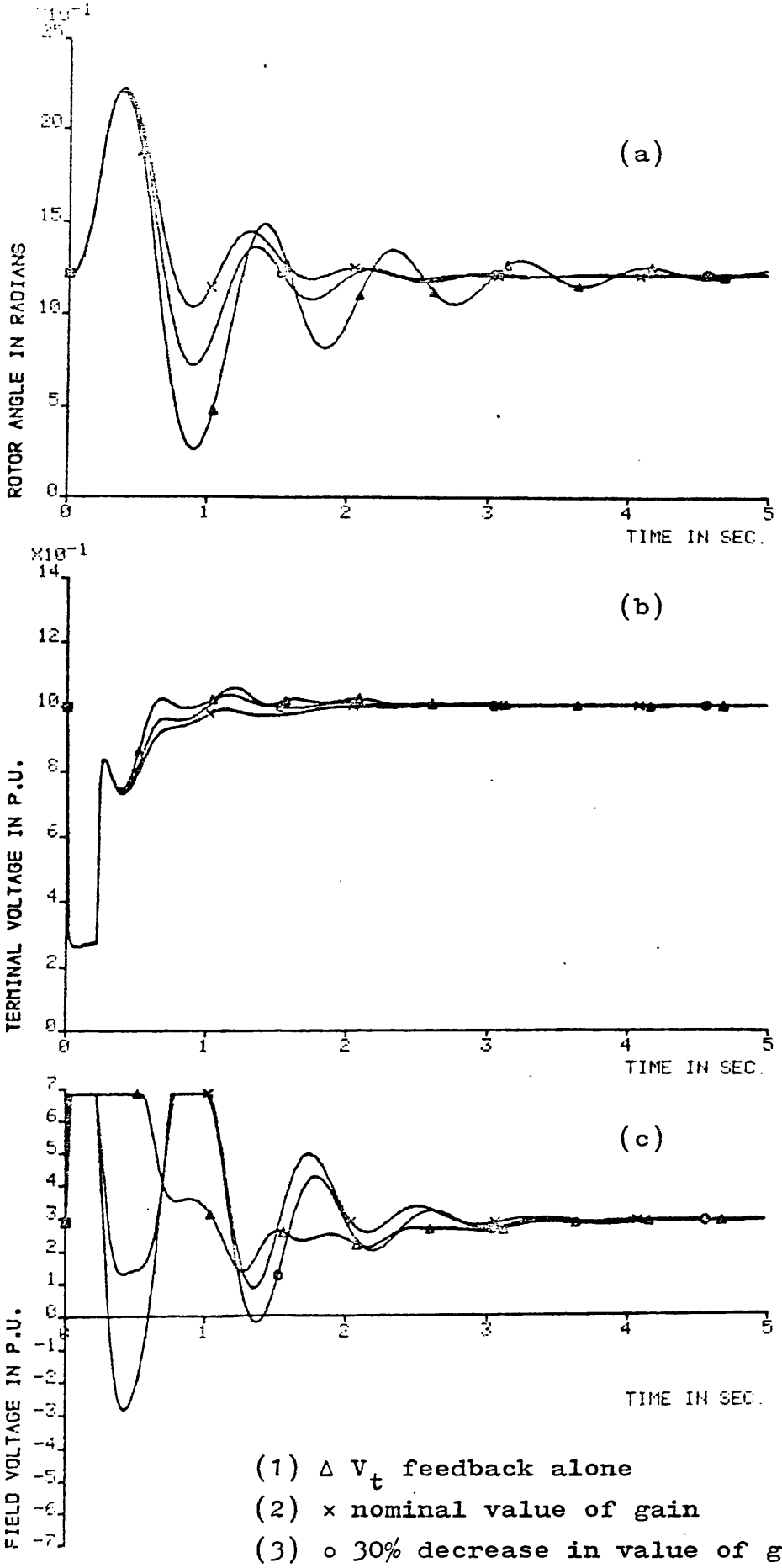

Fig. 5.8 Theoretical response curves for Δi_d feedback

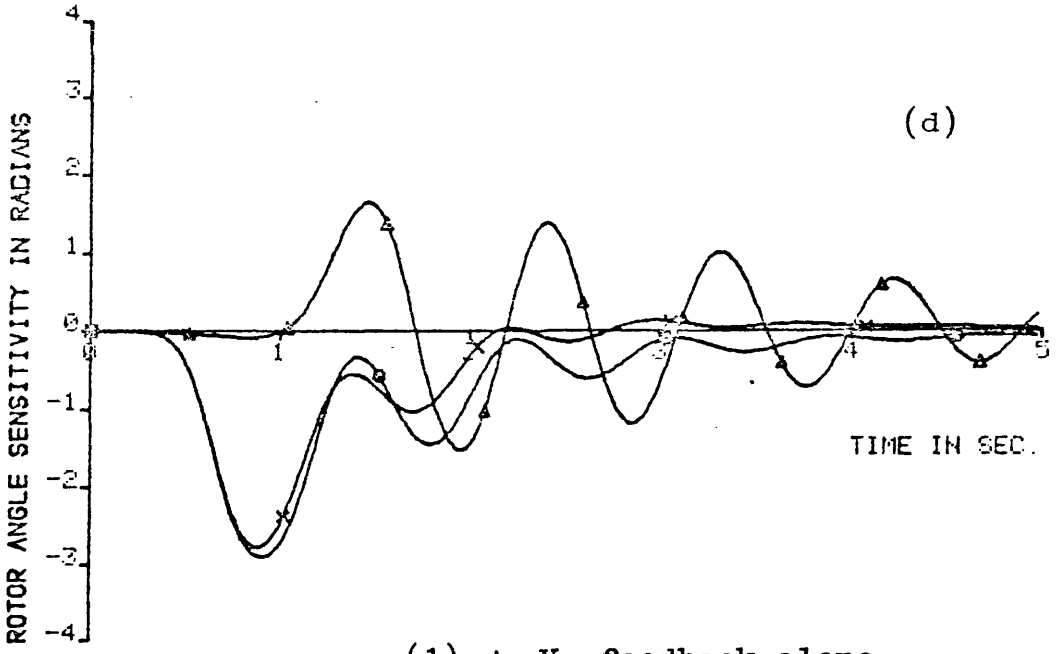

(1) Δ V_t feedback alone
(2) x nominal value of gain
(3) o 30% decrease in value of gain

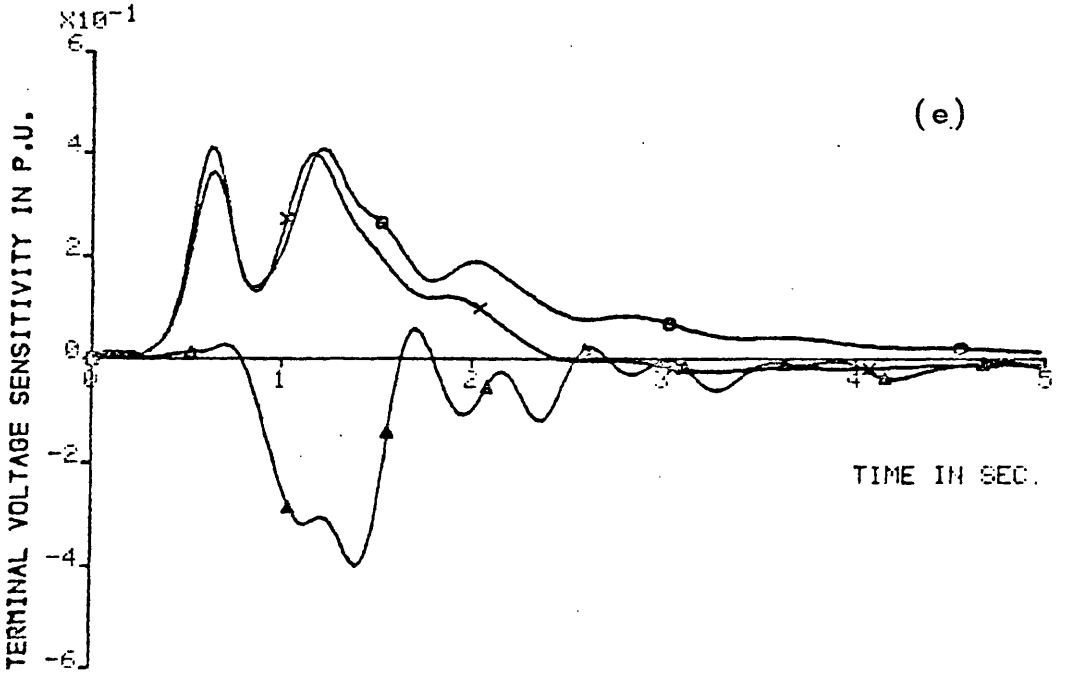

feedback acting alone. In all cases, except curve (3) of Fig. 5.8c where the feedback gain constant is 30% less than the nominal value, there is a short excursion into negative field voltage. The rapid decrease in field voltage and its subsequent reversal are, of course, only possible with the modern thyristor excitation systems and are not possible with rotating diode excitation systems.

Inspection of the load angle curves of Figs. 5.7a and 5.8a shows that, in all cases, when the extra control signal is fed back into the excitation system, an improvement in the damping in rotor oscillations after the first peak, is obtained. Since all the excitation controllers considered force the excitation to the same positive ceiling value, they all give the same value in the first peak in rotor angle.

Because the prime object of feedback of terminal voltage alone is to regulate terminal voltage, the terminal voltage response curves of Fig. 5.7b and 5.8b confirm this fact. However, the terminal voltage responses obtained with feedback of Δi_d are very acceptable.

A study of the variation in the value of the given performance index with the feedback gains is shown in Fig. 5.9. The value of the performance index with feedback of terminal voltage acting alone is when the gain constant K is zero on the curve. It can be seen that the feedback system is quite insensitive to changes in the feedback constant and this result is confirmed by the sensitivity

curves shown in Figs. 5.7 and 5.8. Figures 5.7d and 5.8d give the rotor angle sensitivity curves, and clearly show that the system angle response is quite insensitive to the large change in feedback constant. The corresponding curves shown in Figs. 5.7a and 5.8a confirm this fact. Corresponding curves for terminal voltage sensitivity and response are given in Figs. 5.7c, 5.7e, 5.8c and 5.8e. Because the prime object of terminal voltage feedback acting alone is to control the terminal voltage, the corresponding terminal voltage sensitivity and response curves, shown as curve (1) in the above-mentioned figures confirm this point.

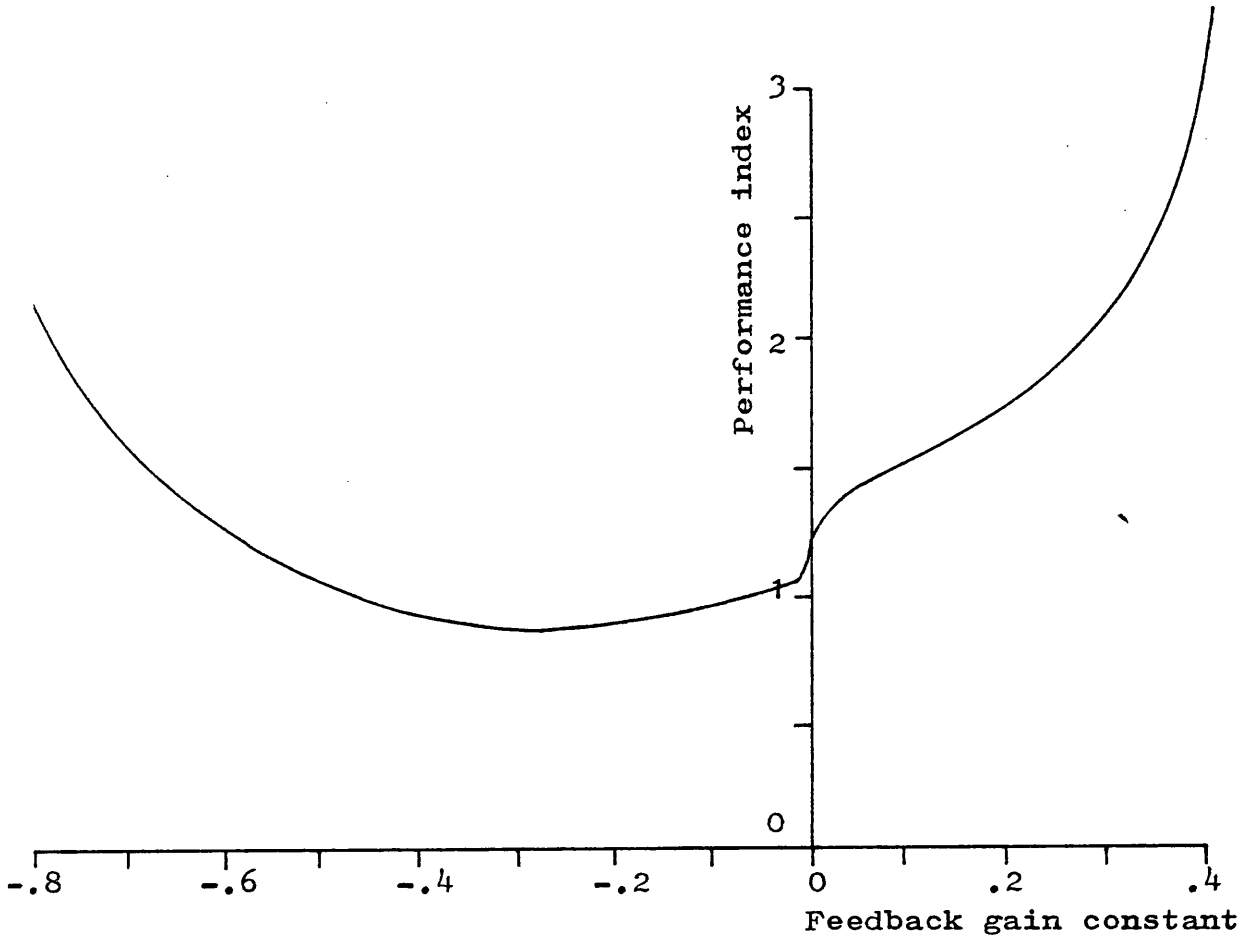

Fig. 5.9 Variation of performance index with change in feedback gain

5.5 Discussion of Results

The open-ended design/synthesis approach, based on Bode techniques and nonlinear single variable optimisation, has been successfully applied to the problem of excitation controller for an a.c. turbogenerator. Such a controller incorporates feedback of only one extra control signal, in addition to the conventional terminal voltage feedback. This particular stabilising signal, the direct-axis current, has not been used in the past as a single-state excitation feedback controller.

A previous investigation using nonlinear multi-variable optimisation technique involves the combination of feedback signals of voltage behind transient reactance, e_q', and load angle, δ. That powerful gradient technique does indeed suggest feedback of the highly disguised direct-axis current signal, i_d, through some algebraic manipulations. The choice of such a signal amongst all the possible system states has become obvious when signal-flow graphs and Bode techniques are used in this design exercise.

The transient response curves of the feedback system suggest that this new stabilising feedback controller can lead to an improvement in the response of the power system when subjected to a large disturbance. The sensitivity functions of the system states, which are generated as a by-product of the synthesis program, can give extra useful information. When the feedback system has been optimised, the corresponding output responses were found to be highly insensitive to parameter changes.

CHAPTER 6 EXPERIMENTAL STUDIES

6.1 Introduction

This chapter describes the experimental results using various control laws of the form discussed in Chapters 4 and 5. It is preferable to be able to implement optimal controllers obtained by theoretical studies on a real machine system, and a small laboratory model system or so-called micromachine system has been developed for this purpose.

The microalternator and transmission line system has its per unit quantities scaled to closely resemble those of the Pembroke power station, which is a large capacity generating complex, situated remote from the grid system. Thus , it represents the classical situation of a generator, long transmission line, infinite busbar problem, often used in transient stability analysis.

Past research has concentrated on the improvement of transient stability by the use of excitation control, and, in particular, the use of multi-state feedback techniques has been fully investigated[74,75]. In the present study, however, the proposed controller has been incorporating only one extra feedback signal into the excitation system in addition to the normal terminal voltage feedback signal. These extra feedback signals are

(a) the change in operating load angle $\Delta\delta$,

(b) the change in rotor velocity from synchronous speed, Δw,

(c) the rotor acceleration $p^2\delta$,

(d) the transient electrical output power ΔP_e and

(e) the transient direct-axis current Δi_d.

The first four signals have all previously been used by various authors. The transient direct-axis current controller is the result of the design exercise of Chapter 5, and such a controller has not been used in the past. The transduced feedback signals have all been generated digitally such that the noise problem is reduced.

All the experiments have been performed using a constant torque drive to simulate the steam turbine, which was assumed to contribute little to the transient stability problem in the present study.

6.2 Laboratory Micromachine System

In order to realise an excitation controller of the state feedback form, and to facilitate suitable comparison of different schemes, it is vital to have an efficient data collection and storage system. Previous attempts at purely analogue methods failed, in a control sense, due to noise problems. Only when digital methods were implemented[88] was it possible to provide relatively noise free state feedback, and efficient data collection. The micromachine system[89] and the more recent digital excitation control schemes[88] at the University of Bath have been fully documented elsewhere. Therefore, only a brief summary

of the control system is given below.

The block diagram of the digital system is shown in Fig. 6.1[90]. The philosophy of the system is to use the power of the PDP11/20 minicomputer as the interface between the operator and control system, as a data logger, and also as a floating point arithmetic unit for the I8080 microprocessor. The necessary control laws are generated within the remote minicomputer system and transmitted to the microprocessor in digital form, through 30m of multi-core cable, where they are decoded into a form suitable for the input to the main transistor d.c.-coupled linear power amplifier supplying the excitation system. The whole system operates in a real-time mode, and allows data acquisition under both steady and transient operating conditions, with the relevant system states obtained using dedicated transducers. The particular transducer used to obtain signals corresponding to the change in angle $\Delta\delta$, the change in rotor speed Δw, and the acceleration $p^2\delta$, has been described in Reference 88. The transient electrical power signal ΔP_e has been obtained using a standard electronic multiplier circuit with its inputs as all the 3-phase system voltages and currents. The direct-axis current, which is obtained from a Hall-effect multiplier, has also been described in Reference 88.

Test data may be optionally overwritten or directed to magnetic disc storage. Such data stored on the computer system is then available for subsequent off-line plotting and inspection. The microprocessor is responsible for

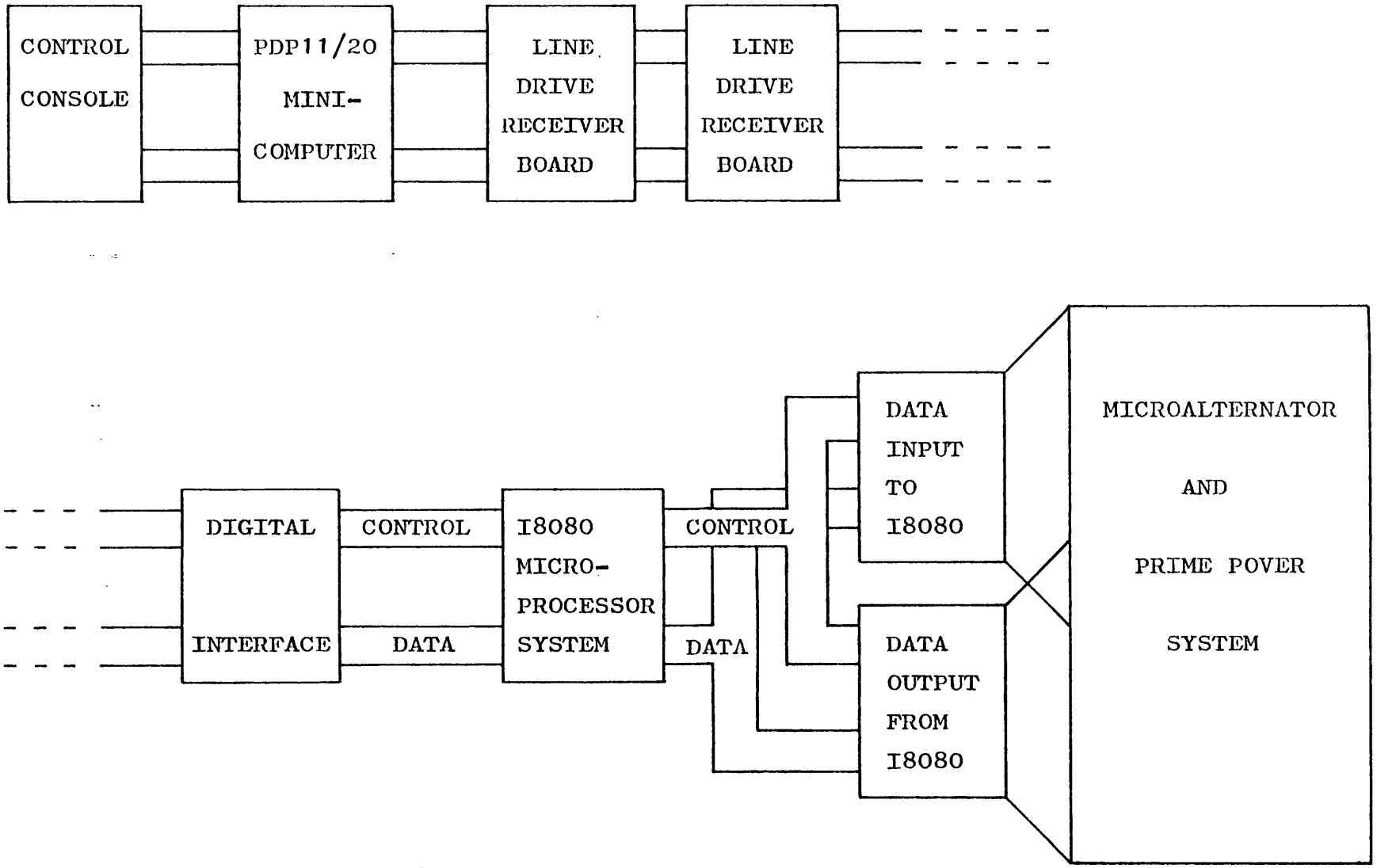

Fig. 6.1 Block diagram of the digital system

data collection from the micromachine transducers, and for processing the data prior to sending a complete package of data to the PDP11/20.

6.3 Validity of Model

The accuracy of various mathematical models of an a.c. turbogenerator used in theoretical studies has been the object of much discussion over the past decade[91]. In deriving suitable feedback gains for optimised performance, the validity of a particular model must influence which feedback system is used. Systems with high sensitivity to changes in the feedback constant should be treated with caution, since the actual optimised value of the feedback constant is itself dependent on the chosen form of mathematical model and the parameter values used in that particular model.

The problem is probably even more pronounced with laboratory-scale experimental studies using micromachines. Values for the micromachine parameters do, of course, exist, but to the best knowledge of the author, the accuracy of these parameters has not been firmly established. In these circumstances, because the accuracy of a comparison between theoretical results with experimental results depends on the parameter values used in the theoretical studies, it should only be used to confirm trends in changes in system performance obtained with different extra feedback signals. In particular,

configurations involving $\Delta\delta$ feedback, which are highly sensitive to changes in the optimised value of the feedback constant, and, therefore, by definition, sensitive to the accuracy of the machine parameters, will only be examined to confirm this fact. However, a more meaningful comparison between theoretical and experimental results can be made when the introduction of an extra feedback signal, such as ΔP_e or Δi_d feedback, has been shown to have low sensitivity to parameter changes.

6.4 Experimental Results

The results of a typical experimental study with a fault duration of 0.22s, incorporating additional feedback of either transient electrical power ΔP_e or transient load angle $\Delta\delta$, are given in Fig. 6.2, which also shows the results obtained using terminal voltage feedback acting alone. The expected significant improvement in subsequent damping in rotor oscillations introduced by ΔP_e feedback is clearly shown in Fig. 6.2a. The high sensitivity introduced by the use of $\Delta\delta$ feedback is shown in the input field voltage response of Fig. 6.2c. The output response of load angle is shown in Fig. 6.2a, and the terminal voltage response is shown in Fig. 6.2b.

These experimental results clearly confirm the expected trends in the change of system transient behaviour in the presence of one extra feedback signal into the excitation system. Corresponding results obtained with either $p^2\delta$ or Δw feedback showed the same trends as those produced by

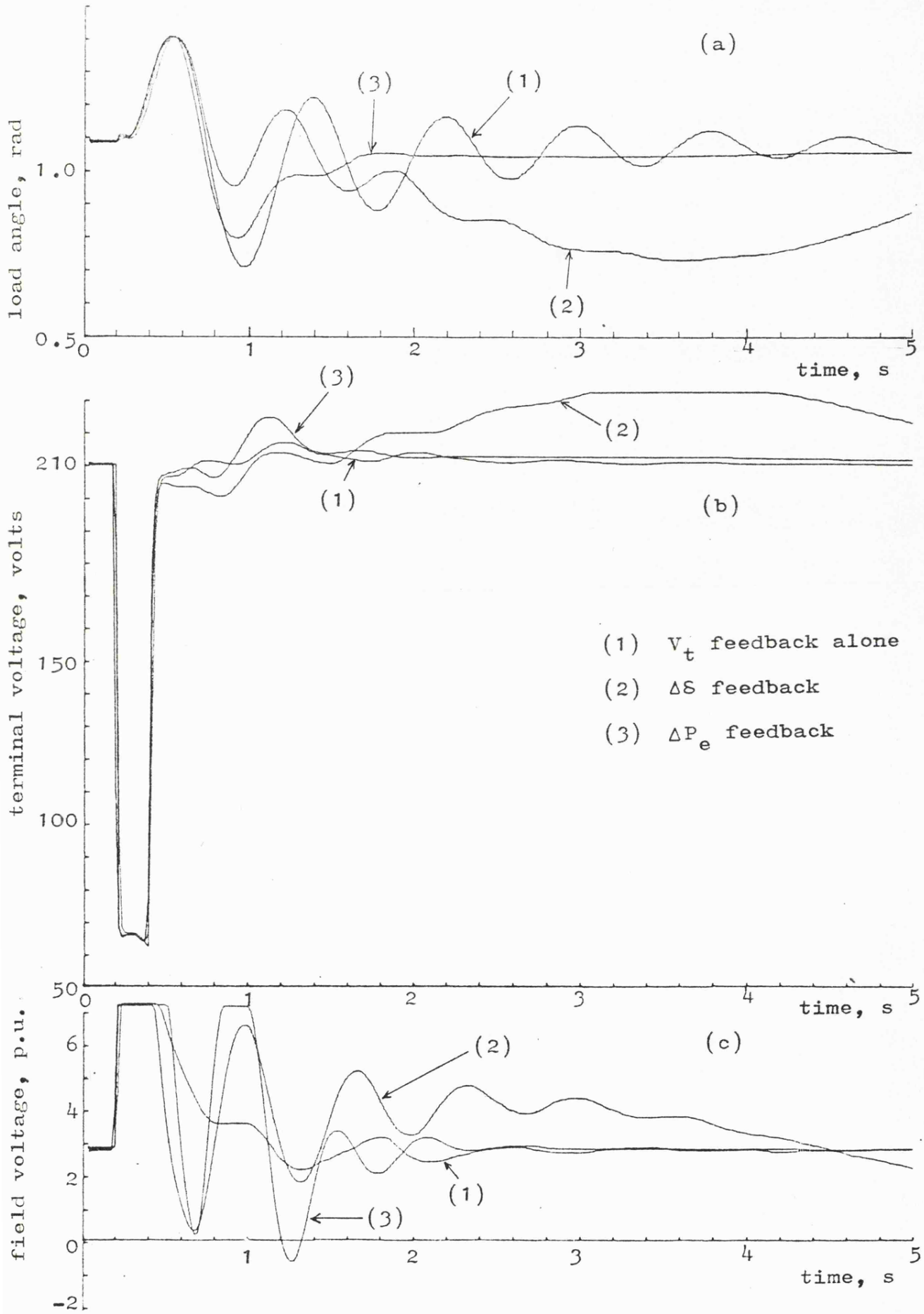

Fig. 6.2 Experimental response curves

theoretical studies. Similar conclusions can be drawn from the results obtained for a fault duration of 0.14s.

The design/synthesis approach to the optimisation of excitation control system in Chapter 5 suggests that the suboptimal control law obtained with transient direct-axis current feedback can improve system transient performance. Inspection of the output response curves for transient rotor angle and terminal voltage, shown in Figs. 6.3a and 6.3b respectively, confirms the usefulness of the proposed suboptimal excitation controller in improving transient response over that obtained using feedback of terminal voltage acting alone. Figure 6.3 also shows the results correspond to a 30% increase in the nominal Δi_d feedback constant. In all cases investigated, the suboptimal controller produced improvements in damping of rotor-angle oscillations without introducing a significant modification in terminal-voltage response

6.5 Sensitivity Studies

It has been suggested in the previous chapters that the suboptimal control law obtained with a feedback of one extra system state can remain near optimum for a change in system configuration. In particular, the results of Fig. 4.7 suggest that, with feedback of ΔP_e, the value of the performance index and therefore the transient response, remains near optimal for relatively large changes in the value of the optimised feedback constant from its nominal value. This result has been confirmed experimentally, and

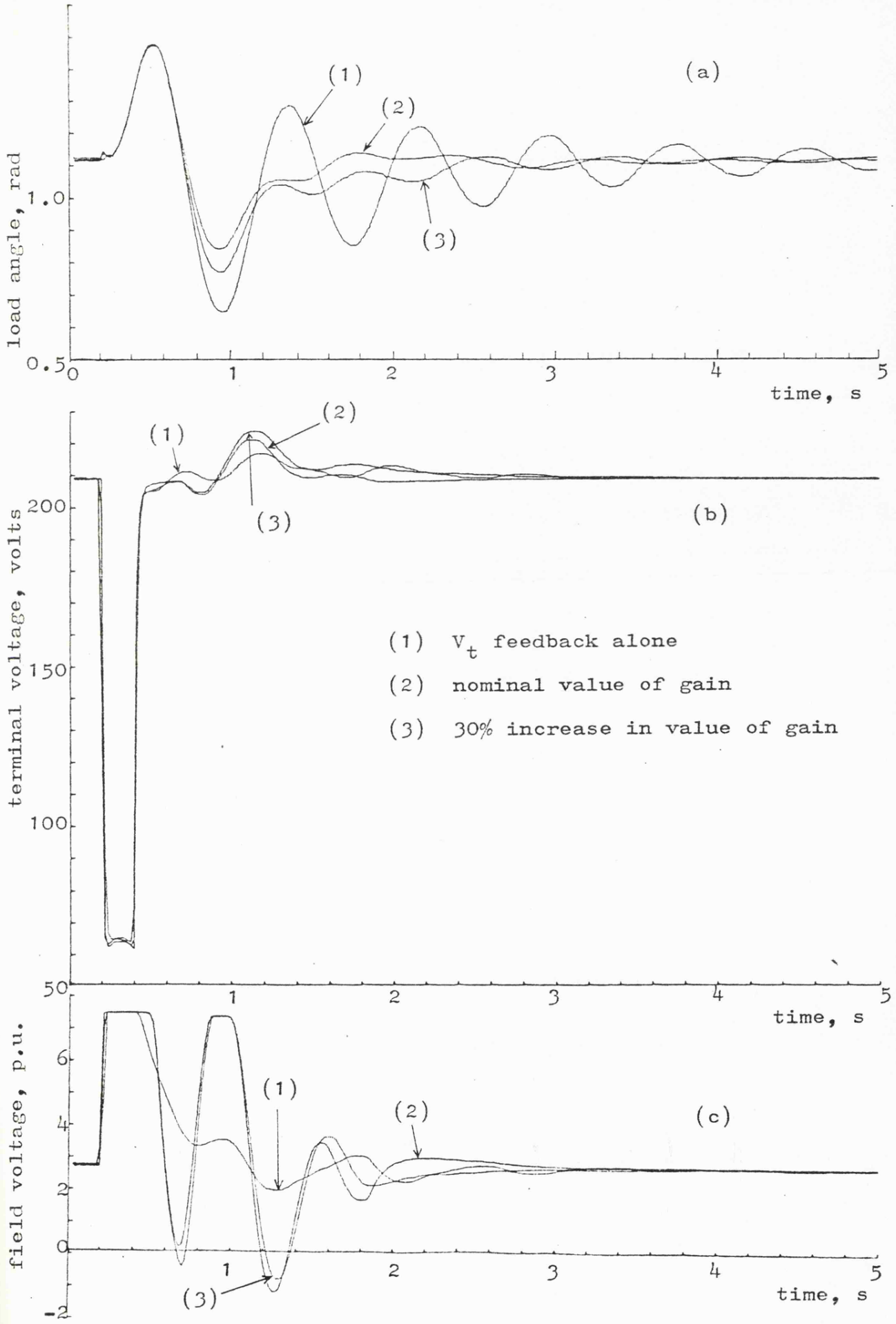

Fig. 6.3 Experimental response curves for Δi_d feedback

is illustrated by the curves shown in Fig. 6.4, in which curve (1) is that obtained with the nominal feedback constant. Curve (2) corresponds to a 30% increase and curve (3) corresponds to a 30% decrease in the value of this feedback constant. Inspection of the angle and terminal voltage responses of Fig. 6.4 confirms that the system response remains close to optimal for these large changes in feedback constant, thereby confirming that the use of ΔP_e feedback results in a system that is relatively insensitive to machine parameter values. Similar conclusions can be drawn from the results using Δi_d feedback with the output response curves given in Fig. 6.3.

The final experimental results given in Fig. 6.5 were obtained for ΔP_e feedback applied to the system with new operating conditions such that the tapchanging has been used to produce steady-state initial operating conditions in the leading v.a.r. condition with an initial system load angle of 80^o. Curve (1) in Fig 6.5 shows the response obtained when the value of the feedback constant obtained for the standard initial conditions of unity power factor at the busbar is used with the new initial conditions. Curve (2) in Fig. 6.5 corresponds to the presence of terminal voltage feedback acting alone. Inspection of Fig. 6.5 shows that the use of ΔP_e feedback has maintained a significant improvement in system performance for a large change in the initial operating conditions, thereby confirming the insensitivity of the response to changes in system configuration obtained with

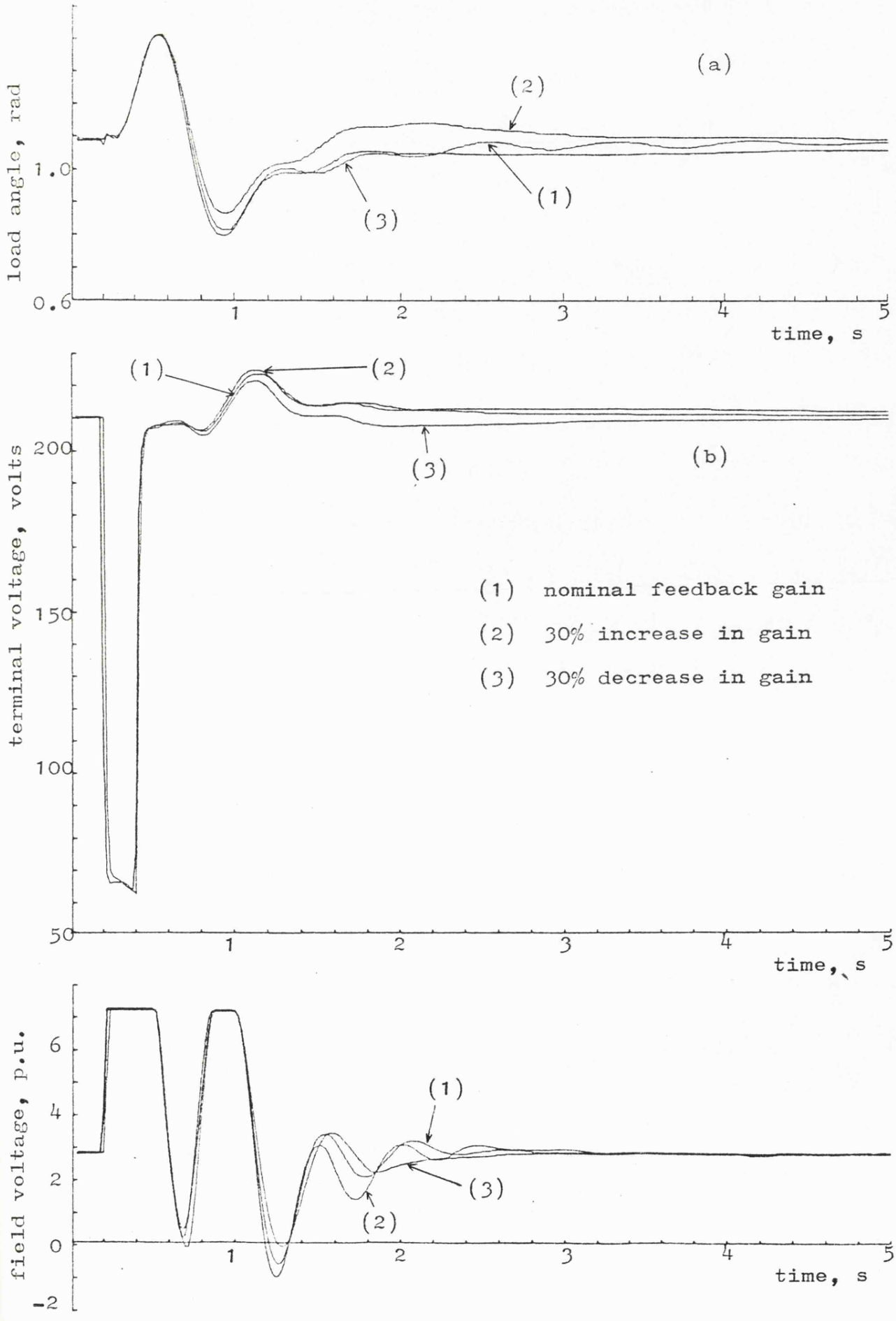

Fig. 6.4 Experimental response curve for ΔP_e feedback

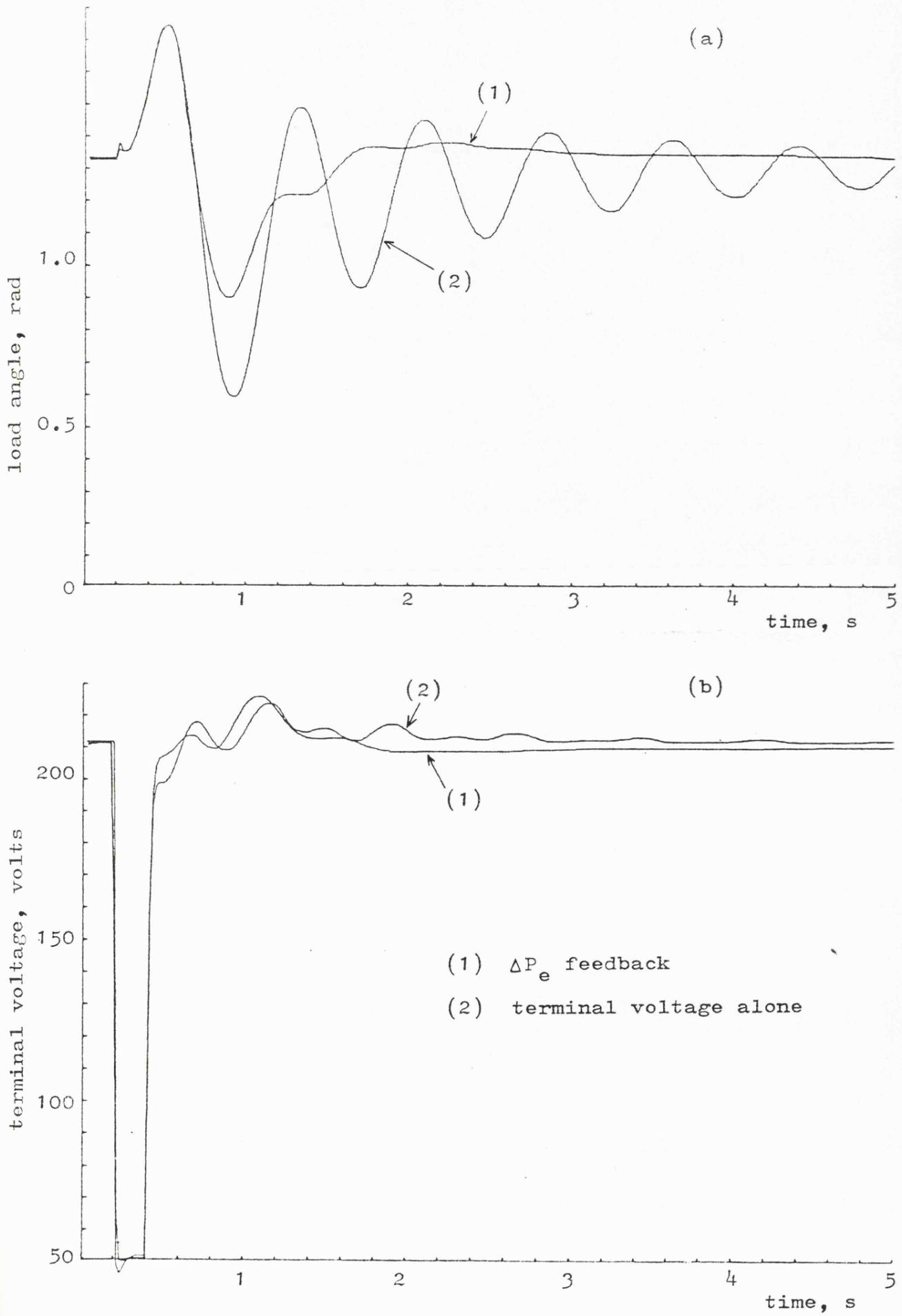

Fig. 6.5 Experimental investigation of sensitivity

ΔP_e feedback. Similar conclusions can be drawn from experimental investigations conducted with either Δi_d feedback or further changes in configuration such as values of fault duration and transfer impedance.

6.6 Discussion of Results

The experimental investigation has been performed on a real, although small, laboratory model, scaled on the Pembroke power station. In all cases, the trends in the system transient performance predicted by theoretical studies, using one of five different feedback signals, have been confirmed experimentally. These experimental studies have also confirmed that the proposed suboptimal control laws obtained for one set of operating conditions remain near optimal for wide change in system parameters or operating conditions.

Successful operation of such controllers require fast-acting excitation system capable of applying full reverse voltage to the generator field. Such a system is not generally available at the present time, and, indeed, the Pembroke power station, used for modelling purpose, has a rotating diode excitation system, which is not capable of producing reverse excitation. However, thyristor excitation controllers, incorporating the necessary facilities, are likely to be generally available in the near future.

CHAPTER 7 CO-ORDINATED CONTROL STUDIES

7.1 Introduction

It has been shown in the previous chapters how excitation control can be employed to improve the system transient performance through an extra suboptimal state feedback control. In this chapter, the use of steam-flow control and combined excitation and steam-flow control to further improve the system transient performance are investigated.

Modern large turbines are now fitted with fast electro-hydraulic governing systems and these too have a potential role in the enhancement of stability. In certain circumstances, this could duplicate the role of a fast excitation system. However, in practice, there are limitation arising from the interceptor valve sequencing required for thermodynamic reasons, and the practical difficulties of increasing the governor transient gain above defined limits[21]. In terms of first-swing performance for transient faults, the technique known as fast valving can make a significant contribution and is being provided on a large number of large machines. The future co-ordination of the governing and a.v.r. functions into a single controller is a desirable objective which would assist the improvement of stability by control means.

In recent years, some methods of optimal control theory have been applied to the design of excitation controllers and governing systems of synchronous generators[92-96].

Most of these studies were based on a linearised model of the power system about a particular operating point[92-94]. Optimal controls with respect to a quadratic performance index have been obtained by the solution of the matrix Riccati equation, which involve feedback of all the state variables[92,93]. Suboptimal controls based on a linearised model employing feedback of measurable output variables through the solution of the Lyapunov matrix equation have been derived[94]. Attempts have also been made to achieve optimal controls by some form of open-loop controls[95]. The majority of these papers describe theoretical studies, but a number of more recent experimental investigation has been undertaken[34,35,97].

Although the optimal and suboptimal controls derived using a linearised model produce optimum performance for small disturbance, these controls may not remain optimum under large disturbances because the linearised model is no longer valid under these conditions and the original nonlinear model must be used for the optimisation of system performance under large disturbance conditions. On the other hand, open-loop controls, though theoretically sound, are difficult to apply in practice. An open-loop control optimised with respect to a particular set of operating conditions and parameter values will not, in general, remain optimum or even near-optimum when system conditions and parameters are changed.

The main object of this investigation is to apply multi-variable nonlinear optimisation technique to the improve-

ment of power system performance and to study the sensitivity characteristics of the system. These studies are made using the nonlinear machine model which is valid for all forms of disturbances, large or small. The optimum control investigated is a form of closed-loop linear state feedback which is amenable to practical implementation.

7.2 Multi-variable Optimisation Program

The optimisation program is illustrated by the flow chart as shown in Fig. 7.1. Machine data and initial operating conditions are read in, and the steady-state values of the state variables and auxiliary variables are determined. The function minimisation subroutine is then called to minimise the chosen performance index. The multi-variable function minimisation subroutine used in this investigation is the Fortran version of the original Algol procedure based on the Quasi-Newton method of Gill, Murray and Pitfield[50].

The minimisation process consists of a systematic sequence of linear searches with the directions of search determined using the sensitivity functions of the performance index, which are evaluated by solving the sensitivity equations. The value of the performance index at each point is evaluated by solving the system equations. During each linear search, polynomial interpolation is used to locate the minimum in that direction. Linear searches are continued until either the convergence criterion is satisfied or

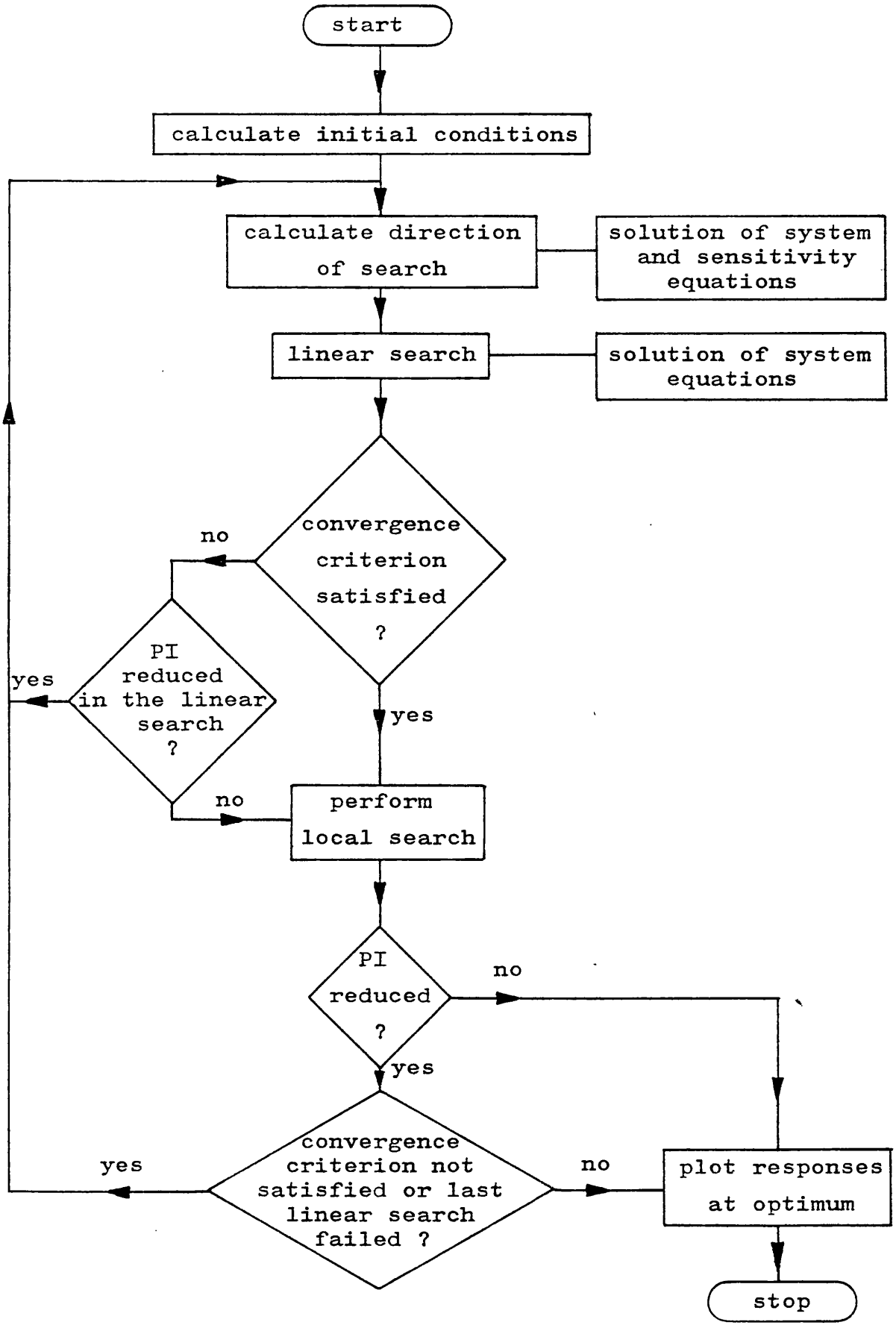

Fig. 7.1 Flow chart for optimisation program

reduction in the performance index is not achieved in a certain direction. A local search is then performed to ensure that the point arrived at is not a saddle point. If the local search fails to reduce the performance index further, the minimisation process is stopped and the response curves at the optimum are plotted. If the local search succeeds in reducing the performance index further, then the linear searches are continued if either the convergence criterion is not satisfied or the last linear search failed. Otherwise, the minimisation process is stopped and the optimum responses are plotted.

Since the problem under study is a nonlinear system, it is expected that there are more than one single local minimum in the region of practical interest in the parameter space. Optimisation results show that the local minimum actually arrived at during an optimisation run and the rate of convergence are influenced by the initial point chosen to start the function minimisation.

In practice, it is very difficult to device a performance index which represents precisely what is required of the system being designed. The design procedure adopted here is to make a few optimisation runs using a performance index which represents resonably well what is required of the system to obtain a few local optima. These optima are then compared in terms of system performance and system sensitivity. The one which is best suited to the requirements is picked out. If required, the response of this optimum can be further shaped, to a certain extent, using the sensitivity informations.

7.3 System Representation

7.3.1 System Under Study

In this investigation, the single-machine system described in Chapter 3 is used. The schematic layout of the system, including the prime mover, has been shown in Fig. 3.1. Simplified models capable of representing the pertinent characteristics of the various parts are used to represent the system and the resulting block diagram representation is illustrated in Fig. 7.2. Both the excitation control system and the prime mover system are represented by second order models, with V_i and T_i available at the input summing junctions for the extra feedback signals. The synchronous machine representation is described by the seventh order model.

7.3.2 Optimisation Problem

The transient performance of the single-machine system is optimised by linear state feedback using the nonlinear optimisation method. The signal in the excitation control system is a linear function of only one extra state variable, x, such that

$$V_i = K_1 \Delta x_1 \qquad (7.1)$$

and similarly, the extra feedback signal in the governing system is in the form of

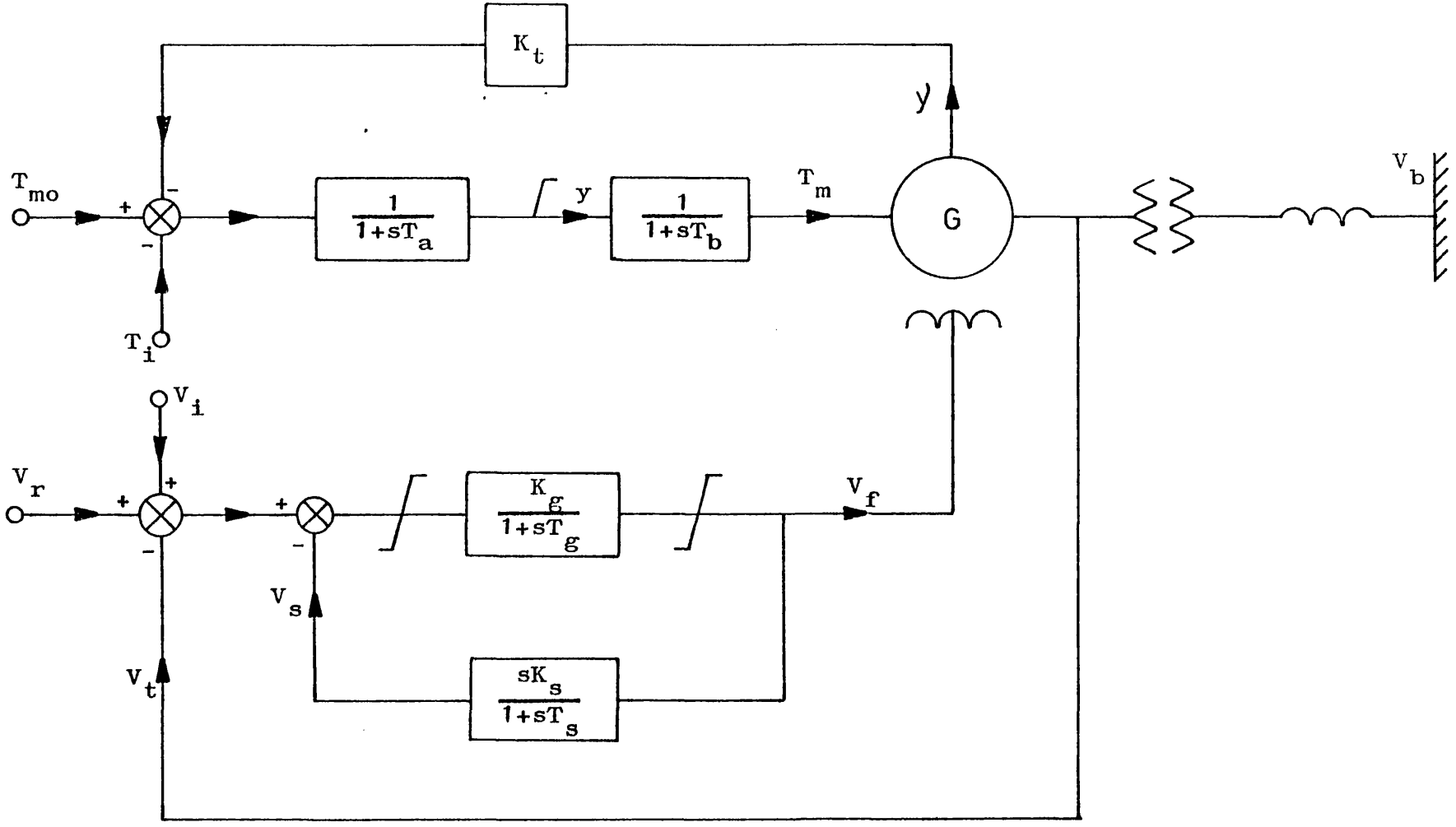

Fig. 7.2 Block diagram representation

$$T_i = K_2 \Delta x_2 \qquad (7.2)$$

where Δx is the change in the proposed state feedback and K_1, K_2 are the optimising parameters.

Initially, the same performance index as used in Chapter 4 was adopted, which is of the form

$$I = \int_o^T (A_1 \Delta V_t^2 + \frac{A_2}{0.1+t} \Delta\delta^2)dt \qquad (7.3)$$

It was found however that the weighting factor placed on the initial rotor swing as given by the inverse time factor is so great that the control obtained gave large reduction in the initial swing but left the subsequent response rather sluggish. This form of performance index is suitable for the optimisation of the excitation system, because, as have been seen in the previous chapters, the improving of the suboptimal excitation control over the conventional a.v.r. on first swing stability is very limited. The optimisation program had little choice but to make as much improvement on the damping of subsequent oscillations as it could. This is no longer the case when steam-flow control is incorporated which makes improvement on the first swing stability possible. The optimisation program now tries to improve first swing stability and subsequent damping according to the weighting placed on them. In this circumstance, a new performance index was adopted which took the form

$$I = \int_o^T ((\Delta V_t^2 + A_1 \Delta\delta^2)(1 + A_2 t))dt \qquad (7.4)$$

The time factor is added to limit the terminal voltage V_t and the rotor angle δ deviations. It penalises any states fluctuation which takes a long time to die out, and thus tends to produce a rapid return to the steady state. Although there is no inverse time factor in the rotor angle excursion, the squaring of the rotor angle excursion inherently puts more weight on the first swing. It is therefore, possible, by properly choosing the weighting factors A_1 and A_2, to balance the weighting between terminal voltage recovery, first swing stability, subsequent damping and speed of response.

In order to evaluate the contributions made by each of the excitation system, the governing system and the co-ordinated control, optimisation was carried out first for the combined excitation and steam-flow control and then the excitation and steam-flow control separately.

7.3.3 Scaling for Optimisation

Scaling often has a significant influence on the performance of optimisation methods. Probably the simple most fruitful action a user can take to ensure success in solving his problem is to scale the problem in a sensible manner. Since the convergence tolerances and other criteria are necessarily based on an implicit definition of 'small' and 'large', problems with unusual or unbalanced scaling may cause difficulties for some algorithms. In the light of the present state of the art[98], it is considered that

sensible scaling by the user is likely to be more effective than any automatic routine.

One method of scaling is to transform the variables from their original representation, which may reflect the physical nature of the problem, to variables that have certain desirable properties in terms of optimisation. It is generally helpful for the following conditions to be satisfied. Firstly, the variables are all of similar magnitude in the region of interest. Secondly, a fixed change in any of the variables results in similar changes in the performance index. Ideally, a unit change in any variable produces a unit change in the performance index. Normally, this transformation is limited to linear transformations of variables, although occasionally non-linear transformations are possible. The most common such transformation, and often the most appropriate, is of the form

$$\underline{x}_{new} = D\,\underline{x}_{old} \qquad (7.5)$$

where D is a diagonal matrix with constant coefficients.

In the present investigation, the extra excitation feedback signal is scaled as

$$V_i = K_1\,\Delta x_1/\text{SCALE1} \qquad (7.6)$$

while scaling for the additional feedback for the governing system is in the form of

$$T_i = K_2\,\Delta x_2/\text{SCALE2} \qquad (7.7)$$

where 1/SCALE1 and 1/SCALE2 are the diagonal elements of the diagonal matrix D. However, for analysing the sensitivity of the system, these scaling factors SCALE1 and SCALE2 should be put back to unity.

The solution of a given problem is unaltered if the objective function $f(\underline{x})$ is multiplied by a positive constant, or if a constant value is added to $f(\underline{x})$. It is generally preferable for the objective function to be of the order of unity in the region of interest; thus, if in the original formulation $f(\underline{x})$ is always of the order of 10^{+5}(say), then the value of $f(\underline{x})$ should be multiplied by 10^{-5} when evaluating the function within the optimisation routine.

7.3.4 Derivation of Sensitivity Equations

The sensitivity equations are derived by differentiating the system equations with respect to the various feedback gain constants as illustrated in section 4.4.3. The differences being that the parameter $K = K_1, K_2$ in turn and the effect of the prime mover has been taken into account as shown in the last two system differential equations given below. The system equations are as follws:

$$pe_d'' = ((x_q - x_q'')i_q - e_d'')/T_{qo}'' \qquad (7.8)$$

$$pe_q' = (V_f - (x_d - x_d'')i_d - e_q'')/T_{do}'' \qquad (7.9)$$

$$pe_q'' = (e_q' - (x_d' - x_d'')i_d - e_q'' - (T_1(e_q'' - x_d''i_d) + T_2x_di_d - T_{kd}V_f)/T_{do}')/T_{do}'' \qquad (7.10)$$

$$p\delta = \gamma \tag{7.11}$$

$$p\gamma = (T_m - T_e - K_{dd}\gamma)/M \tag{7.12}$$

$$pV_f = ((V_r - V_t + V_i - V_s)K_g - V_f)/T_g \tag{7.13}$$

$$pV_s = (K_s pV_f - V_s)/T_s \tag{7.14}$$

$$pI = (\Delta V_t^2 + A_1 \Delta\delta^2)(1 + A_2 t) \tag{7.15}$$

$$pi_d = (pe_q" - w_o(V_b \sin\delta + (R_t+R_a)i_d) + w(e_d" + (x_q"+X_t)i_q))/(X_t+x_d") \tag{7.16}$$

$$pi_q = (-pe_d" + w(e_q" - (X_t+x_d")i_d) - w_o(V_b\cos\delta + (R_t+R_a)i_q))/(X_t+x_q") \tag{7.17}$$

$$py = (T_{mo} - T_i - K_t\gamma - y)/T_a \tag{7.18}$$

$$pT_m = (y - T_m)/T_b \tag{7.19}$$

The auxiliary equations are given by

$$V_i = K_1 \Delta x_1 \tag{7.20}$$

$$T_e = e_d"i_d + e_q"i_q - (x_d"-x_q")i_d i_q \tag{7.21}$$

$$w = w_o + \gamma \tag{7.22}$$

$$v_d = V_b \sin\delta + X_t pi_d/w_o + R_t i_d - wX_t i_q/w_o \tag{7.23}$$

$$v_q = V_b\cos\delta + X_t pi_q/w_o + R_t i_q + wX_t i_d/w_o \tag{7.24}$$

$$V_t = \sqrt{(v_d^2 + v_q^2)} \tag{7.25}$$

$$T_i = K_2 \Delta x_2 \tag{7.26}$$

where $K_{dd} = K_d/w_o$.

The sensitivity equations with respect to the feedback gain constants K_1 and K_2 are as follows:

$$p\left(\frac{\partial e_d''}{\partial K}\right) = \left((x_q - x_q'')\frac{\partial i_q}{\partial K} - \frac{\partial e_d''}{\partial K}\right)/T_{qo}'' \tag{7.27}$$

$$p\left(\frac{\partial e_q'}{\partial K}\right) = \left(\frac{\partial V_f}{\partial K} - (x_d - x_d'')\frac{\partial i_d}{\partial K} - \frac{\partial e_q''}{\partial K}\right)/T_{do}' \tag{7.28}$$

$$p\left(\frac{\partial e_q''}{\partial K}\right) = \left(\frac{\partial e_q'}{\partial K} - (x_d' - x_d'')\frac{\partial i_d}{\partial K} - \frac{\partial e_q''}{\partial K} - \left(T_1\left(\frac{\partial e_q''}{\partial K} - x_d''\frac{\partial i_d}{\partial K}\right)\right.\right.$$
$$\left.\left. + T_2 x_d \frac{\partial i_d}{\partial K} - T_{kd}\frac{\partial V_f}{\partial K}\right)/T_{do}'\right)/T_{do}'' \tag{7.29}$$

$$p\left(\frac{\partial \varepsilon}{\partial K}\right) = \frac{\partial \gamma}{\partial K} \tag{7.30}$$

$$p\left(\frac{\partial \gamma}{\partial K}\right) = \left(\frac{\partial T_m}{\partial K} - \frac{\partial T_e}{\partial K} - K_{dd}\frac{\partial \gamma}{\partial K}\right)/M \tag{7.31}$$

$$p\left(\frac{\partial V_f}{\partial K}\right) = \left(\left(\frac{\partial V_t}{\partial K} + \frac{\partial V_i}{\partial K} - \frac{\partial V_s}{\partial K}\right)K_g - \frac{\partial V_f}{\partial K}\right)/T_g \tag{7.32}$$

$$p\left(\frac{\partial V_s}{\partial K}\right) = \left(K_s p\left(\frac{\partial V_f}{\partial K}\right) - \frac{\partial V_s}{\partial K}\right)/T_s \tag{7.33}$$

$$p\left(\frac{\partial I}{\partial K}\right) = 2.0\left(\Delta V_t \frac{\partial V_t}{\partial K} + A_1 \Delta\varepsilon \frac{\partial \varepsilon}{\partial K}\right)(1 + A_2 t) \tag{7.34}$$

$$p\left(\frac{\partial i_d}{\partial K}\right) = \left(p\left(\frac{\partial e_q''}{\partial K}\right) - w_o\left(V_b \cos\varepsilon \frac{\partial \varepsilon}{\partial K} + (R_t + R_a)\frac{\partial i_d}{\partial K}\right)\right.$$
$$+ w\left(\frac{\partial e_d''}{\partial K} + (x_q'' + X_t)\frac{\partial i_q}{\partial K}\right)$$
$$\left. + \left(e_d'' + (X_t + x_q'')i_q\right)\frac{\partial w}{\partial K}\right)/(X_t + x_d'') \tag{7.35}$$

$$p\left(\frac{\partial i_q}{\partial K}\right) = \left(-p\left(\frac{\partial e_d''}{\partial K}\right) - w_o\left(-V_b \sin\varepsilon \frac{\partial \varepsilon}{\partial K} + (R_t + R_a)\frac{\partial i_q}{\partial K}\right)\right.$$
$$\left. + w\left(\frac{\partial e_q''}{\partial K} - (X_t + x_d'')\frac{\partial i_d}{\partial K}\right) + \left(e_q'' - (X_t + x_d'')\right)\frac{\partial w}{\partial K}\right)/(X_t + x_q'') \tag{7.36}$$

$$p\left(\frac{\partial y}{\partial K}\right) = \left(\frac{\partial T_i}{\partial K} - K_t\frac{\partial y}{\partial K} - \frac{\partial y}{\partial K}\right)/T_a \tag{7.37}$$

$$p\left(\frac{\partial T_m}{\partial K}\right) = \left(\frac{\partial y}{\partial K} - \frac{\partial T_m}{\partial K}\right)/T_b \tag{7.38}$$

where $K = K_1, K_2$ in turn.

The auxiliary sensitivity equations are described by

$$\frac{\partial V_i}{\partial K_1} = K_1\frac{\partial x_1}{\partial K_1} + \Delta x_1 \tag{7.39}$$

$$\frac{\partial V_i}{\partial K_2} = K_1\frac{\partial x_1}{K_2} \tag{7.40}$$

$$\frac{\partial T_e}{\partial K} = \frac{\partial e_d''}{\partial K}i_d + \frac{\partial i_d}{\partial K}e_d'' + \frac{\partial e_q''}{\partial K}i_q + \frac{\partial i_q}{\partial K}e_q'' - (x_d''-x_q'')\left(i_d\frac{\partial i_q}{\partial K} + i_q\frac{\partial i_d}{\partial K}\right) \tag{7.41}$$

$$\frac{\partial w}{\partial K} = \frac{\partial y}{\partial K} \tag{7.42}$$

$$\frac{\partial V_t}{\partial K} = \left(v_d\frac{\partial v_d}{\partial K} + v_q\frac{\partial v_q}{\partial K}\right)/V_t$$

$$= \left(v_d\left(V_b\cos\delta\frac{\partial \delta}{\partial K} + X_t p\left(\frac{\partial i_d}{\partial K}\right)/w_o + R_t\frac{\partial i_d}{\partial K} - wX_t\frac{\partial i_q}{\partial K}/w_o - X_t i_q\frac{\partial w}{\partial K}/w_o\right) + v_q\left(-V_b\sin\delta\frac{\partial \delta}{\partial K} + X_t p\left(\frac{\partial i_q}{\partial K}\right)/w_o + R_t\frac{\partial i_q}{\partial K} + wX_t\frac{\partial i_d}{\partial K}/w_o + X_t i_d\frac{\partial w}{\partial K}/w_o\right)\right)V_t \tag{7.43}$$

$$\frac{\partial T_i}{\partial K_1} = K_2\frac{\partial x_2}{\partial K_1} \tag{7.44}$$

$$\frac{\partial T_i}{\partial K_2} = K_2\frac{\partial x_2}{\partial K_2} + \Delta x_2 \tag{7.45}$$

where $K = K_1, K_2$ in turn.

7.4 Optimisation Studies

7.4.1 General

The choice of extra feedback signals into the excitation system has been limited to three particular signals, all of which have been previously used. These three signals are $p^2\delta$, the rotor acceleration, ΔP_e, the transient electrical output power and Δi_d, the change in direct-axis current. On the governing side, the PID governors[99] have attracted much attention with signals as proportional, integral and derivative of the speed signal. However, the acceleration feedback in the steam-flow control system has been found[100] to be more effective than the rotor angle and speed feedback. In fact, comparable suboptimal controls has been reported[101] employing only the acceleration feedback. To achieve economic operation without impairing the optimum performance of the suboptimal control, only this extra signal is chosen in the governing system in this present investigation.

Weighting factors of A_1=0.1 and A_2=70.0 in eqn. 7.4 have been chosen as a result of several optimisation scaling runs. In this form, the objective function not only satisfies the transient response requirements but also fulfils the necessity for problem scaling. The scaling factors SCALE1 and SCALE2 for the feedback signals have different values for different feedback combinations. The object of the scaling is such that per unit change in the

gain constants of the feedback will produce roughly a per unit change in the objective function. The convergence criterion has been assumed to be satisfied when the gradient norm is less than the specified accuracy,i.e.

$$\sqrt{\sum_{i=1}^{2} g(i)} < \epsilon$$

The integral of eqn. 7.4 is evaluated over 3.5s in attempts to find the optimised values of the parameters K_1 and K_2 of eqns. 7.1 and 7.2. The quadratic approximation single variable optimisation has also been applied for the assessment of the individual contribution by each of the excitation and steam-flow control loop.

7.4.2 Co-ordinated Control

A large number of optimisation runs have been performed to optimise the transient performance of the single-machine system by incorporating both suboptimal excitation and steam-flow control using the performance index given in eqn. 7.4. Four typical optimum controls, A1a, A1b, A2 and A3 are described in Table 7.1 where the conventional control, A_o(conventional a.v.r. and conventional governor), is also included for comparison. Controls A1a and A1b are two separate local minima arrived using acceleration signal in both the excitation and the governing system. All controls use acceleration signal as the extra feedback in the governing system.

Control Number	Excitation Feedback Signal	Excitation Controller Gain K_1	Steam-flow Controller Gain K_2	Value of PI
A_o	/	0.0	0.0	39.77
A1a	$p^2\delta$	0.0365	0.12	5.55
A1b	$p^2\delta$	0.0543	0.147	7.57
A2	ΔP_e	0.6946	0.03	8.69
A3	Δi_d	-0.4692	0.0392	8.79
B1a	/	0.0	0.0217	35.13
B1b	/	0.0	0.05	/
C1	$p^2\delta$	0.0166	0.0	9.98
C2	ΔP_e	0.5486	0.0	9.77
C3	Δi_d	-0.3638	0.0	10.11

Table 7.1 Optimisation results

The transient responses of the systems with Controls A_o, A1a and A1b are shown in Fig. 7.3. The control inputs to the systems are the excitation voltage and the mechanical input power. It can be observed from Figs. 7.3c and 7.3d that the suboptimal controls exercise much more control action than the conventional control. Immediately after fault inception, all three controls push the excitation voltage to the positive ceiling, and whilst the suboptimal controls reduce the mechanical input power sharply, the power input effected by the conventional control remains unchanged for about 0.1s and then reduces at a much slower rate. The electrical power output(Fig. 7.3e) of all three controls are almost zero initially due to the collapse of the terminal voltage. However, by the time the fault is cleared, much more energy has been injected into the system

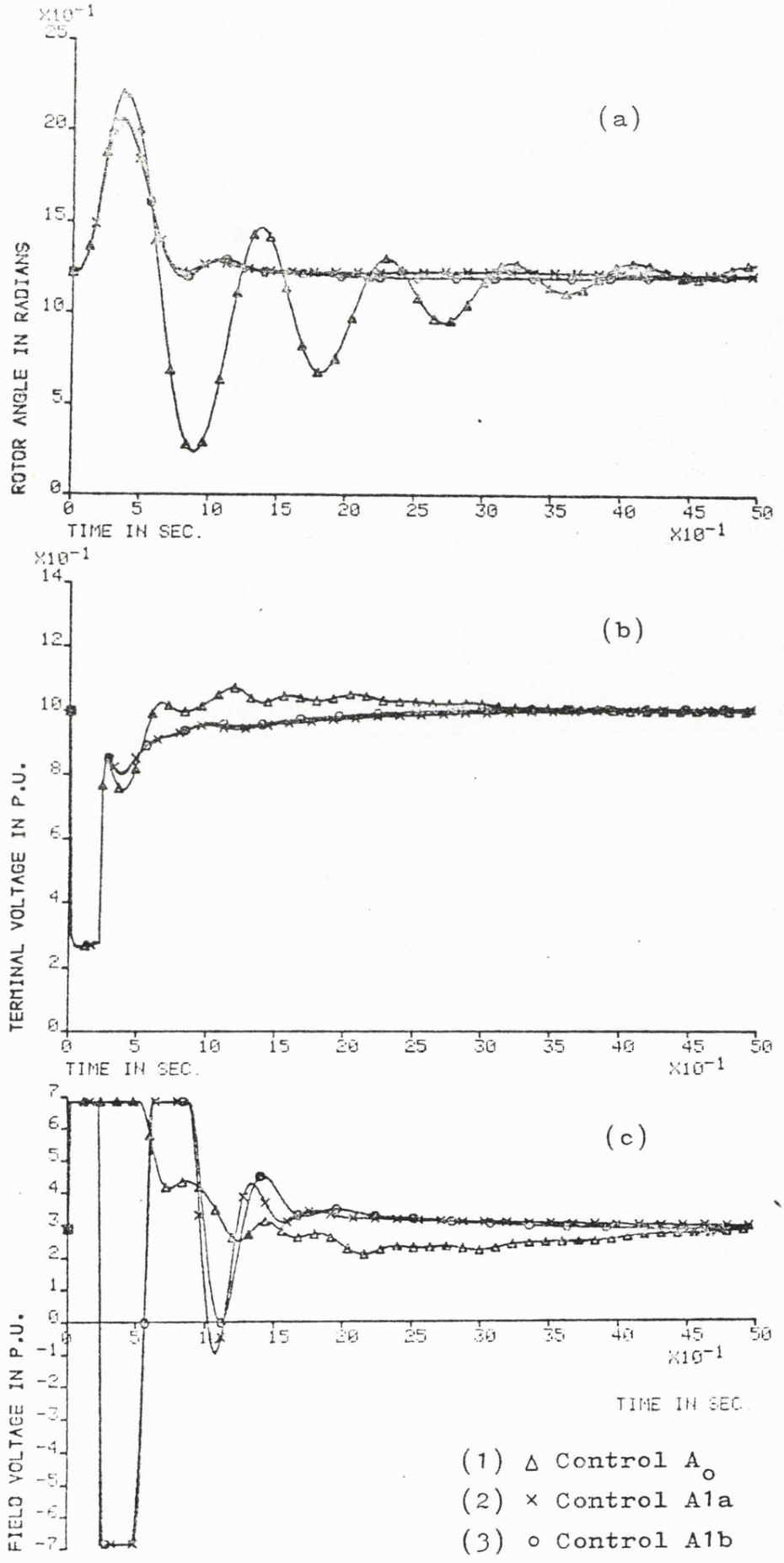

Fig. 7.3 Theoretical response curves

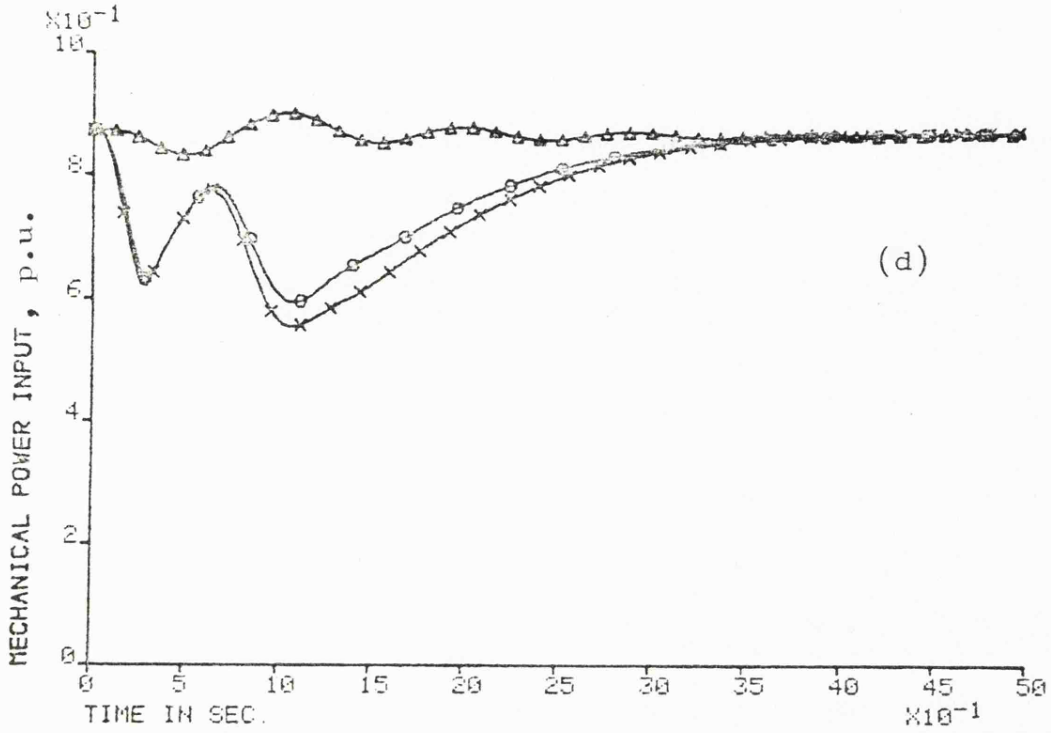

(1) Δ Control A_o

(2) × Control A1a

(3) o Control A1b

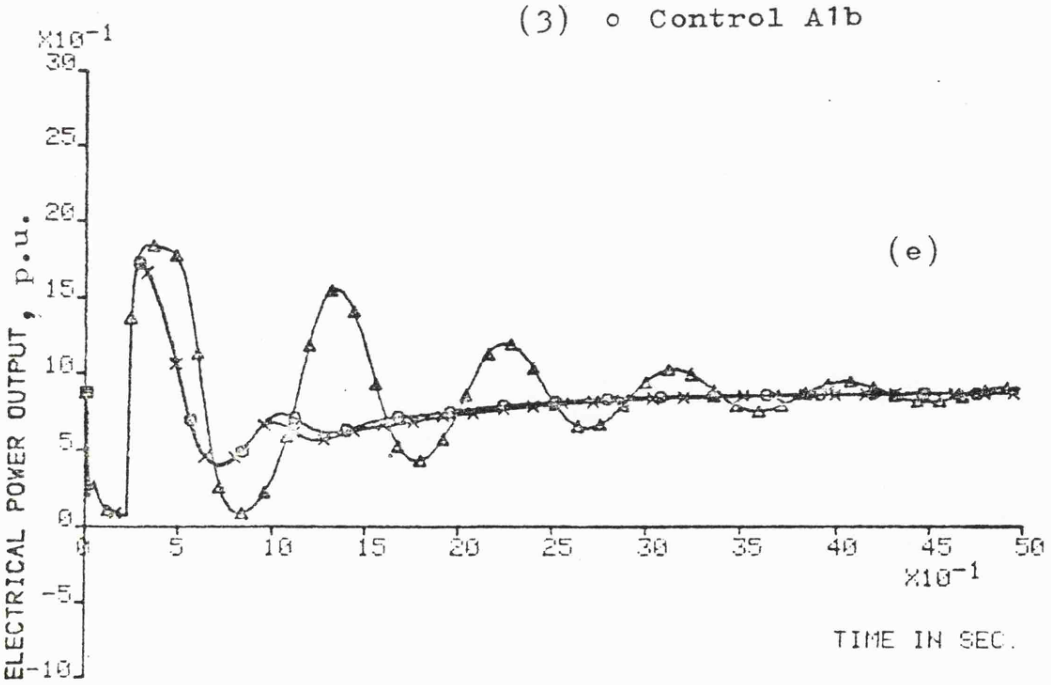

Fig. 7.3 Theoretical response curves

with the conventional control and this extra energy is available to accelerate the rotor, leading to higher first swing in rotor angle. When the fault is removed, all three controls maintain the excitation at a ceiling value, thereby increasing the electrical power output in an attempt to resynchronise. However, the conventional control maintains the excitation at the positive ceiling for too long, resulting in excessive decelerating power, which in turn, leads to a much larger back swing in rotor angle. The suboptimal controls, on the other hand, efficiently co-ordinate the mechanical input and electrical output power to produce more effective damping.

Apart from improving the first swing stability and subsequent damping, the suboptimal controls also furnish better control over the terminal voltage recovery response. These controls reduce the voltage dip after the fault is removed as shown in Fig. 7.3b. It can be seen that the suboptimal excitation control is virtually bang-bang in nature in the first 1s and that the transient performance of the two optimum controls are very similar, though they have different feedback gains.

Control A2 and A3 are systems with transient electrical power, ΔP_e, and change in direct-axis current, Δi_d, as the extra excitation signal respectively. Although it has been found that each of these gives comparable transient performance with acceleration signal in the previous excitation control optimisation studies, they do not seem

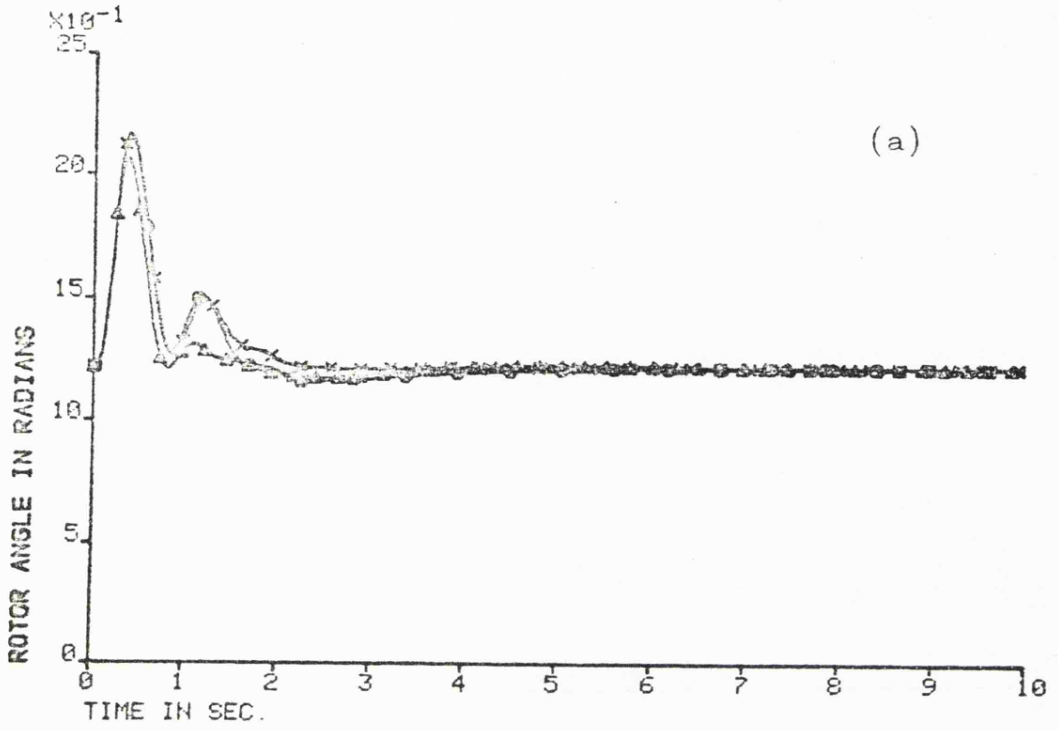

(1) Δ Control A1a

(2) × Control A2

(3) ○ Control A3

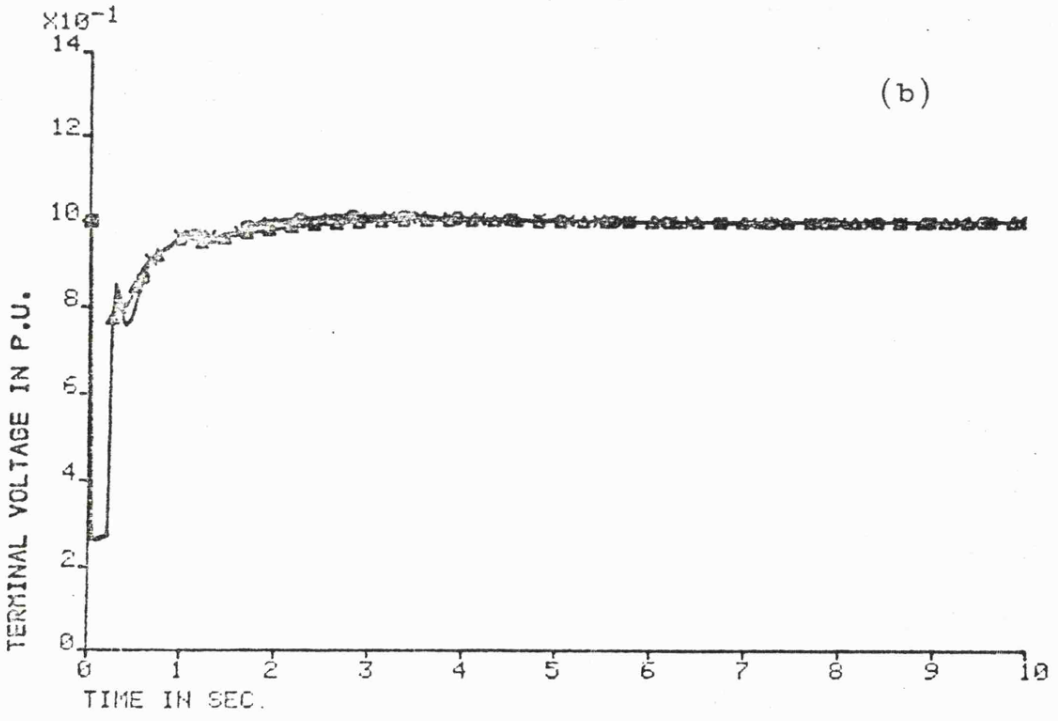

Fig. 7.4 Theoretical response curves

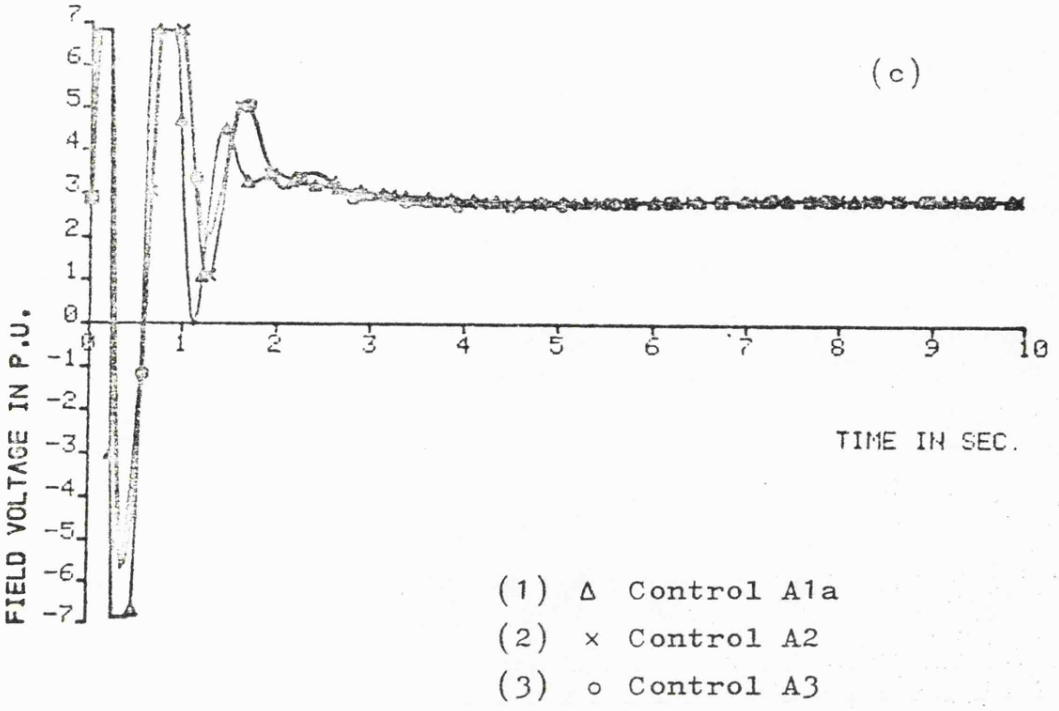

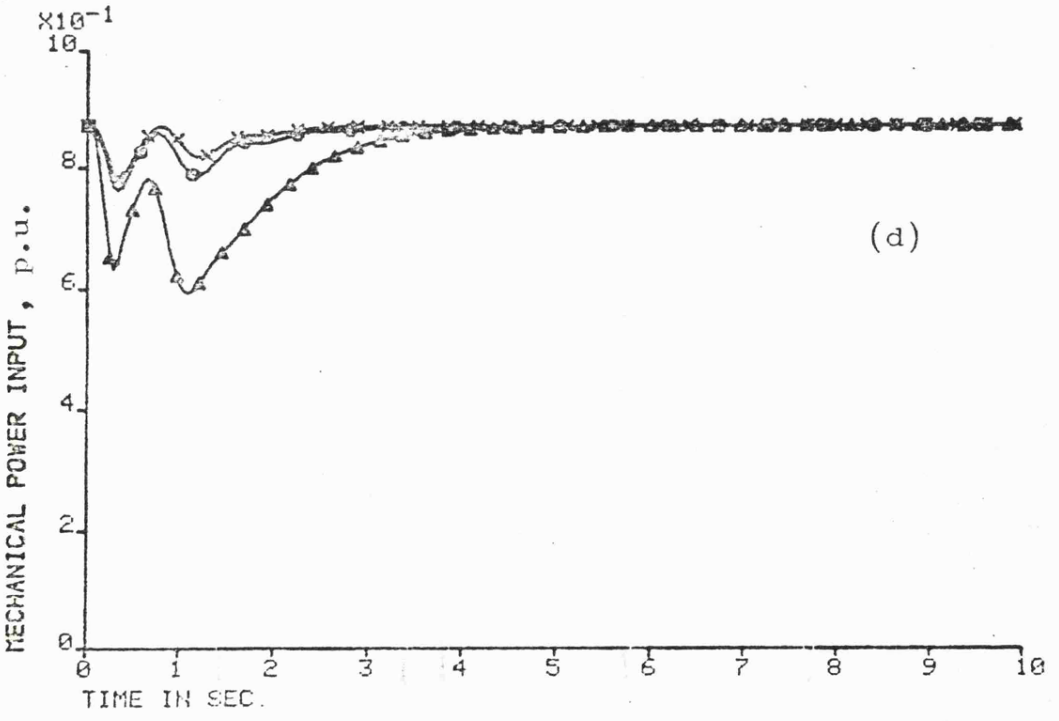

Fig. 7.4 Theoretical response curves

to co-ordinate effectively with the acceleration signal in the governing system. The Control A1a, however, with acceleration signal in both the excitation system and the governing system, stands out to be a better co-ordination as illustrated in Fig. 7.4, when compared with Controls A2 and A3. The 10-second plot gives a much clearer picture that the optimum systems do actually settle to their initial steady state completely after about 4s. It is observed that the gain constants, K_2, for Controls A2 and A3 are small comparing with Control A1a. However, increasing K_2 for Controls A2 and A3 has been found to make the system responses rather sluggish without reducing the first swing.

7.4.3 Suboptimal Steam-Flow Control

In order to evaluate the individual contribution made by steam-flow control towards the transient performance of the single-machine system, a system incorporating a suboptimal state feedback steam-flow control with a conventional a.v.r. was studied. A typical control obtained is described in Table 7.1 as Control B1a. This control was obtained using the performance index described by eqn. 7.4. It has been mentioned previously that the choice of performance index is arbitrary. In the present form, it may not be the most suitable one for the sub-optimal steam-flow control problem. It is, however, possible to arrive at Control B1b using a slightly

modified performance index. The transient response of this system is depicted in Fig. 7.5, in which Controls A_o and A1a are also shown for comparison. From Fig. 7.5a, it can be seen that the system with suboptimal steam-flow control(B1b) has a first swing in rotor angle comparable to that of the system with co-ordinated control A1a, and the behaviour of its subsequent swings resembles that of the system with conventional control A_o, although it is somewhat more damped. This is because of the fact that, while this control reduces the mechanical power input (Fig. 7.5d) sharply at the onset of the fault, as Control A1a, and thereby reduces the first swing, it exports too much electrical power(Fig. 7.5e) after the removal of the fault because of lack of control action by the excitation system and so gives rise to an excessive back swing. This is confirmed by the excitation voltage response(Fig. 7.5c) which shows that the control furnished by Control B1b is similar to that of Control A_o. The terminal voltage response follows the same trend as shown in Fig. 7.5b. While the voltage response of Control B1b is similar to that of Control A1a during the initial period, it resembles that of Control A_o in the subsequent response.

7.4.4 Suboptimal Excitation Control

Studies have been made in the previous chapters to investigate the contribution made by a suboptimal excitation control on the system transient performance with the prime mover assumed to deliver a constant mechanical input

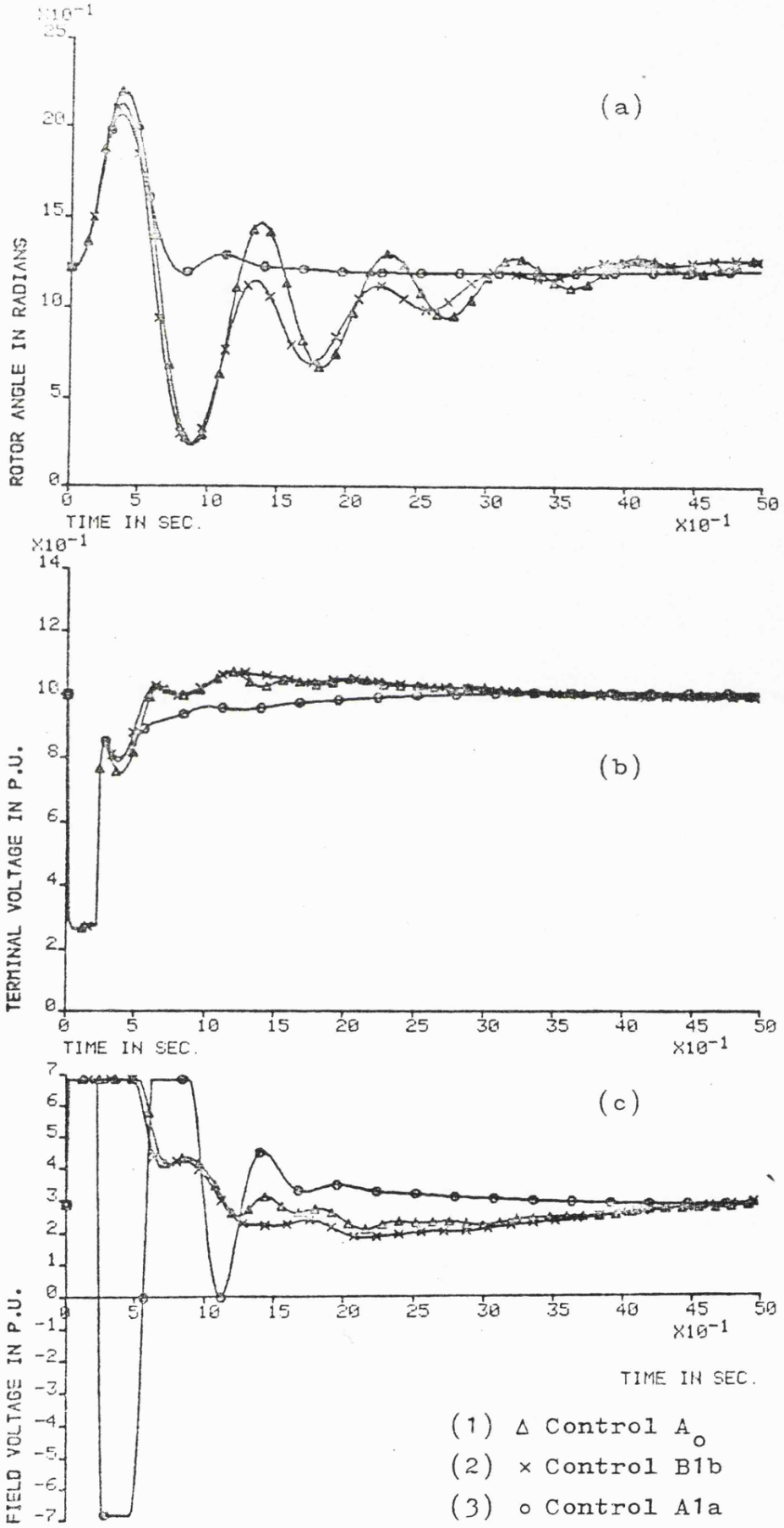

Fig. 7.5 Theoretical response curves

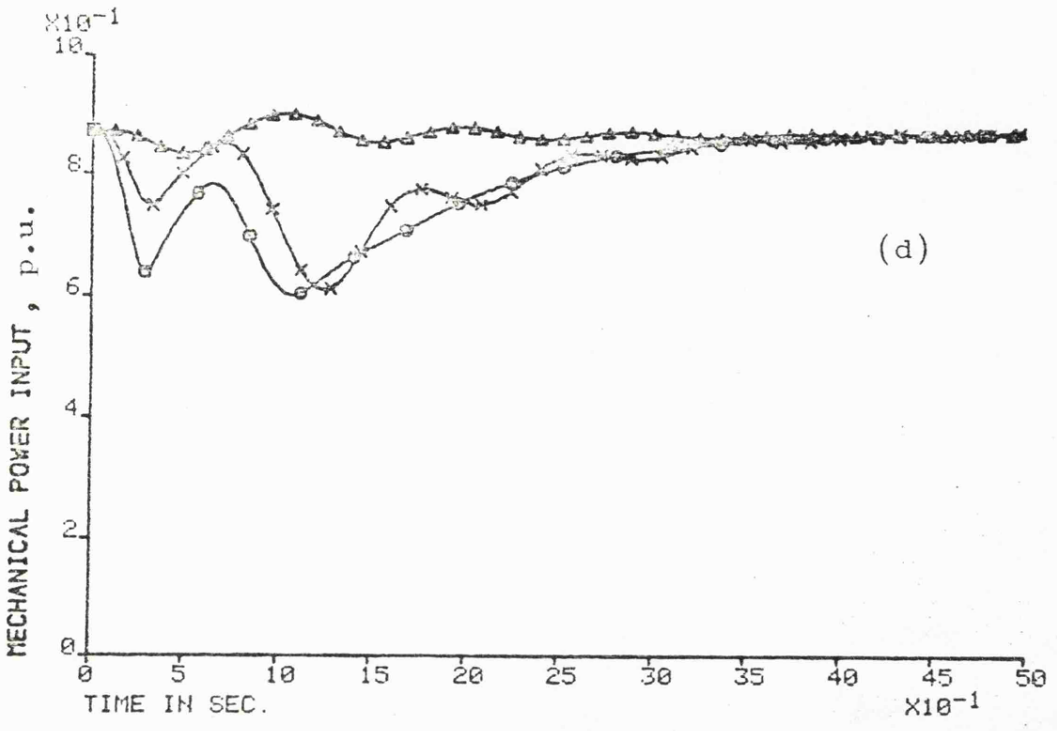

(1) Δ Control A_o

(2) × Control B1b

(3) o Control A1a

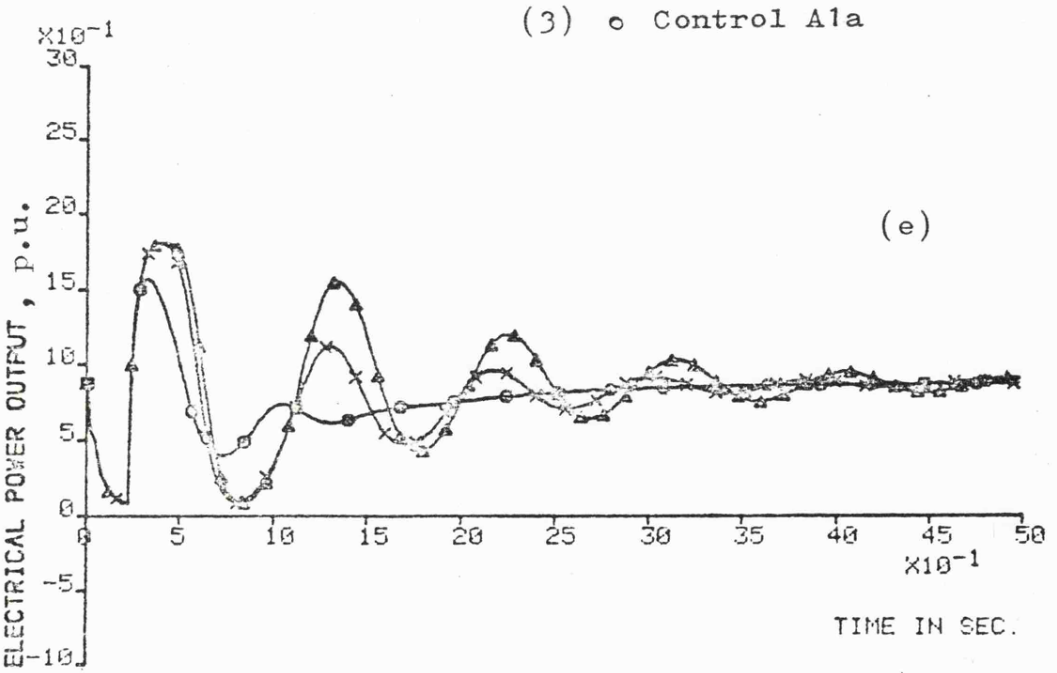

Fig. 7.5 Theoretical response curves

to the generator. These studies show that, while the suboptimal excitation control can make little further improvement on the first swing stability over the conventional a.v.r., it provides much more effective damping on subsequent swings. It also renders better control on the terminal voltage response. In order to investigate this more closely with the prime mover realistically represented, a system with a conventional governing system and incorporating suboptimal excitation was studied.

Typical optimum controls are described in Table 7.1 as Controls C1, C2 and C3. Control C1 is chosen for the comparison study. The transient performance of the system with this control is depicted in Fig. 7.6, where Controls A_o and A1a are also included for comparison. From Fig. 7.6c and 7.6d, it is readily observed that Control C1 has an excitation control similar to that of Control A1a and a steam-flow control resembling that of Control A_o. In fact, the steam-flow controls of Controls A_o and C1 are identical during the first 0.6s after fault inception. This being the case, it is not surprising that the rotor swing response of Control C1, as shown in Fig. 7.6a, has a first peak practically identical to that of Control A_o and subsequent swings comparable to Control A1a. The magnitude of back swing after the first peak of the machine with Control C1 is reduced by excitation control which prevents excessive power export after the fault is removed, as shown in Fig. 7.6e. The terminal voltage response of the machine with Control C1 goes through the same voltage dip

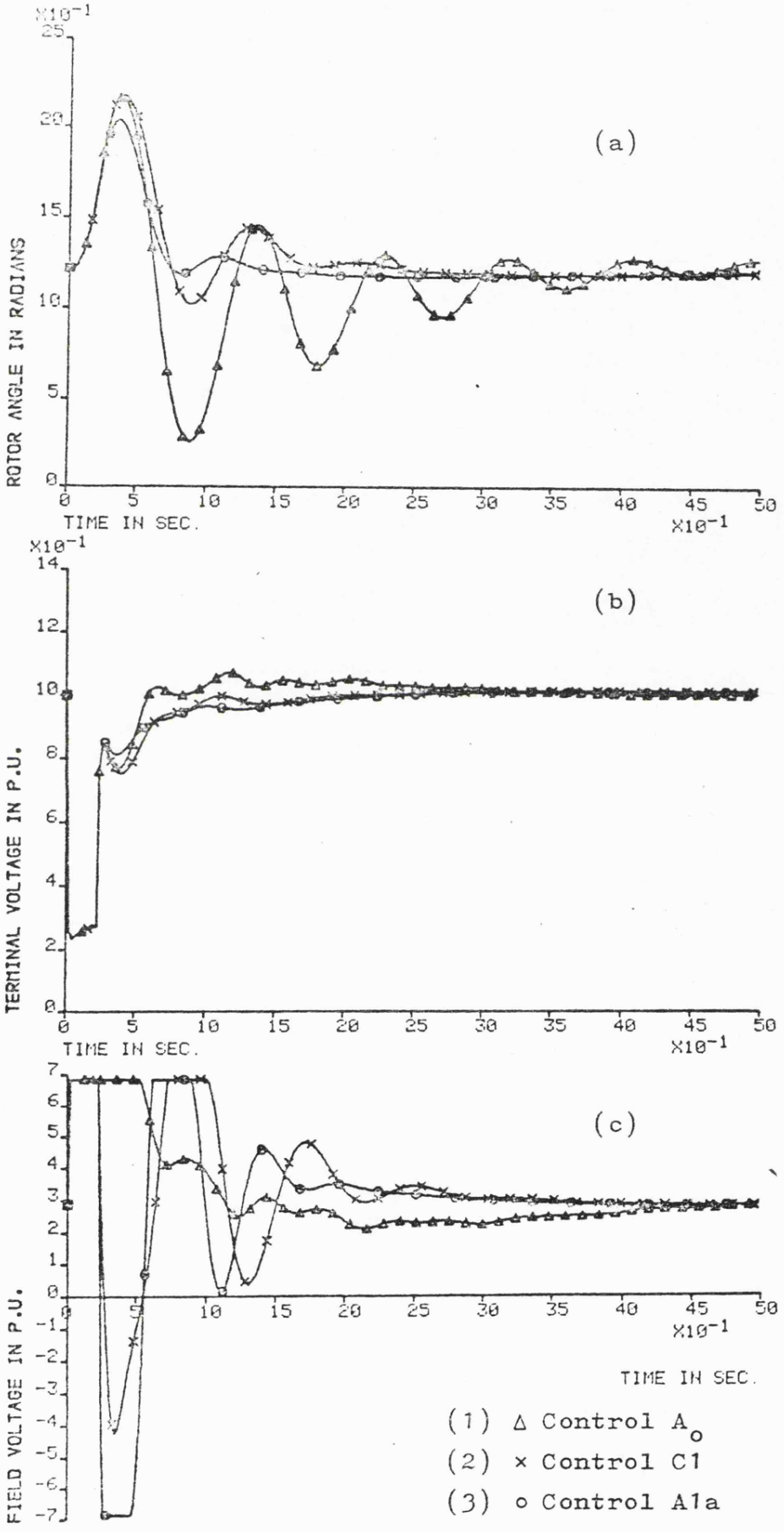

Fig. 7.6 Theoretical response curves

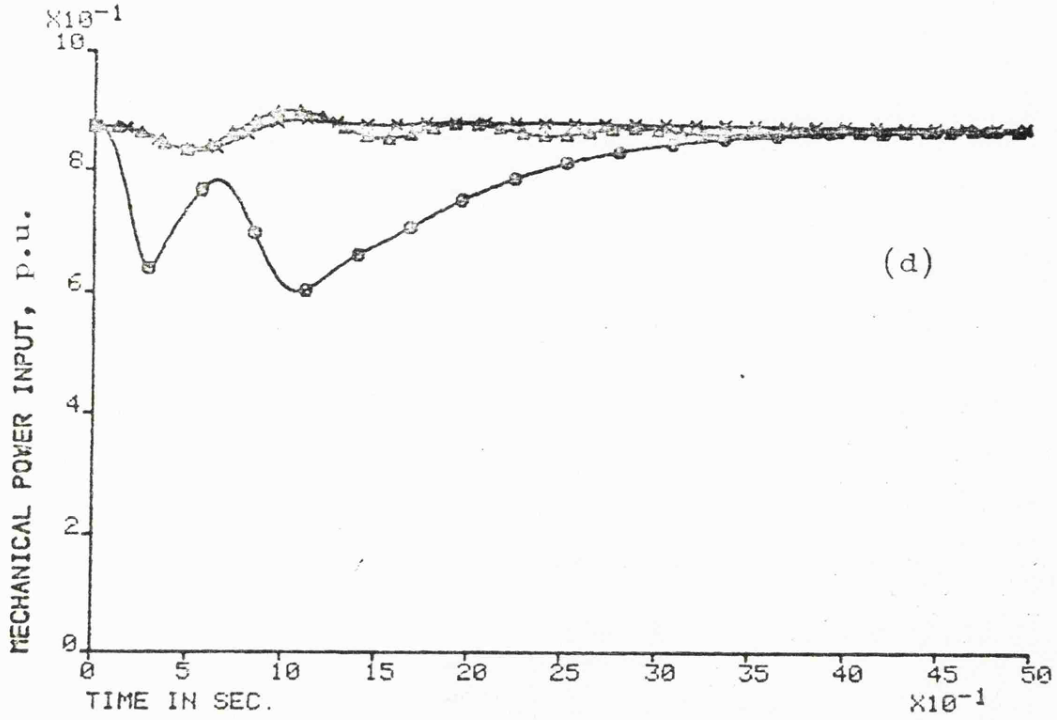

(1) Δ Control A_o
(2) x Control C1
(3) o Control A1a

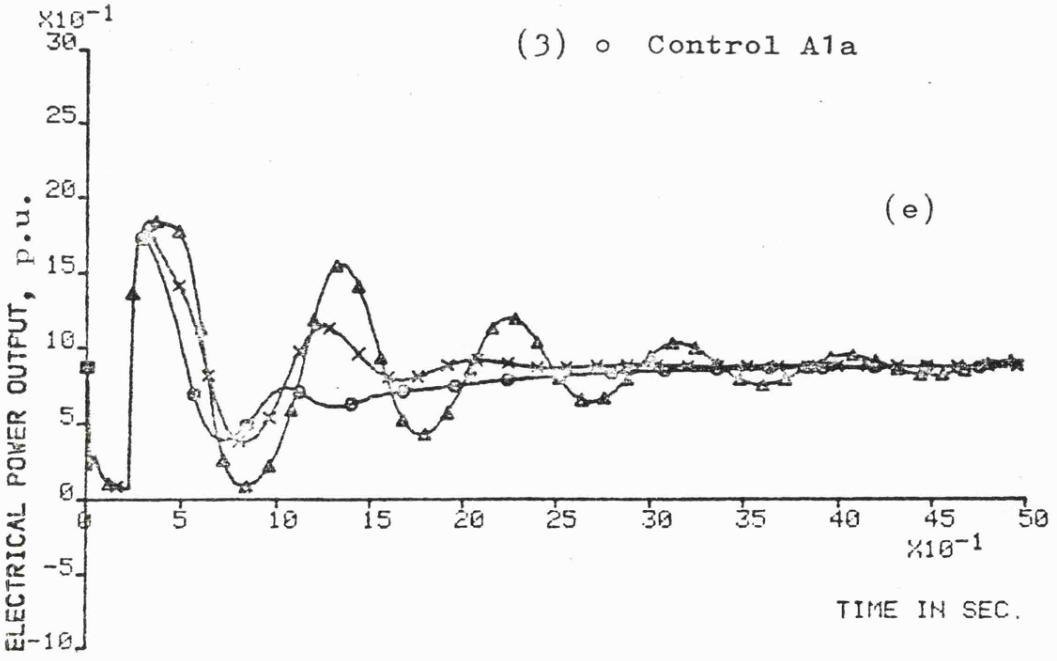

Fig. 7.6 Theoretical response curves

after fault removal as that with Control A_o, but regains its steady-state value much more quickly than Control A_o and slightly ahead of Control A1a.

7.4.5 System Sensitivity

A study has been made of the sensitivity of the single-machine system with respect to each of the excitation single stabilising feedback gain and the steam-flow controller feedback constant, using the sensitivity functions described in Chapter 4. The results of this study are illustrated in Figs. 7.7 and 7.8, where logarithmic sensitivity functions for the rotor angle and the terminal voltage respectively have been plotted for the suboptimal controllers A1a, A2 and A3 described in Table 7.1. Figure 7.7 shows that, although the initial rotor-angle response is totally insensitive to variations in the feedback gain for various signals of the excitation control system for the initial 0.4s after fault inception, it is sensitive to the acceleration gain of the steam-flow control about 0.2s after fault inception. On the other hand, the terminal voltage is more sensitive to the excitation feedback gain through the transient period with the exception of Control A1a.

A useful alternative method of comparing system sensitivities is to compare the areas under the logarithmic sensitivity curves and Table 7.2 shows the integrals of rotor-angle and terminal-voltage sensitivity functions over 5s. Two

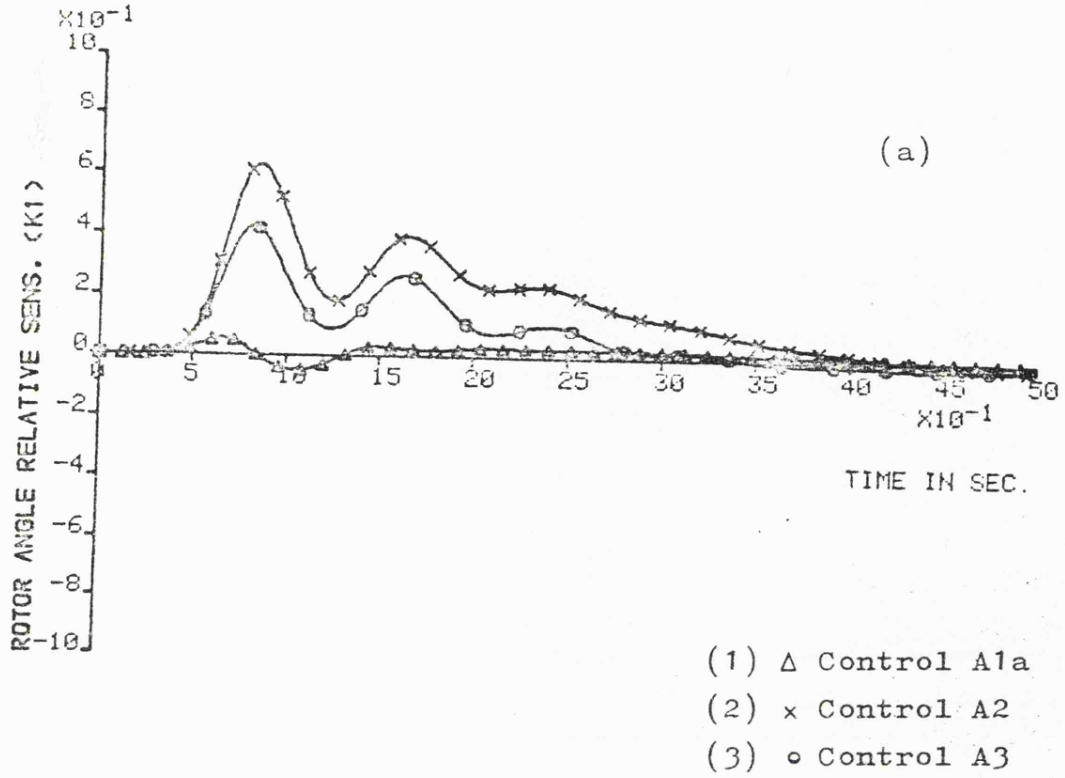

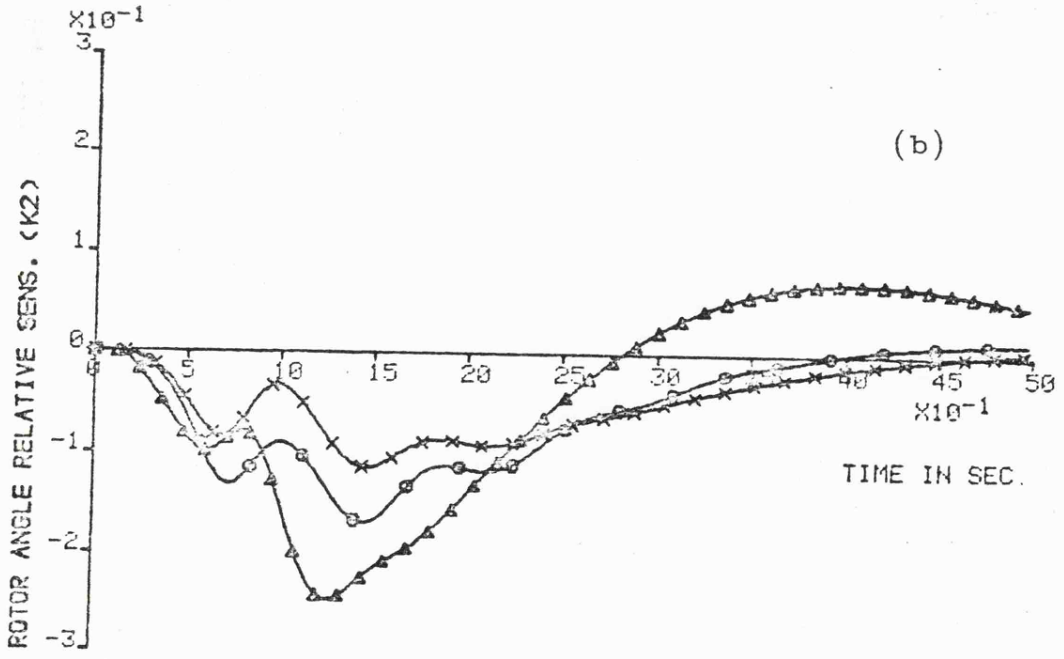

Fig. 7.7 Theoretical sensitivity curves

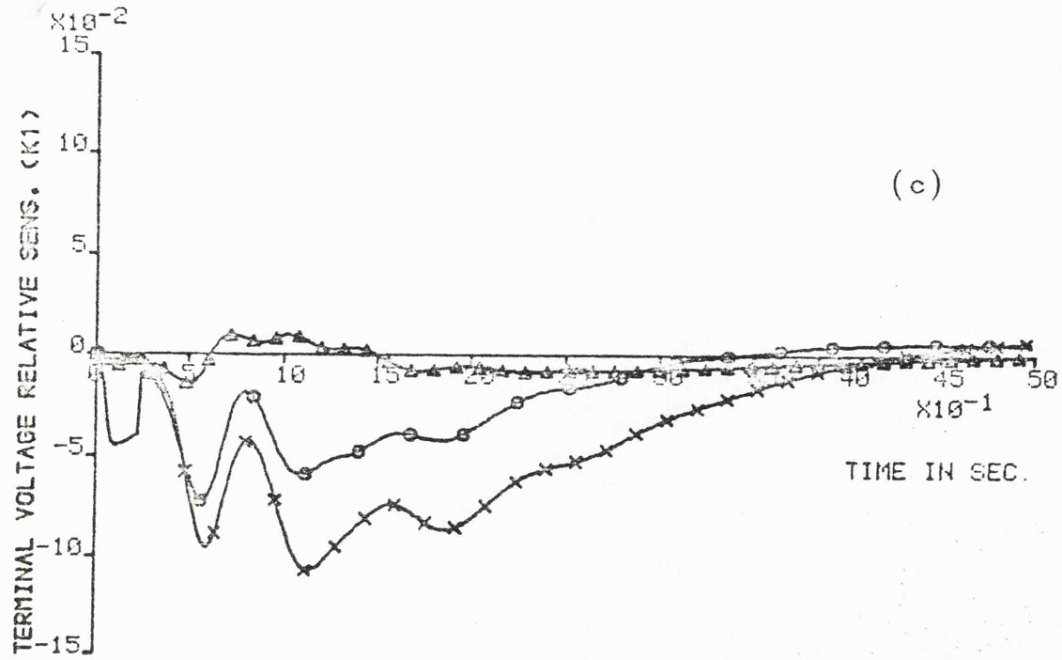

(1) Δ Control A1a

(2) × Control A2

(3) o Control A3

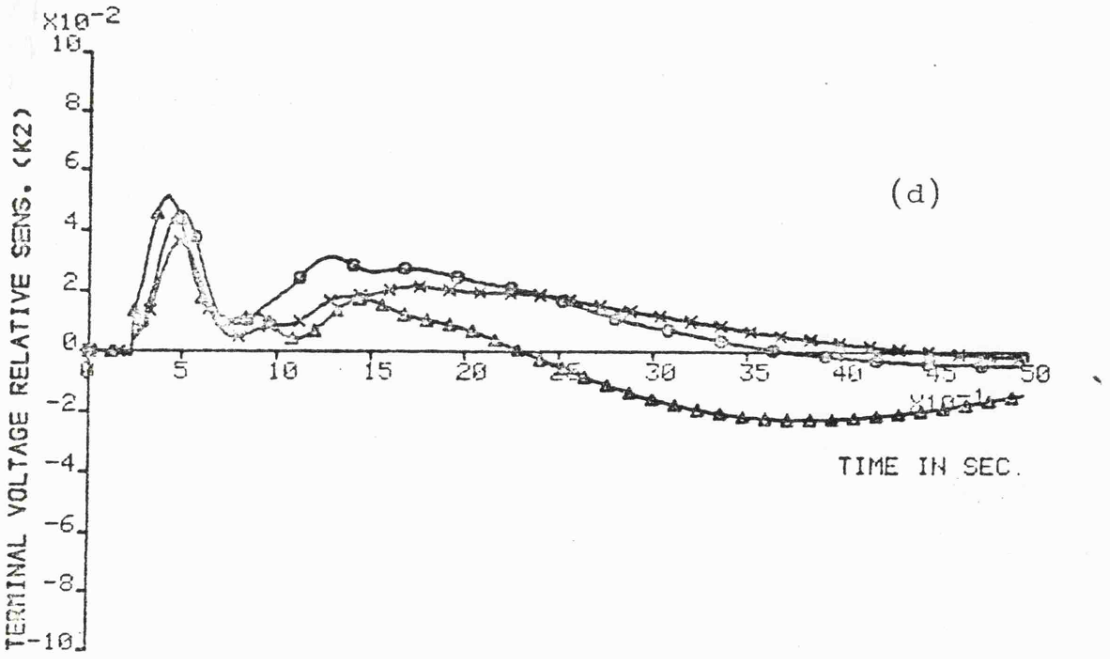

Fig. 7.8 Theoretical sensitivity curves

kinds of sensitivity functions are used in this table, namely, the absolute sensitivity and the logarithmic sensitivity functions and both bave been described earlier in Chapter 2. Control A_o, the conventional system, is the most sensitive of all controls to feedback gain variation on this basis, whereas Controls A1a, A2 and A3, which are co-ordinated suboptimal controllers, are the least sensitive.

Control Number	Absolute Sensitivity Integrals				Logarithmic Sensitivity Integrals			
	$s(K_1)$	$s(K_2)$	$V_t(K_1)$	$V_t(K_2)$	$s(K_1)$	$s(K_2)$	$V_t(K_1)$	$V_t(K_2)$
A_o	63.92	14.4	7.69	0.95	/	/	/	/
B1a	/	8.39	/	0.77	/	0.17	/	0.017
C1	45.02	/	9.295	/	0.61	/	0.16	/
A1a	1.65	4.51	0.32	0.59	0.046	0.44	0.013	0.074
A2	1.41	9.62	0.29	1.75	0.797	0.232	0.203	0.055
A3	1.14	9.67	0.21	1.63	0.43	0.299	0.109	0.067

Table 7.2 Integrals of sensitivity functions

A comparison of the corresponding integrals for the excitation controller and the steam-flow controller shows that this single-machine system is more sensitive to gain variations in the feedback signal K_2 of the steam-flow controller as far as absolute sensitivity function is concerned. From the viewpoint of logarithmic sensitivity function, however, only the Control A1a remains to be dominant in steam-flow controller gain sensitivity. This can be easily confirmed from Figs. 7.7 and 7.8. This fact may attribute to the reason that, while each of the

excitation controller signal used for Controls A2 and A3 has comparable transient responses with Control A1a in the earlier excitation control optimisation studies, they do not co-ordinate effectively as Control A1a with the acceleration steam-flow controller. The combination of acceleration steam-flow controller with single feedback excitation systems other than acceleration excitation controller has been observed to reduce its effectiveness as illustrated in section 7.4.2.

7.4.6 Changes in Operating Conditions

The optimisation studies have all been performed for a particular set of operating conditions. A control law so derived would be of little practical significance if it only gives satisfactory performance for that one set of operating conditions and it follows that the optimality of the control should not be unduly sensitive to system variations. The sensitivity of the response to changes in the state-feedback gains has just been discussed, and the present section deals with the usefulness of the suboptimal controller A1a of Table 7.1 when the operating conditions are varied over a relatively wide range. The results of such an investigation are given in Table 7.3.

Certain general conclusions can be made from the results listed in Table 7.3. Although the range of operating conditions considered is wide, the order of magnitude of the optimum feedback gains is not changed. Mathematically

Control Number	K_1	K_2	Power	Power Factor	New PI	PI for A1a
A1a	0.0365	0.12	0.85	1.0	5.686	5.686
A11	0.036	0.12	0.85	0.95 lag	5.305	5.765
A12	0.031	0.122	0.85	0.95 lead	4.854	5.507
A13	0.032	0.119	0.2	1.0	2.69	2.883
A14	0.037	0.154	0.85	1.0	1.695	2.28

Table 7.3 Effects of system changes

speaking, this means that the optimum points for this wide range of operating conditions are close to each other in the parameter space. When the fault clearance time is changed from 0.22s to 0.14s, Control A1a is only slightly modified by the reoptimisation to obtain Control A14 in Table 7.3, and it can be concluded that the controller remains near-optimal as the fault-clearance time is changed.

All the above results have been confirmed by the use of transient response curves and a typical set of response curves is illustrated in Fig. 7.9 for the operating conditions described by Control A12. The conventional control A_o and the feedback gains derived under Control A1a are also included for comparison, all operating under the same initial conditions.

7.5 Discussion of Results

A combined suboptimal excitation and steam-flow controller, employing a fast, high ceiling excitation system with

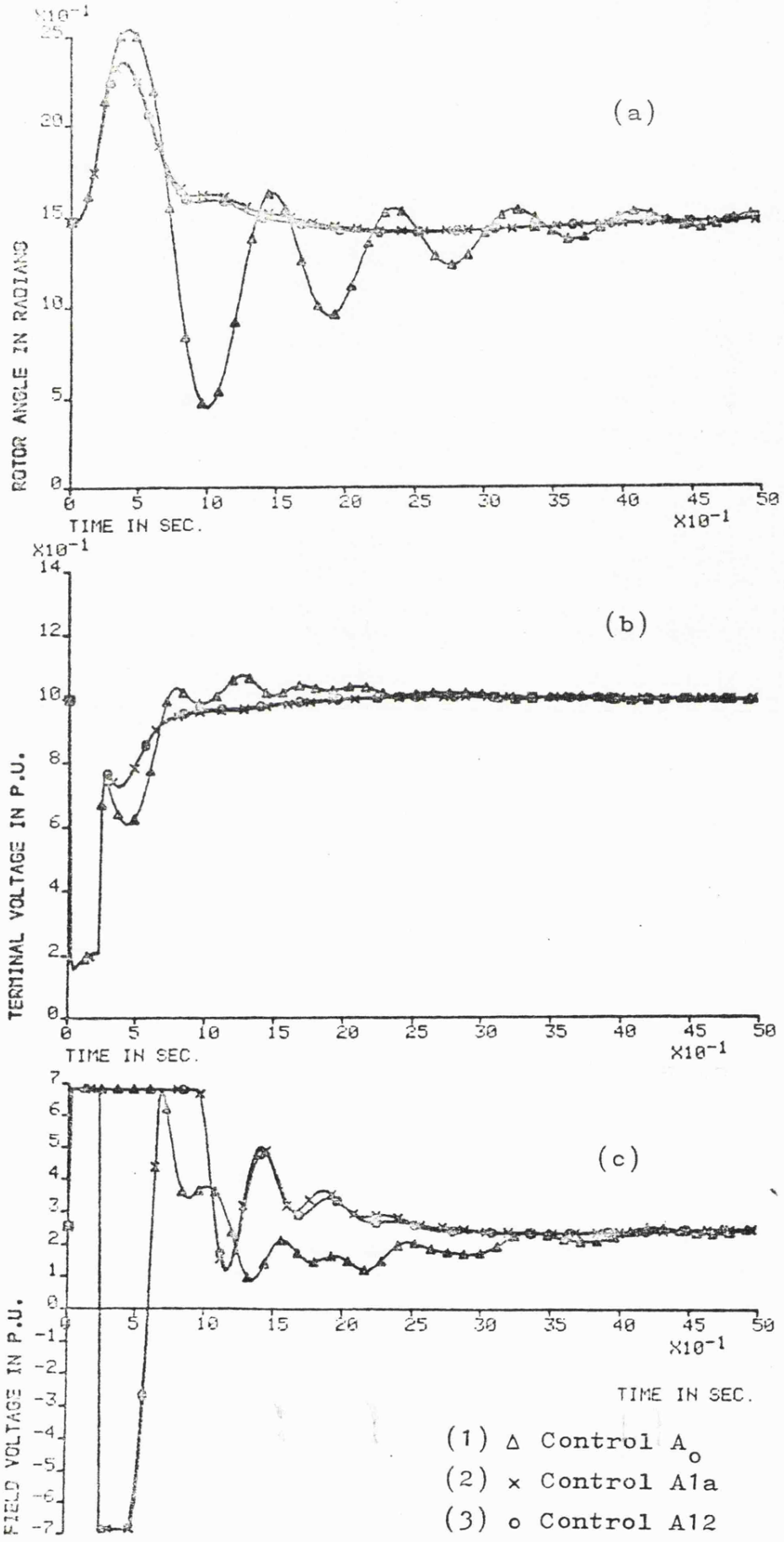

Fig. 7.9 Theoretical investigation of sensitivity

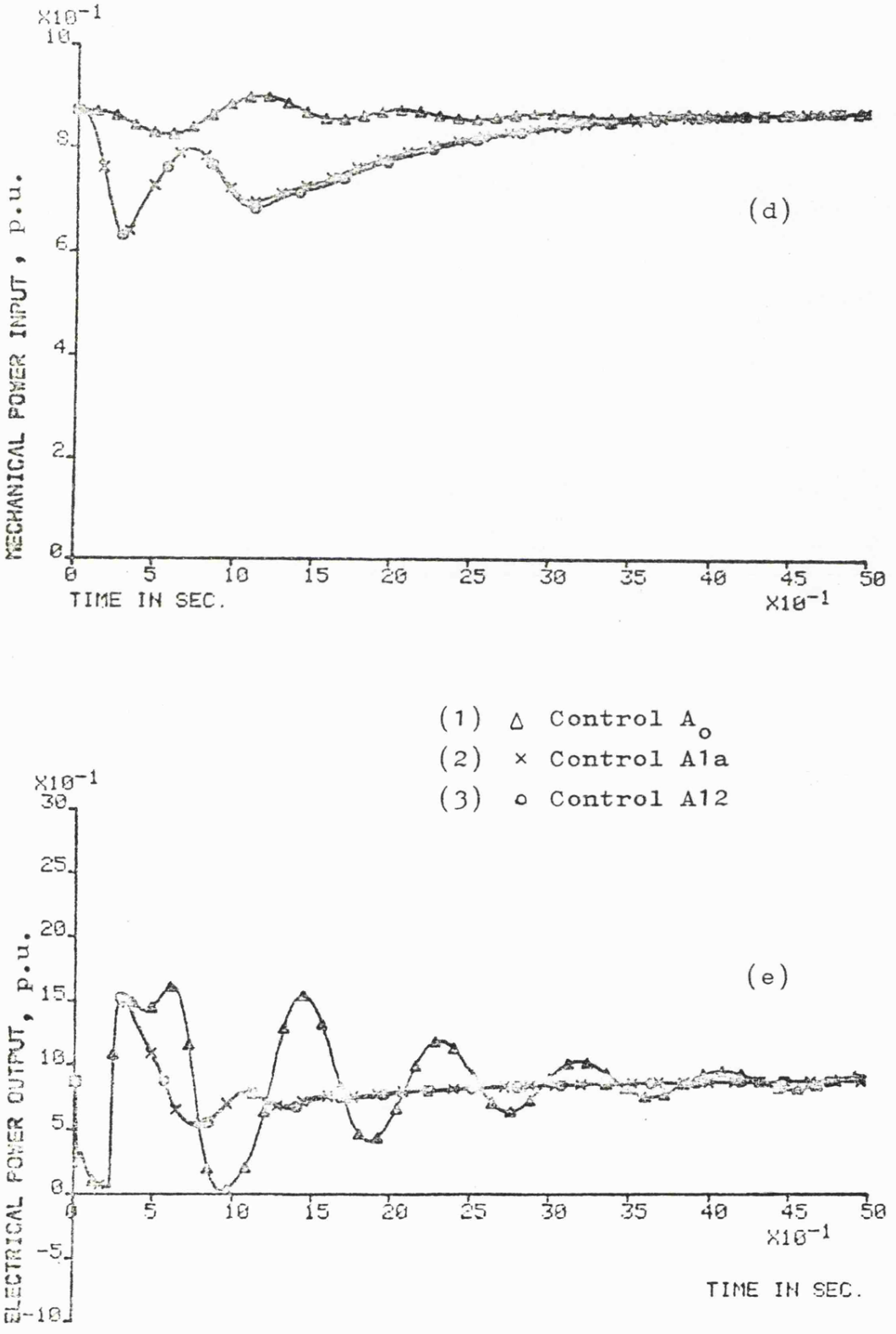

Fig. 7.9 Theoretical investigation of sensitivity

continuous main governing and interceptor-valve control can be very effective in improving the transient response of a single-machine power system, both in terms of first swing stability and subsequent damping. In a previous investigation[101], three states have been used for each of the control loops. It has now been demonstrated that it is possible to reduce the number of extra signals to one into each input. The best combination of the extra feedback signals under study has been found to be acceleration signal for both excitation and steam-flow controllers.

Suboptimal steam-flow control makes its main contribution in the reduction of the first swing in rotor angle, although it also provides some damping on subsequent swings, while the main contribution made by the suboptimal excitation controller is the provision of very effective damping on subsequent swings in rotor angle, beyond the first swing.

Sensitivity studies have shown that, although the suboptimal control law for the nonlinear model was obtained for a given set of operating conditions, this controller provides a substantial improvement in transient performance for a wide range of operating conditions. There is, however, a change in the optimum feedback gains as system conditions are changed, but, for operating conditions near the nominal values, these changes are small.

CHAPTER 8 CONCLUSIONS

8.1 General

Sensitivity theory and nonlinear optimisation techniques have been successfully applied to the optimisation of the transient performance of a power system consisting of an a.c. turbogenerator, connected to an infinite busbar through a transmission network. Systematic methods have been developed for the optimisation problem. By assuming that a suboptimal control could be obtained by a linear combination of the system states, the optimum control problem is transformed into one of parameter optimisation. This is, in turn, formulated as a function minimisation problem, whereby an optimum is located by a search, involving sensitivity functions, to minimise a perfromance index representing the performance of the system. Such a formulation avoids the two-point boundary problem and results in closed-loop state feedback controllers. It also allows suboptimal controllers incorporating feedback of any subset of the system variables to be derived in the same systematic and simple manner. The subset of the system variables may therefore be chosen to consist of only the output variables and not of inaccessible states.

In all the nonlinear optimisation studies, minimisation of the performance index requires the estimation of the partial derivatives of the performance index with respect to the optimising parameters. Although the partial

derivatives can be calculated using difference approximation inside the function minimisation subroutine, exact formulation of the derivatives is desirable for better efficiency. The method of obtaining the required derivatives also indirectly involves calculation of the absolute sensitivity functions of the system states. These sensitivity functions, which are inherent in any study involving gradient techniques, can give additional information about the system states.

The theoretical study in this thesis has progressed along three main lines. Firstly, a synthesis method has been investigated to produce optimised excitation control of an a.c. turbogenerator when subjected to a large disturbance. Secondly, a novel design/synthesis approach has been applied to the excitation control problem. Finally, non-linear multi-variable optimisation method is used to optimise the system performance under co-ordinated excitation and steam-flow control.

8.2 Synthesis Method for Excitation Control

Many analytical studies of the application of modern control methods to the excitation control of a.c. turbogenerators have been reported but there are few reported experimental studies. More recent ones involve direct digital control of excitation using both minicomputer and microprocessor installations. In some cases, the required control law has been obtained using linearised equations,

while, in other cases, certain of the system nonlinearities have been taken into account, to produce multi-variable feedback suboptimal controllers.

In the present study, a relatively simple synthesis approach using a linear search method is applied to the suboptimal excitation control problem. The proposed controller incorporates only one extra feedback signal into the excitation system, in addition to the normal terminal voltage feedback signal. The method uses single variable optimisation techniques, incorporating successive quadratic or cubic approximations of a nonlinear polynomial. Such an optimisation technique has been applied as a powerful method to synthesise a control law based on the existence of a given single system state, available for feedback purposes. When the cubic approximation algorithm is being used, formulation of dynamic sensitivity functions is required. It is suggested that the extra information obtained by these sensitivity functions should always be used to assess the suitability of a particular feedback signal.

8.3 Design/Synthesis Approach

The previous synthesis approach to the excitation control study makes no attempt to complete the design problem. Such a method of synthesis may be used as an ingredient of design but has limited power by itself. Therefore, a combined design and synthesis approach to this particular

excitation control problem has been made. The open-ended design method is based on an application of Bode techniques to the simplified linearised system to obtain a suitable form of compensation with accurate values determined precisely by single variable optimisation of the detailed nonlinear system. Such a controller incorporates feedback of transient direct-axis current which has not been used in the past as a single-state excitation feedback controller. A previous investigation using nonlinear multi-variable optimisation technique involves the combination of feedback signals of voltage behind transient reactance and load angle. That powerful gradient technique does indeed suggest feedback of the highly disguised direct-axis current signal through some algebraic manipulations. The choice of such a signal amongst all the possible system states has become obvious when signal-flow graphs and Bode techniques are used in this design exercise.

8.4 Experimental Studies

An experimental investigation based on the results from the synthesis and design/synthesis approaches has been performed on a real, although small, laboratory model, scaled on the Pembroke power station. The accuracy of various mathematical models of a turbogenerator used in theoretical studies has been the object of much discussion in the past. The accuracy of the values for the micro-

machine parameters has also not been firmly established. In these circumstances, since the accuracy of a comparison between theoretical results with experimental results depends on the parameter values used in the theoretical studies, it should only be used to confirm trends in system performance obtained with different extra feedback signals. In particular configurations involving load angle feedback, which are highly sensitive to changes in the optimised value of the feedback constant and therefore, by definition, sensitive to the accuracy of the machine parameters, will only be examined to confirm this fact. However, a more meaningful comparison between theoretical and experimental results can be made when the introduction of an extra signal, such as transient electrical power feedback, has been shown to have low sensitivity to parameter changes. In all cases, the trends in the system transient performance predicted by theoretical results, using one of five feedback signals, have been confirmed experimentally. These five signals are load angle, rotor velocity, acceleration, electrical power and direct-axis current.

8.5 Co-ordinated Control Problem

The final part of the theoretical study involves co-ordinated excitation and steam-flow control of a turbo-generator. Investigation of such a system becomes important when modern large turbines are fitted with fast

electro-hydraulic governing systems which have a potential role in the enhancement of stability. In certain circumstances, this could duplicate the role of a fast excitation system. In recent years, some methods of optimal control theory have been applied to this area of research. Attempts have also been made to achieve optimal controls by some form of open-loop controls. The majority of the published papers in this field describe theoretical studies, and little, if any, consideration has been given to the application of modern control techniques to practical systems.

The approach adopted in the present investigation uses multi-variable optimisation technique applied to the nonlinear system model. Suboptimal excitation control is achieved by transient feedback of a system state and suboptimal steam-flow control is achieved by proportional feedback of the acceleration signal. The stabilising excitation system states considered are rotor acceleration, electrical output power and direct-axis current. It has been found that the combined controller is very effective in improving the machine transient performance. The main contribution of the suboptimal excitation control is the effective damping of subsequent swings while that of the suboptimal steam-flow control is the reduction of the first rotor swing. The best combination of the extra feedback signals under study has been found to be the acceleration signal for both the excitation controller and the steam-flow controller.

Sensitivity studies suggest that the suboptimal control laws obtained are insensitive to wide range of parameter changes.

8.6 Summary and Suggestions

It is hoped that the synthesis method, demonstrated and the results successfully verified experimentally, will find application in various studies of the optimisation of performance of any engineering systems. The simplicity of the approach can prove advantageous, since these linear search methods can be easily programmed, are computationally compact and make only very modest demand on storage, all of which can be important considerations in practical optimisation projects. However, an initial design based on long-established classical control techniques, followed by final parameter adjustment using nonlinear optimisation methods could well be the best design/synthesis approach to the optimisation of the performance of nonlinear control systems.

The simplicity of the proposed co-ordinated controller which incorporates only one extra signal in each of the excitation and steam-flow control loop is amenable to practical implementation. Such implementation of the co-ordinated control of a single machine and multi-machine systems is, of course, the ultimate aim of the project.

APPENDIX A1

STEADY-STATE CALCULATION FOR SYNCHRONOUS MACHINE

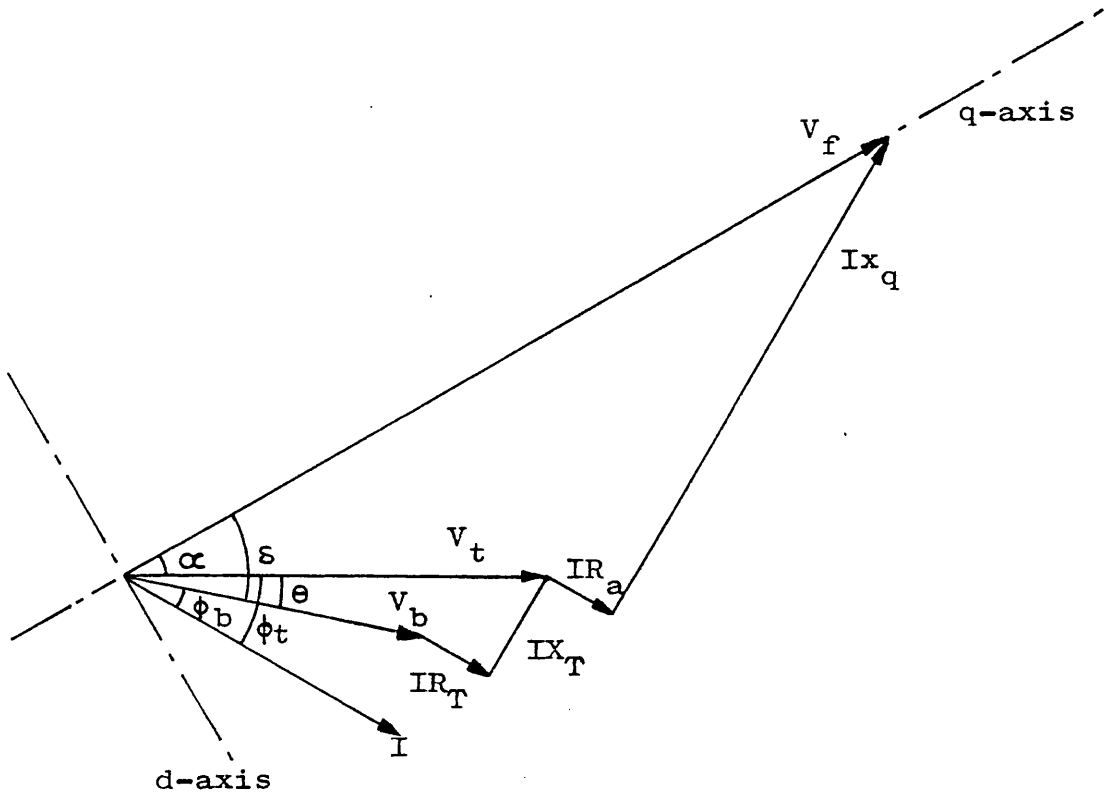

Fig. A1.1 Phasor diagram of a synchronous machine

Specified steady-state conditions:

Machine terminal voltage, V_t = 1 p.u.

Power at infinite busbar, P_b = 0.85 p.u.

Power-factor angle at infinite busbar, ϕ_b = 0.

The generator current, I, is given by

$$I = P_b/V_b\cos\phi_b \qquad \text{(A1.1)}$$

From the steady-state phasor diagram, V_t is described by

$$V_t^2 = (V_b + IR_T\cos\phi_b + IX_T\sin\phi_b)^2 + (IX_T\cos\phi_b - IR_T\sin\phi_b)^2 \qquad \text{(A1.2)}$$

From eqns. A1.1 and A1.2, V_b can therefore be calculated as

$$V_b = \left(\frac{-(2u-V_t^2) + \sqrt{((2u-V_t^2)^2 - 4(u^2+v^2))}}{2}\right)^{1/2},$$

where $u = P_b R_T + X_T \tan\phi_b P_b$,

$v = X_T P_b - R_T \tan\phi_b P_b$,

$R_T = R_l + R_x$,

and $X_T = X_l + X_x$.

The angles can be evaluated as

$$\theta = \sin^{-1}\left(\frac{IX_T\cos\phi_b - IR_T\sin\phi_b}{V_t}\right)$$

$$\phi_t = \phi_b + \theta$$

$$\alpha = \tan^{-1}\left(\frac{Ix_q\cos\phi_t - IR_a\sin\phi_t}{V_t + IR_a\cos\phi_t + Ix_q\sin\phi_t}\right)$$

$$\delta = \alpha + \theta$$

where θ is the angle between V_t and V_b,

ϕ_t is the power-factor angle at machine terminal,

α is the angle between V_f and V_t, and

δ is the rotor angle.

The following steady-state quantities can then be evaluated as

$$V_d = V_t\sin\alpha \qquad V_q = V_t\cos\alpha$$

$$I_d = I\sin(\delta+\phi_b) \qquad I_q = I\cos(\delta+\phi_b)$$

$$V_f = V_q + x_d I_d \qquad P_e = V_t I\cos\phi_t$$

where P_e is the electrical power at the machine terminals.

APPENDIX A2 MACHINE AND SYSTEM DATA

All values are per unit values unless otherwise stated. The machine rating is 588 MVA, 500 MW, 22kV, 3000 rpm with the following parameters:

$R_a = 0.0079$, $x_d = 2.8$, $x_q = 2.72$

$x_d' = 0.361$, $x_d'' = 0.18$, $x_q'' = 0.23$

$T_{do}' = 7.29s$, $T_{qo}'' = 0.116s$, $T_1 = 0.0914s$

$T_2 = 0.039s$, $T_{kd} = 0.00375s$, $H = 4.46$

$K_d = 6.0$, $M = 0.0284$

The generator transformer has $R_x = 0.013$, $X_x = 0.157$.
The transmission line has $R_l = 0.00794$, $X_l = 0.103$.

The excitation system allows full reversal of field voltage with a ceiling value of ± 6.87 (twice the full load value) with the following parameters:

$K_g = 200$, $T_g = 0.5s$, $K_s = 0.035$, $0.5s \leq T_s \leq 2.0s$.

APPENDIX A3 DERIVATION OF QUADRATIC APPROXIMATION

The assumed value of the quadratic function $q(\lambda)$ takes the general form:

$$q(\lambda) = q_o + q_1\lambda + q_2\lambda^2 \qquad (A3.1)$$

such that, for function values, f_a, f_b and f_c at the three points a, b and c,

$$f_a = q_o + q_1 a + q_2 a^2$$
$$f_b = q_o + q_1 b + q_2 b^2$$
$$f_c = q_o + q_1 c + q_2 c^2$$

This set of equations can then be solved to give q_o, q_1 and q_2 in terms of f_a, f_b, f_c, a, b and c.

Equation A3.1 has a turning point at

$$\lambda = \lambda_m = -\frac{q_1}{2q_2}$$

and has a minimum at this point if $q_2 > 0$. It follows from the above equations that

$$2\lambda_m = \frac{(b^2-c^2)f_a + (c^2-a^2)f_b + (a^2-b^2)f_c}{(b-c)f_a + (c-a)f_b + (a-b)f_c} \qquad (A3.2)$$

and this turning point is a minimum if

$$\frac{(b-c)f_a + (c-a)f_b + (a-b)f_c}{(a-b)(b-c)(c-a)} < 0 \qquad (A3.3)$$

APPENDIX A4

DERIVATION OF CUBIC APPROXIMATION

The assumed cubic approximation $C(\lambda)$ takes the general form

$$C(\lambda) = f_o + G_o\lambda + C_2\lambda^2 + C_3\lambda^3 \qquad (A4.1)$$

such that, at any point, h, $C(h) = f_h$ is the function value and G_h is the gradient value at that point. When eqn. A4.1 is differentiated with respect to λ, it follows that

$$C'(\lambda) = G_o + 2C_2\lambda + 3C_3\lambda^2 \qquad (A4.2)$$

Then, given the function values, f_o and f_h, the gradient values, G_o and G_h at two points, 0 and h, it follows from eqns. A4.1 and A4.2 that, with $\lambda = h$,

$$h^2C_2 + h^3C_3 = f_h - f_o - G_oh \qquad (A4.3)$$

$$2hC_2 + 3h^2C_3 = G_h - G_o \qquad (A4.4)$$

Equations A4.3 and A4.4 can then be solved for hC_2 and h^2C_3 to give

$$hC_2 = -(G_o + Z)$$

$$3h^2C_3 = (G_o + G_h + 2Z)$$

where $$Z = 3(f_o - f_h + G_o + G_h)/h$$

When these values of hC_2 and h^2C_3 are substituted into eqn. A4.2 it follows that

$$C'(\lambda) = G_o - \frac{2}{h}(G_o+Z)\lambda + \frac{\lambda^2}{h^2}(G_o+G_h+2Z)$$

The corresponding minimum value of $\lambda = \lambda_m$ is obtained by equating $C'(\lambda_m)$ to zero, so that

$$\frac{\lambda_m}{h} = \frac{G_o + Z \pm W}{G_o + G_h + 2Z} \qquad (A4.5)$$

where

$$W = (Z^2 - G_oG_h)^{1/2}$$

The ambiguity in the sign can be resolved by considering the second derivative of $C(\lambda_m)$, which must be greater than zero for a minimum value. Then, under this constraint, eqn. A4.5 becomes

$$\frac{\lambda_m}{h} = \frac{G_o + Z + W}{G_o + G_h + 2Z}$$

$$= 1 - \frac{G_h + W - Z}{G_h - G_o + 2W} \qquad (A4.6)$$

APPENDIX A5 SIGNAL-FLOW GRAPH MANIPULATION

Standard manipulation of the basic flow diagram of Fig. 5.1 can be used to eliminate the unwanted vertices v_q and e_q'. Consider the flow graph around the vertices v_q, i_d and e_q':

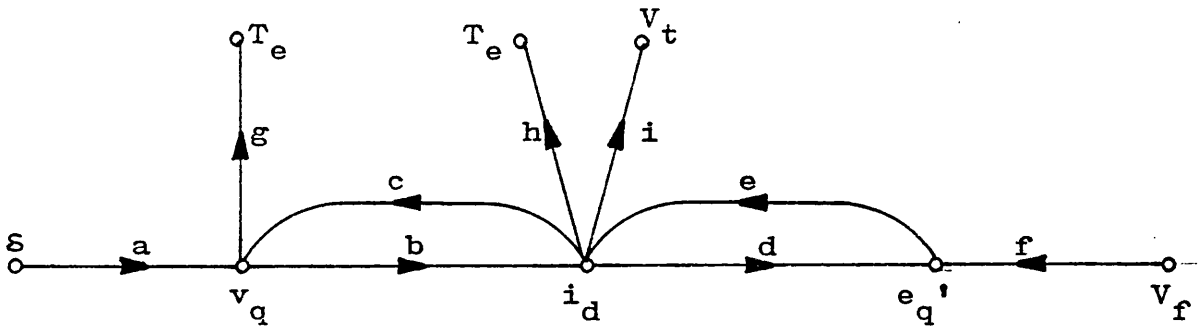

Fig. A5.1

where $a = -V_b \sin\delta_o$

$b = -1/x_d'$

$c = X_t$

$d = -(x_d - x_d')/(1+Ts)$

$e = 1/x_d'$

$f = 1/(1+Ts)$

$g = i_{qo}$

$h = v_{do}$

$i = X_t v_{qo}/V_{to}$

The vertex v_q is first removed, which generates a self circuit round i_d and results in the flow graph of Fig. A5.2. Similarly, removing vertex e_q' generates another self circuit round i_d as shown in Fig. A5.3. Finally, the self loops round i_d are removed, showing all the transmittance paths via i_d as illustrated in Fig. A5.4.

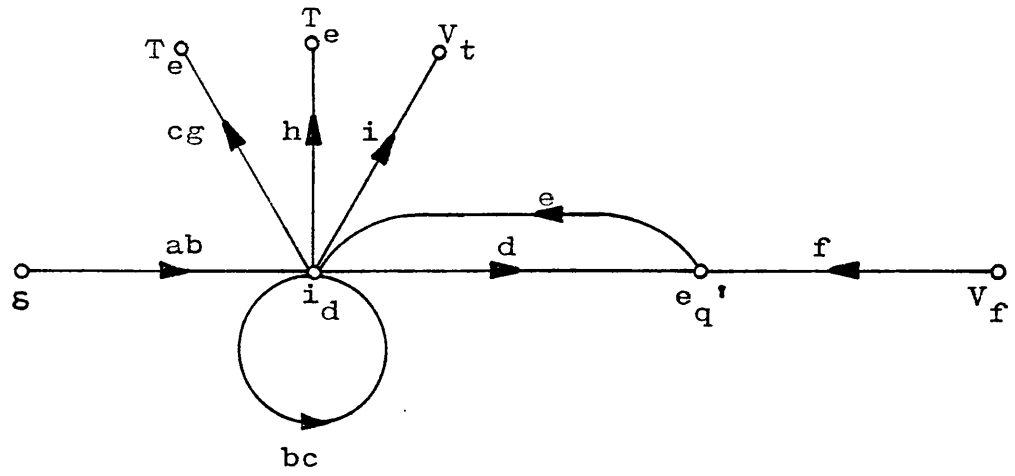

Fig. A5.2

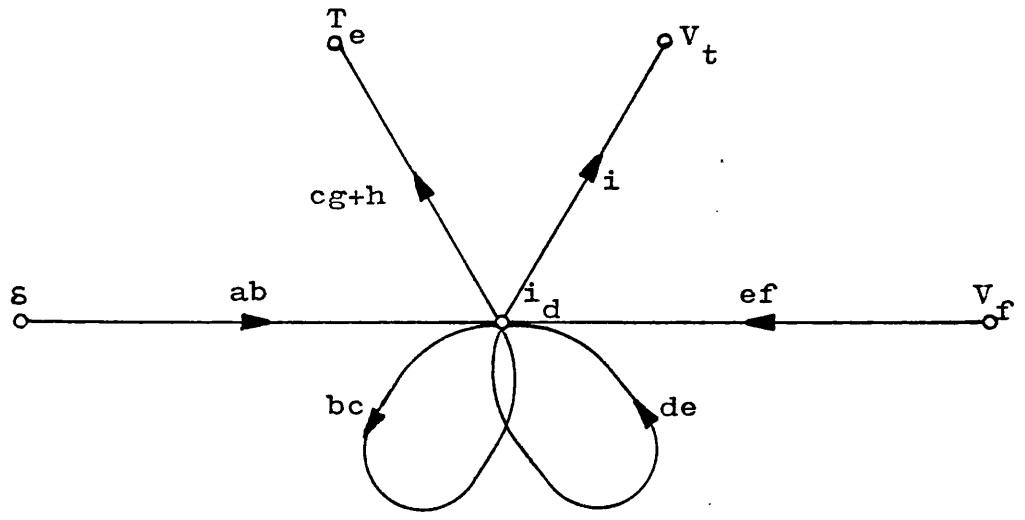

Fig. A5.3

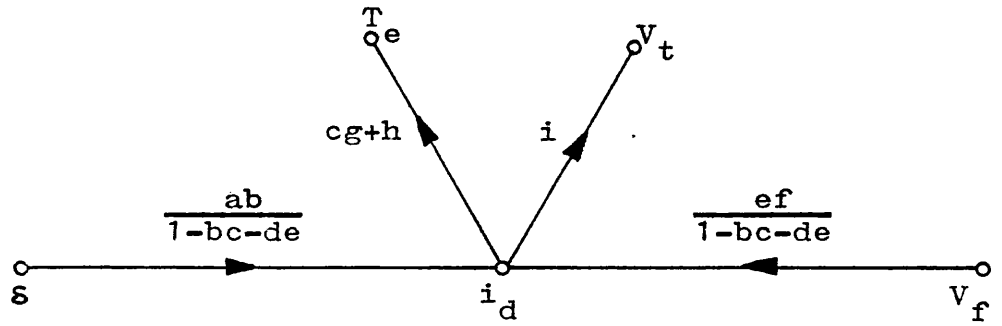

Fig. A5.4

Substituting the values back for a to i into the transmittance paths of Fig. A5.4 gives the simplified representation as shown in Fig. 5.2, where

$$cg + h = v_{do} + X_t i_{qo}$$

$$i = X_t v_{qo}/V_{to}$$

$$\frac{ab}{1 - bc - de} = \frac{V_b \sin\delta_o / x_d'}{1 + \frac{X_t}{x_d'} + \left(\frac{x_d - x_d'}{1+Ts}\right)\frac{1}{x_d'}}$$

$$= \frac{(V_b \sin\delta_o)(1+Ts)}{(x_d + X_t) + (x_d' + X_t)Ts}$$

$$\frac{ef}{1 - bc - de} = \frac{1}{x_d'(1+Ts)} \quad \frac{1}{1 + \frac{X_t}{x_d'} + \frac{x_d - x_d'}{x_d'(1+Ts)}}$$

$$= \frac{1}{(x_d + X_t) + (x_d' + X_t)Ts}$$

APPENDIX A6 RELATIONSHIP BETWEEN δ, e_q' and i_d

From Fig. A5.2, retaining only the transmittance paths onto i_d gives the following highly simplified flow graph:

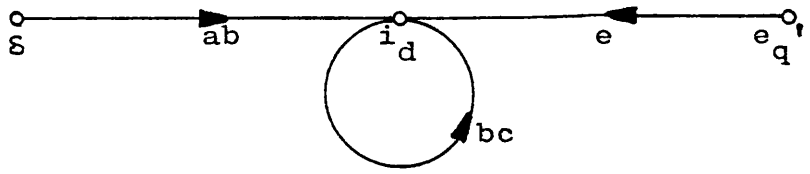

Fig. A6.1

where $a = -V_b \sin\delta_o$

$b = -1/x_d'$

$c = X_t$

$e = 1/x_d'$

Removing the self loop round i_d gives

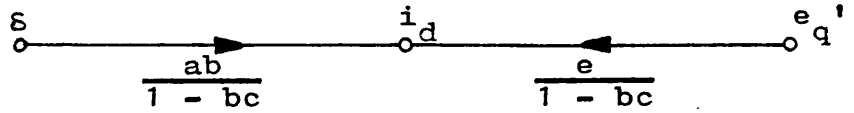

Fig. A6.2

Substituting the values back for a, b, c and e into the transmittance paths gives the simple relationship between δ, e_q' and i_d as described by eqn. 5.35, where

$$\frac{ab}{1 - bc} = \frac{V_b \sin\delta_o / x_d'}{1 + X_t/x_d'} = \frac{V_b \sin\delta_o}{X_t + x_d'}$$

$$\frac{e}{1 - bc} = \frac{1/x_d'}{1 + X_t/x_d'} = \frac{1}{X_t + x_d'}$$

REFERENCES

1 CRARY, S.B. "Power system stability", Vol 1, John Wiley, New York, 1954

2 KIMBARK, E.W.: "Power system stability", Vol 1 and 3, John Wiley, New York, 1948 and 1956

3 BRUCK, R.W., and MESSERLE, H.K.: "The capability of alternators", Proc. IEE, 1955, 102(A), pp. 611-618

4 HUGHES, F.M.: "Improvement of turbogenerator transient performance by control means", ibid., 1973, 120, pp. 233-240

5 SULLIVAN, A.C., and YEE, H.: "Fast governing of turbo-generators during transients", ibid., 1973, 120, pp. 371-378

6 CUSHING, E.W., DRECHSLER, G.E., KILLGOAR, W.P., MARSHALL, H.G., and STEWART, H.R.: "Fast valving as an aid to power system transient stability and prompt resynchronisation and rapid reload after full load rejection", IEEE Trans., 1972, PAS-91, pp. 1624-1636

7 DINLEY, J.L., MORRIS, A.J., and PREECE, C.: "Optimised transient stability from excitation control of synchronous generators", ibid., 1968, PAS-87, pp. 1696-1705

8 ELLIS, H.M., HARDY, J.E., BLYTHE, A.L., and SKOOGLUND, J.W.: "Dynamic stability of the Peace River transmission system", ibid., 1966, PAS-85, pp. 586-600

9 KIMBARK, E.W.: "Improvement of system stability by switched series capacitors", ibid., 1966, PAS-85, pp. 180-188

10 KIMBARK, E.W.: "Improvement of power system stability by changes in the network", ibid., 1969, PAS-88, pp. 773-781

11 WILSON, A.T., and PORAY, A.T.: "Comparison of methods of improving the transient performance of power stations", System Technical Report No. PL-ST/3/73, CEGB

12 O'KELLY, D., and MUSGRAVE, G.: "Improvement of power system transient stability by phase-shift insertion", Proc. IEE, 1973, 120, pp. 247-252

13 REITAN, D.K., and RAO, N.R.: "A method of improving transient stability by bang-bang control of tie-line reactance", IEEE Trans., 1974, PAS-93, pp. 303-311

14 HUMPAGE, W.D., and STATT, B.: "Effect of autoreclosing circuit breakers on transient stability in e.h.v. transmission systems", Proc. IEE, 1964, 111, pp. 1287-1298

15 DANIELS, A.R., and LEE, Y.B.: "Optimal and suboptimal control of dual-excited synchronous generators", ibid., 1976, 123, pp. 989-992

16 SHACKSHAFT, G.: "Generator stability improved by an interconnected winding rotor", Elect. Times, 29th Jan. 1971, pp. 33-37

17 SKOOGLUND, J.W., and BLYTHE, A.L.: "Discussion on reference 22", IEEE Trans., 1970, PAS-89, pp. 975

18 SMITH, J.M.: "Power system transient control by capacitor switching", ibid., 1969, PAS-88, pp. 28-35

19 FENWICK, D.R., and WRIGHT, W.F.: "Review of trends in excitation systems and possible future developments", Proc. IEE, 1976, 123, pp. 413-420

20 HAM, P.A.L.: "Generator stability - a manufacturer's viewpoint", IEE Colloquium on Generator Dynamic Control, Savoy Place, London, Feb. 1978

21 HAM, P.A.L., JENKINS, K., and MIKHAIL, S.E.: "Performance and control capabilities of electro-hydraulic governing systems for steam turbine-generators", Reyrolle Parsons Review, Vol 2, No 5, Summer 1976

22 RAMARAO, N., and REITAN, D.K.: "Improvement of power system transient stability using optimal control - bang bang control", IEEE Trans., 1970, PAS-89, pp. 975-984

23 SOPER, J.A., and FAGG, A.R.: "Divided-winding-rotor synchronous generator", Proc. IEE, 1969, 116, pp. 113-126

24 GUILE, A.E., and PATERSON, W.: "Electrical power systems", Vol 2, 2nd Edition, Oliver and Boyd, Edingburgh, 1978

25 DINELEY, J.L., and POWNER, E.T.: "Power system governor simulation", Proc. IEE, 1964, 111, pp. 115-125

26 POWER NEWS: "New electronic governor saves wear and tear", CEGB Newspaper, March 1979, pp. 3

27 BUSEMANN, F., and CASSON, W.: "Results of full-scale stability tests on the British 132 kV Grid system", Proc. IEE, 1958, 105(A), pp. 347-362

28 SCOTT, E.C., CASSON, W., CHORLTON, A., and BANKS, J.H.: "Multi-generator transient stability performance under fault conditions", ibid., 1963, 110, pp. 1051-1064

29 SHACKSHAFT, G., and NEILSON, R.: "Results of stability tests on an underexcited 120 MW generator", ibid., 1972, 119, pp. 175-188

30 BARTLETT, J.P., GIBBARD, M.J., and WOODWARD, J.L.: "Performance of a 5 kVA synchronous generator with an optimal excitation regulator", ibid., 1973, 120, pp. 1250-1256

31 ELEMETWALLY, M.M., RAO, N.D., and MALIK, O.P.: "Expermental results on the implementation of an optimal control for synchronous machines", IEEE Trans., 1975, PAS-94, pp. 1192-2000

32 DANIELS, A.R., DAVIES, D.H., and PAL, M.K.: "LINEAR and nonlinear optimisation of power system performance", ibid., 1975, PAS-94, pp. 810-818

33 YU, Y.N., SOWADA, J.H., and WVONG, M.D.: "A dynamic power system model for teaching and research", ibid., 1976, PAS-95, pp. 1507-1514

34 NEWTON, M.E., and HOGG, B.W.: "Optimal control of a micro-alternator system", ibid., 1976, PAS-95, pp. 1822-1830

35 MOYA, O.E.O., and CORY, B.J.: "Online control of generator stability by minicomputer", Proc. IEE, 1977, 124, pp. 252-258

36 BURROWS, P.J., and DANIELS, A.R.: "Digital excitation control of a.c. turbogenerators using a dedicated microprocessor", ibid., 1978, 125, pp. 237-240

37 ANDERSON, J.H., HUTCHISON, M.A., WILSON, W.J., ZOHDY, M.A., and APLEVICH, J.D.: "Microalternator experiments to verify the physical realisibility of simulated optimal controllers and associated sensitivity studies", Trans. IEEE, 1978, PAS-97, pp. 649-658

38 PHUNG, V.A., and GIBBARD, M.J.: "Practical implementation on a 5 kVA synchronous generator of an adaptive excitation controller strategy for a wide range of operating conditions", Proc. IEE, 1978, 125, pp. 1009-1014

39 SPEEDY, C.B., BROWN, R.F., and GOODWIN, G.C.:"Control theory - identification and optimal control", Oliver and Boyd, Edingburgh, 1970

40 FRANK, P.M.: "Introduction to system sensitivity theory", Academic Press, New York, 1978

41 RALSTON, A., and RABINOWITZ, P.: "A first course in numerical analysis", 2nd Edition, McGraw Hill, 1978

42 BEVERIDGE, G.S.G., and SCHECHTER, R.S.: "Optimisation theory and practice", McGraw Hill, 1970

43 WALSH, G.W.: "Methods of optimisation", John Wiley, 1975

44 NELDER, J.A., and MEAD, R.: "A simplex method for function minimisation", The Computer Journal, 1965, 7, pp. 308-313

45 GILL, P.E., and MURRAY, W.: "Quasi-Newton methods for unconstrained optimisation", J. Inst. Maths. Appl., 1972, 9, pp. 91-108

46 HASDORFF, L.: "Gradient optimisation and nonlinear control", John Wiley, New York, 1976

47 GILL, P.E., and MURRAY, W.: "Software for numerical optimisation", National Physical Laboratory Conference, Russell Hotel, London, March 1978

48 POWELL, M.J.D.: "An efficient method of finding the minimum of several variables without calculating derivatives", The Computer Journal, 1964, 7, pp. 155-162

49 DAVIDSON, W.C.: "Variable metric method for minimisation", AEC Research and Development Report, ANL-5990

50 GILL, P.E., MURRAY, W., and PITFIELD, R.A.: "The implementation of two revised Quasi-Newton algorithms for unconstrained optimisation", National Physical Laboratory Report NAC 11, April 1972

51 Private communication with Professor K.V. Diprose

52 SANFORD, R.S.: "Physical Network", Prentice Hall, 1965

53 THALER, G.J.: "Design of feedback systems", 1973

54 MACFARLANE, A.G.J.: "Dynamic system models", Harrap, 1970

55 PARK, R.H.: "Two-reaction theory of synchronous machines; generalised methods of analysis", Part 1, IEEE Trans., 1929, 48, pp. 716-730; Part 2, 1933, 52, pp. 352-355

56 PARK, R.H.: "Definition of an ideal synchronous machine and formula for the armature flux linkages", General Electrical Review, 1928, 31, pp. 332

57 RANKIN, A.W.: "Per-unit impedance of synchronous machines", Trans. AIEE, Part 1, 1945, 64, pp. 569-573; Part, pp. 839-841

58 ADKINS, B., and HARLEY, R.G.: "The general theory of a.c. machines", Chapman and Hall, 1975

59 SHACKSHAFT, G.: "General purpose turbo-alternator model", Proc. IEE, 1963, 110, pp. 707-713

60 HUMPAGE, W.D., and SAHA, T.N.: "Digital-computer methods in dynamic-response analysis of turbogenerator units", ibid., 1967, 114, pp. 1115-1130

61 PAL, M.K.: "Mathematical methods in power system stability studies", Ph.D. Thesis, University of Aston in Birmingham, 1971

62 VENIHOV, V.A.: "Transient phenomena in electrical power systems", Pergamon, 1964

63 MEHTA, D.B., and ADKINS, B.: "Transient torque and load angle of a synchronous generator following several types of system disturbance", Proc. IEE, 1960, 107, pp. 61-74

64 PAL, M.K.: "Synchronous machine representation in power system stability", Nelson Research Laboratory, English Electric, NSY 190, May 1968

65 FENWICK, D.R., and WRIGHT, W.F.: "Review of trends in excitation systems and possible future developments", Proc. IEE, 1976, 123, pp. 413-420

66 HUGHES, F.M.: "Improvement of turbogenerator transient performance by control means", ibid., 1973, 120, pp. 233-240

67 IEEE STD 421A-1978: "Guide for identification, testing, and evaluation of the dynamic performance of excitation control systems", IEEE Standard, June 1978

68 WATSON, W., and MANCHUR, G.: "Experience with supplementary damping signals for generator static excitation systems", IEEE Trans., 1973, PAS-92, pp. 199-204

69 HERNANDEZ MILLAN, R., MENDOZA, J.A., CARDOZO, C., and DE LIMA, A.: "Dynamic stability and power system stabilisers - analysis and tests on the Venezuelean system", ibid., 1977, PAS-96, pp. 855-862

70 BAYNE, J.P., LEE, D.C., and WATSON, W.: "A power system stabiliser for thermal units based on derivation of accelerating power", ibid., 1977, PAS-96, pp. 1777-1783

71 DEMELLO, F.P., HANNETT, L.N., and UNDRILL, J.M.: "Practical approaches to supplementary stabilising from accelerating power", ibid., 1978, PAS-97, pp. 1515-1522

72 KEAY, F.W., and SOUTH, W.H.: "Design of power system stabiliser sensing frequency deviation", ibid., 1971, PAS-90, pp. 707-713

73 DANIELS, A.R., DAVIS, D.H., and PAL, M.K.: "Linear and nonlinear optimisation of power system performance", ibid., 1975, PAS-94, pp. 810-818

74 DANIELS, A.R., LEE, Y.B., and PAL, M.K.: "Nonlinear power-system optimisation using dynamic sensitivity analysis", Proc. IEE, 1976, 123, pp. 365-370

75 CHANA, G.S., and DANIELS, A.R.: "Turboalternator excitation control incorporating nonlinear state feedback", ibid., 1978, 125, pp. 1245-1246

76 LEE, Y.B.: "Sensitivity and optimal control studies of power systems", Ph.D. Thesis, University of Bath, 1975

77 CONCORDIA, C.: "Steady-state stability of synchronous machines as affected by voltage-regulator characteristics", IEEE Trans., PAS-63, 1944, pp. 215-220

78 ALDRED, A.S., and SHACKSHAFT, G.: "A frequency-response method for the predetermination of synchronous-machine stability", IEE Monograph No 340S, Aug. 1959

79 STAPLETON, C.A.: "Root-locus study of synchronous-machine regulation", Proc. IEE, 1964, 111, pp. 761-768

80 JACOVIDES, L.J., and ADKINS, B.: "Effect of excitation regulation on synchronous-machine stability", ibid., 1966, 113, pp. 1021-1034

81 KASHKARI, C.N.: "Effect of feedback signals on transient stability - phase plane approach", IEEE Trans., 1971, PAS-90, pp. 2228-2232

82 DEMELLO, F.P., and CONCORDIA, C.: "Concepts of synchronous machine stability as affected by excitation control", ibid., 1969, PAS-88, pp. 316-329

83 KEAY, F.W., RACZKNOWSKI, C., and SOUTH, W.H.: "Excitation control system complex compensation", ibid., 1974, PAS-93, pp. 1444-1448

84 BOLLINGER, K., LAHA, A., HAMILTON, R., and HARRAS, T.: "Power system stabiliser design using root locus methods", ibid., 1975, PAS-94, pp. 1484-1488

85 HUGHES, F.M., and HAMDON, H.M.A.: "Design of turbo-alternator excitation controllers using multi-variable frequency-response methods", IEE Colloquium on Generator Dynamic Control, Savoy Place, Feb. 1978

86 AHSON, S.I., and HOGG, B.W.: "Integrated control and governing of turbogenerators using the Inverse Nyquist Array design method", Thirteenth Universities Power Engineering Conference, April 1978

87 DANIELS, A.R., LU, H.: "Nonlinear single variable optimisation studies of a.c. turbogenerator performance", Accepted for publication, Proc. IEE, March 1979

88 BURROWS, P.J.: "Direct digital method of a micro-machine model power system", Ph.D. Thesis, University of Bath, 1977

89 MARTIN, M.A.: "Micromachine studies of power systems", M.Sc. Thesis, University of Bath, 1973

90 HAZELL, P.A.: "Development and use of a digital real time model of a steam governor and turbine of a large turbogenerator, for use on a micromachine system", Transfer Report, University of Bath, 1978

91 SHACKSHAFT, G., and PORAY, A.T.: "Implementation of a new approach to determination of synchronous machine parameters from tests", IEE Discussion Meeting on Determination of Turbogenerator Characteristics On Load, Savoy Place, Dec. 1978

92 YU, Y.N., VONSURIYA, K., and WEDMAN, L.N.: "Application of an optimal control theory to a power system", IEEE Trans., 1970, PAS-89, pp. 55-62

93 ANDERSON, J.H.: "The theory of a synchronous machine using optimal control theory", Proc. IEEE, 1971, 59, pp. 25-35

94 DAVISON, E.J., and RAU, N.S.: "The optimal output feedback of a synchronous machine", IEEE Trans., 1971, PAS-90, pp. 2123-2134

95 IYER, S.N., and CORY, B.J.: "Optimisation of turbo-generator transient performance by differential dynamic programming", ibid., 1971, PAS-90, pp. 2149-2157

96 IYER, S.N., and CORY, B.J.: "Optimal control of a turbogenerator including an exciter and governor", ibid., 1971, PAS-90, pp. 2142-2148

97 PULLMAN, R.T., and HOGG, B.W.: "Discrete state-space controller for a turbogenerator", Proc. IEE, 1979, 126, pp. 87-92

98 NPL: "Aspects of mathematical modelling which affect algorithmic choice and performance", National Physical Laboratory Conference on Software for Numerical Optimisation, Russell Hotel, London, March 1978

99 DHALIWAL, N.S., and WICHERT, H.E.: "Analysis of P.I.D. governors in multimachine system", IEEE Trans., 1978, PAS-97, pp. 456-463

100 DINELEY, J.L., and MIKHAIL, S.E.: "Effect of feedback signals in excitation and governor/turbine systems on transient and dynamic stability", IEEE PES Meeting Paper A 76 113-1, Jan. 1976

101 DANIELS, A.R., LEE, Y.B., and PAL, M.K.: "Combined suboptimal excitation control and governing of a.c. turbogenerators using dynamic sensitivity analysis", Proc. IEE, 1977, 125, pp. 473-478